THE EFFECTS OF ALKALI-AGGREGATE REACTIVITY ON THE MECHANICAL PROPERTIES OF CONCRETE

SHELDON LANGDON

The Effects of Alkali-Aggregate Reactivity on the Mechanical Properties of Concrete

By

© Sheldon Langdon, B.Eng.

A THESIS SUBMITTED TO THE SCHOOL OF GRADUATE STUDIES
IN PARTIAL FULFILMENT OF THE REQUIREMENTS FOR
THE DEGREE OF MASTER OF ENGINEERING

APRIL 1998

FACULTY OF ENGINEERING AND APPLIED SCIENCE

MEMORIAL UNIVERSITY OF NEWFOUNDLAND

ST. JOHN'S NEWFOUNDLAND CANADA

Abstract

Alkali-aggregate reactivity is an internal chemical reaction between the sodium and potassium alkaline components in the concrete mix and active mineral constituents of some aggregates. The reaction results in the formation of a gel which absorbs water, expands, and therefore exerts internal pressures which sometimes can be far in excess of that which concrete can sustain, thereby causing the formation of micro cracks.

In this investigation, a potentially highly reactive aggregate, and a potentially marginally reactive aggregate (identified by accelerated mortar bar testing, and petrographic examination) were used in concrete specimens, in both normal and high strength mix designs. After the initial 28 day curing period, the number of samples allocated for each testing procedure were equally divided, and then submerged in a holding tank containing either a solution of 1M sodium hydroxide or de-ionized water at 80 °C over an extended period of time. Research has proven that a sodium hydroxide solution can accelerate an alkali-aggregate reaction.

From these specimens, the mechanical properties such as the compressive strength, direct tensile strength, modulus of rupture, freeze - thaw characteristics, as well as the creep characteristics were determined for all samples at different time intervals. In comparing the mechanical properties of samples located in the sodium hydroxide solution, and those determined from samples located in the de-ionized water, the effect of an alkali-aggregate

reaction on the mechanical properties of concrete could be examined.

In general, normal strength concrete samples subjected to the sodium hydroxide solution containing the potentially highly reactive aggregate experienced increased losses in mechanical properties than that of specimens containing the potentially marginally reactive aggregate. However, for high strength concrete samples subjected to the solution, there were little, if any, loss of mechanical properties for either specimens containing the potentially reactive or marginal aggregates. This is explained by the improved micro structure of high strength concrete as a result of the secondary pozzolanic reaction.

The normal strength samples containing the highly reactive aggregate experienced a loss in ultimate compressive strength of 28%, and a decrease in the modulus of elasticity of 80% over the testing period. Samples containing the moderately reactive aggregate experienced no loss in compressive strength over the testing period, and a decrease in the modulus of elasticity of 20%. The ultimate tensile strength of both normal strength concrete samples containing the highly and moderately reactive aggregate decreased by 37 %, and 31 % respectively. The freeze - thaw effects revealed that normal strength specimens containing the moderately reactive aggregate experienced larger decrease in mechanical properties than that of specimens containing the highly reactive aggregate. Creep of the normal strength concrete containing the highly reactive aggregate experienced a 94% increase in creep strain with respect to the control, whereas normal strength specimens containing the moderately reactive aggregate experienced a 48% increase in creep strain with respect to the control. This is

attributed to the weaker cement paste resulting from a more aggressive alkali-aggregate reaction.

A theoretical investigation of the moment - curvature response of a typical I - section, and Tee - section were examined assuming expansive strains resulting from an alkali - aggregate reaction. From the investigation, it was apparent that the effects of an alkali-aggregate reaction on the ultimate moment capacity, and curvature of both sections was not significant (< 5%). These results are consistent with that determined from research conducted during the past decade involving pre-stressed, and well reinforced sections.

Acknowledgements

The author wishes to thank the Provincial Government of Newfoundland, and the Natural Sciences and Engineering Council of Canada for funding of the study contained in this thesis.

The author also wishes to extend his sincere thanks to Dr. H. Marzouk, and Mr. Dan Bragg, who have made this study possible. The author would also like to thank Mr. Austin Bursey, Mr. Calvin Ward, Mr. John Tucker, Mr. Tom Ring, and Mr. Colin Crane, whose assistance has been greatly appreciated.

Table of Contents

List of Figures

List of Tables

List of Symbols

a	constant depending on the properties of concrete and the storage environment
A_c	area of concrete section (mm^2)
A_p	area of prestressing strands (mm^2)
A_s	area of non-prestressed reinforcement (mm^2)
A_{trans}	transformed area (mm^2)
b	constant depending on the properties of concrete and storage environment
c	distance from centroid of section to the moment axis (y_{trans}) (mm)
d	average depth of specimen (mm)
E	modulus of elasticity (MPa)
E_d	dynamic modulus of elasticity (MPa)
E_{ci}	initial tangent modulus of elasticity (MPa)
E_s	non - prestressed reinforcement modulus of elasticity (MPa)
$E_{p,eff}$	effective modulus of elasticity of prestressed reinforcement (MPa)
E_p	modulus of elasticity of prestressed reinforcement (MPa)
f_c	stress in concrete section (MPa)
f_p	stress in prestressing strands (MPa)
f_s	stress in non-prestressed reinforcement (MPa)
f'_c	ultimate concrete strength (MPa)
I_{xx}	transformed section modulus (mm^4)
N	sum of axial loads on a section (MPa)

M	sum of moments on a section (MPa)
R	modulus of rupture (MPa)
y_{trans}	section centroid (mm)
ϵ_{AAR}	strains present due to alkali - aggregate reactivity
ϵ_c	strain in the concrete determined from geometry at the particular location
ϵ'_c	ultimate strain of concrete corresponding to ultimate strength
ϵ_{cf}	final strain in the concrete section
ϵ_{cth}	strain in concrete due to temperature effects
$\Delta \epsilon_p$	initial strain in the prestressing strands due to pre-stressing
ϵ_p	final strain in the pre-stressing strands
ϵ_{pf}	final strain in the pre-stressing strands
ϵ_{pth}	strains in prestressed reinforcement due to temperature
ϵ_s	strain in the non-prestressed reinforcement
ϵ_{sf}	final strain in non-prestressed reinforcement
ϵ_t	strain in concrete at top of section
ϵ_{sth}	strain in non-prestressed reinforcement due to temperature
ϕ	creep coefficient (assumed as 2.7)

1.0 Introduction

1.1 General

Concrete is known as the first construction material, proving to be very cost effective, reliable, and has shown to provide long time durability. Many of the structures located in Europe, even though the concrete was not made with modern portland cement, have been in service for hundreds of years, and are still found without appreciable deterioration. For the most part, deterioration of modern concrete structures has resulted from inadequate cover of reinforcing steel, and the penetration of chloride ions which lead to corrosion of the steel, as well as spalling of the concrete cover.

However, due to extensive field and laboratory investigations during the past few decades, researchers have discovered that a chemical reaction which occurs within the concrete when certain constituents are present can cause serviceability problems. This phenomenon is called alkali-aggregate reactivity (AAR), and was first recognized in the western region of the United States of America in the late 1930's (Stanton, 1940). Research conducted on nearly

400 concrete structures located in Newfoundland revealed that almost 32 % were showing signs of premature deterioration due to alkali-aggregate reactivity, with the greater number of these structures being located on the Avalon Peninsula (refer to Figure 1). However, of this 32%, 11.2 % showed moderate to severe deterioration as a result of alkali-aggregate reactivity (Bragg, 1996).

Figure 1 - Concrete structures with moderate to severe deterioration caused by AAR (Bragg, 1996)

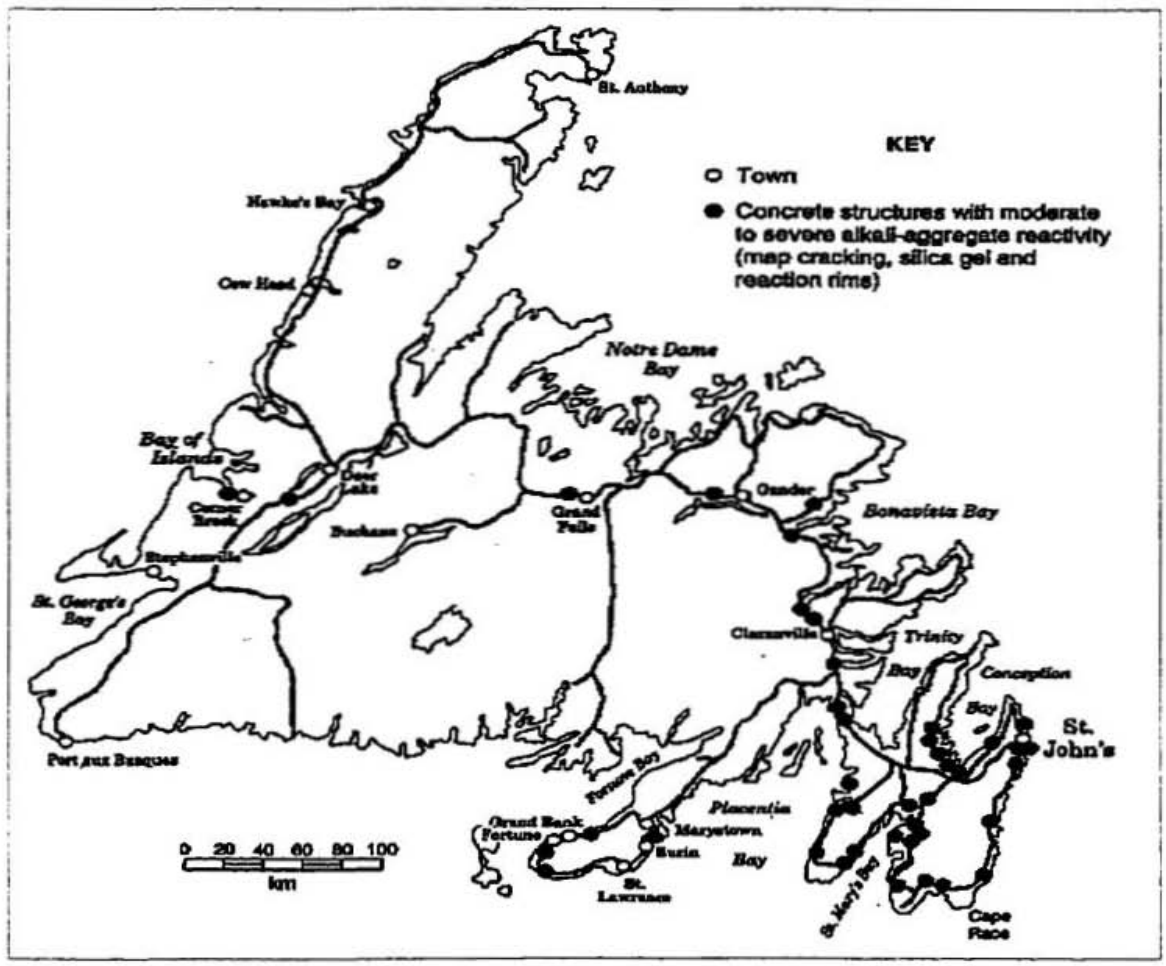

In the past, visible evidence of surface cracking was attributed to such processes as stress, freeze-thaw cycles, shrinkage, and creep. However, today many researchers believe that internal expansive alkali-aggregate reactions may be a catalyst to cause crack formation in many cases, and that all of the other processes act synergistically in causing the observed damage of field structures.

Today, evidence of AAR can be seen in almost all regions of Canada, even in concrete using different types of aggregate. In general, there are three types of alkali aggregate reactivity: alkali-silica, alkali-carbonate, and alkali-silicate reactivity. However, alkali-silica reactivity (ASR) is more widespread, and is the reaction of which this thesis is concerned.

ASR is an internal chemical reaction between the sodium and potassium alkaline components in the concrete mix and active mineral constituents of some aggregates. The reaction results in the formation of a gel which absorbs water, expands, and therefore exerts internal pressures which sometimes can be far in excess of that which concrete can sustain, thereby causing the formation of micro cracks. These cracks can thereby act as channels for water movement leading to increased saturation, increasing the structure's freeze-thaw susceptibility, and increasing the potential for chloride attack of the reinforcement.

Extensive investigations made by scientists all over the world have concluded that there are three main components necessary to facilitate the alkali-silica reaction. They include a sufficient amount of alkalies in the pore solutions, a critical amount of reactive mineral

phases in the aggregate particles, and sufficient moisture or humidity.

Currently, there are several different test methods used for determining the potential reactivity of a given aggregate. However, at the present, the three most accepted tests used in Canada include the Accelerated Mortar Bar Test (CSA A23.2-25A, NBRI, ASTM C9-P214), the Concrete Prism Test (CAN3-CSA A23.2-14A), and the Mortar Bar Test (ASTM C227). Nonetheless, to date, there is no test that can guarantee that a structure will not be affected by alkali-aggregate reactivity.

It must be remembered that AAR is a time dependent function. It may not occur or may go undetected for a long period of time. However, as conditions of the structure or the local environment change, the reaction may progress at a relatively rapid pace. It is for these reasons that AAR is still largely an unpredictable phenomenon. There are too many interdependent and highly interactive factors necessary which make the assessment and testing techniques quite complex. However, if the correct material constituents are present, along with the appropriate environmental conditions, concrete can be found to deteriorate at early stages of the service life of the structure, and thereby resulting in costly and time consuming repair and/or reconstruction.

The effects of ASR on the properties of concrete have been investigated under laboratory conditions and field conditions, using both reinforced and unreinforced concrete specimens. For the most part, the detrimental effects of ASR are much more pronounced in plain

concrete, and under laboratory conditions. In many instances, laboratory investigations have shown a markedly larger decrease in mechanical properties such as compressive strength, indirect and direct tensile strength, modulus of rupture, modulus of elasticity, and dynamic modulus of elasticity, when in fact, cores obtained from structures known to be affected by ASR do not indicate the same extreme level of mechanical property loss. Research conducted throughout the world during recent years has shown that "well reinforced" structures resist the detrimental effects ASR can have on the structural integrity of the system.

While concrete is considered to be theoretically homogeneous, it is not usually the case. It may be such that aggregates from certain areas of a quarry may be more reactive than others, resulting in certain areas of the structure containing more reactive aggregate. Furthermore, quality control of concrete must always be exercised to as great an extent as possible.

The understanding of an alkali-aggregate reaction, its causes and consequences, are also very important in the development of numerical and finite element models. At present, many of the existing models are too simplistic, and thus misrepresent the nature of the reactivity.

1.2 Research Scope

In Newfoundland, ASR research has been limited to Accelerated Mortar Bar Testing, Concrete Prism Testing, and petrographic examination. However, with the increasing interest in oil reserves located in the Grand Banks, the possibility of several hydro development projects, and the trans Labrador highway construction, it is important to try to achieve a greater understanding of this phenomenon.

The work reported herein includes the experimental investigation of several mechanical properties of concrete involving a reactive and marginally aggregate from two Newfoundland sources. In addition, an investigation of the effect of ASR induced strains on the Moment-Curvature of two structural elements is investigated.

1.3 Research Objectives

The research objective of this thesis is to compare the effects of ASR on the mechanical properties of concrete containing a reactive and marginally reactive aggregate obtained from two Newfoundland concrete suppliers. In addition, an attempt will be made to try and bridge the gap between laboratory investigations and field performance of such concrete.

1.4 Thesis Outline

In addition to this chapter, there are 5 more chapters in the thesis.

Chapter 2 is a literature review of recent research work relevant to this topic. This chapter reviews the effects of aggregates, cement type, moisture, the environment, and

supplementary cementing materials on an alkali-silica reaction. In addition, research conducted during the past few decades regarding the effects of an alkali-silica reaction on the mechanical properties of plain and reinforced concrete are reviewed. Furthermore, analytical models that have been developed in order to understand the phenomenon are examined.

Chapter 3 contains the methodology used in this study, as well as the relevant information regarding the experimental setup. This information includes the petrographic examination, and associated accelerated mortar bar results from each aggregate source, as well as, aggregate property testing and geochemistry. In addition, the mix design to be used throughout these experiments, and the cement test reports are also included. Finally, the testing regime for the compression, direct and in-direct tension, creep, freeze-thaw, and expansion testing are included within this chapter, as well as the testing set-up for each experiment.

Chapter 4 presents the results obtained from the experimental investigation, and compares how these results obtained compare with those of previous researchers.

Chapter 5 investigates the theoretical effect of ASR induced strains on the Moment-Curvature response of two prestressed concrete beams. In this chapter, both the short and long term moment curvature response of the section are investigated, in conjunction with theoretical strains resulting from expansive alkali-aggregate reactivity.

In Chapter 6, the main conclusions from the thesis research are collated and further supplemented.

2.0 Literature Review

2.1 General

During the past few decades there has been extensive research conducted by engineers and scientists all over the world on AAR. During the initial stages, much of the phenomenon associated with alkali-aggregate reactivity was not well understood. However, as time progressed, and more researchers became involved in this area of study, substantial gains have been made in understanding alkali-aggregate reactions. The following chapter presents an extensive review of recently published literature.

2.2 ASR - The Reaction

Research conducted over the past 50 years has indicated that alkali-aggregate reactivity is a complex chemical process. Most researchers have explained the phenomenon in the following manner.

The alkaline components, sodium and potassium, derived from cement, and other constituents, cause the dissolution of siliceous components of the aggregate to result in the formation of a non-deforming gel. This dissolution is possible due to the fact that the hydroxyl ion, the critical reacting ion, penetrates the aggregate particles and produces large numbers of Si-OH bonds. These bonds have the ability to bond with large numbers of water molecules, which in turn, causes the swelling of the aggregate particles. The swelling of the aggregate particle is not uniform, but instead decreases with depth inside the particle. The alkalis become concentrated on the aggregate / paste interface where they attract water molecules from the residual mixing water by way of an osmotic process, thereby resulting in expansion. This expansion is, for the most part, confined within an inelastic medium, and is largely an irreversible anisotropic volumetric expansion. It is the expansion that exerts disruptive tensile forces in the concrete, that when exceeding the tensile capacity of the concrete, causes the formation of micro-cracks. As the gel continues to imbibe moisture, the micro-cracks are widened. On the surface, the crack formation formed is known as map-cracking, and often resembles the formation of a spiders web. Extensive research of field structures has indicated that crack widths can range from 0.1mm to 10mm in extreme cases, and even extend beyond the reinforcement (Neville (1995), Swamy (1992), and Vivian (1992)).

However, identification of deterioration that is observed in the field being solely the result of ASR has been quite difficult. Often, other processes such as thermal shrinkage, freeze-thaw processes, and concentrations of stress contribute to what many see as AAR activity.

"The most evident signs to diagnose significant ASR effects are relative movements, closure of joints and distortions, and concrete spalling associated with stress buildup in concrete and reinforcement. The appearance of surface cracking is also an important feature associated with ASR. However, it should be recognized that surface cracking might be due to a number of different causes" (Leger et al, 1990, p.695). Although the presence of gel products does not imply that ASR was the sole cause of the observed cracking, the visible map cracking on the surface together with the presence of gel products indicate that ASR might have a major role in the observed deterioration. Nonetheless, the involvement of the particular factors necessary to cause the formation of the reaction will be investigated in the following sections.

2.3 The Three Basic Requirements for ASR

2.3.1 Alkalis in the cements

All Portland cement based concrete contain alkalis to some degree. These alkalis are derived from the raw materials used in the manufacture of the portland cement such as clay, limestone, chalk, and shale (Hobbs, 1989). "Alkali compounds in the clinker are alkali sulphates, alkali aluminates and aluminoferrites, and alkali silicates. The alkalis combine preferentially with the clinker SO_3 and any remaining alkali is present in the silicates, aluminates, and aluminoferrites" (Hobbs, 1989, p.11)

The Portland Cement provided by North Star Cement of Corner Brook, as used in this study, contains an alkali content of approximately 1.05% equivalent Na_2O. For normal Type I

cements produced across Canada in 1988, the Na_2O/K_2O ratio ranged from 1.09 to 0.07, with a mean of 0.38 (median 0.31) (Rodgers, 1990). Therefore, since a low alkali content is considered to be less than 0.7% soda equivalent (the actual Na_2O content plus 0.658 times the K_2O content of the cement), the possibility of ASR in Newfoundland is quite high.

The hydration of portland cement results in the formation of sodium ions (Na^+), potassium ions (K^+), calcium ions (Ca^{+}), and hydroxyl ions (OH^-) being formed in the pore water solution. The possibility of a reaction is dependant on the hydroxyl ion concentration, and thereby the chemical composition of the portland cement being used (Hobbs, 1989).

Neville (1995) provides the rationale for using a cement containing a low alkali content when a potentially reactive aggregate is being used. Since a high-alkali cement leads to a pore water pH of between 13.5 and 13.9, while a low-alkali cement leads to a pore water pH of between 12.7 and 13.1, an increase in pH of 1.0 represents a ten-fold increase in hydrogen ion concentration. In addition, Hobbs (1989) determines that it is only in pore solutions of high hydroxyl ion concentration that significant attack of reactive silica occurs.

Many researchers are now specifying low alkali cements for all aspects of construction. "In Alberta, an engineer recently proposed the use of a maximum alkali cement content of 0.3% for dam construction. Such a cement is not available in Canada, but such caution is understandable, given the high costs of remedial work on large concrete structures affected by alkali-aggregate reactivity" (Rodgers, 1990, p. 5).

It is important to realize, however, that the alkali percentage in the mix can be increased from alkali-bearing aggregates, irrespective of whether they are reactive or not, and can also draw alkalis from external sources such as deicing salts and sea water as ions penetrate into the concrete, and even supplementary cementing materials. Therefore, prescribing the use of a low alkali cement does not ensure that the overall alkali content of the mix will not increase after the mix has been put in place. Moreover, laboratory investigations have shown that even the use of a low alkali cement does not effectively prevent an alkali-aggregate reaction when concrete is used in a severe alkaline environment (Alasali et al., 1990).

2.3.2 Aggregates

In Canada, there are three types of alkali-aggregate reactions recognized in Portland cement concrete. However, all three types cannot be evaluated by using the same testing procedures. This is due to the wide range of rock types capable of causing ASR, and that some rock types show different expansions when using different testing procedures. Rodgers (1990) has conducted extensive research into determining which testing procedures provide the most accurate evaluation of the potential reactivity of the aggregate. The main findings reported by Rodgers (1990) have been summarized as the following.

Alkali-carbonate reaction (ACR) is a reaction between the carbonates of the aggregate and the alkaline pore solution of the concrete. ACR is common with dolomotic limestones and calcitic dolostones of Ordovician Age. The rock cylinder expansion test (ASTM C 586) and the concrete prism expansion test (CAN#-A23.2-14A) are useful for identifying these rocks.

Alkali-silica reaction (ASR), an acid-base reaction between the alkaline pore solution and the silica content of the aggregate, is common with various varieties of quartz or with poorly crystalline or metastable silica minerals such as chalcedony, opal, cristobalite, and volcanic glass. The Mortar Bar Expansion Test (ASTM C 227), Concrete Prism Expansion test at 38°C with high cement contents, and the rock cylinder expansion test are used for assessing the potential reactivity of these rock types. The Quick Chemical Expansion test (ASTM C 289) is also used, but gives misleading results when carbonates are present.

For the case of late/slow alkali-silica/silicate reaction with sandstones and granites containing strained quartz and metamorphosed sediments such as phyllite, argillite, and greywacke, where exfoliation of phyllosilicates causes swelling of aggregate particles. This is the most common form of ASR, and is the reaction under investigation.

The expansion caused by the alkali-silica reaction increases with increasing content of reactive silica in the aggregate. However, this is only true up to a certain percentage of reactive silica content. Exceeding this certain percentage, known as the pessimum content, the excess silica acts as a deterrent to the reaction (Hobbs, 1989). In addition, Hobbs (1989) also indicates that the time at which cracking is induced in specimens subjected to AAR decreases as the reactive silica content of the aggregate increases, however, at very high silica contents no cracking or expansion is observed. The percentage at which this limiting of the expansion occurs is higher at lower water/cement ratios and at higher cement contents (Neville, 1995). The following figure depicts the typical pessimum behaviour observed by

Hobbs (1989) using opaline silica as the reactive aggregate.

Figure 2 - Pessimum Behaviour of Opaline Silica (Hobbs, 1989)

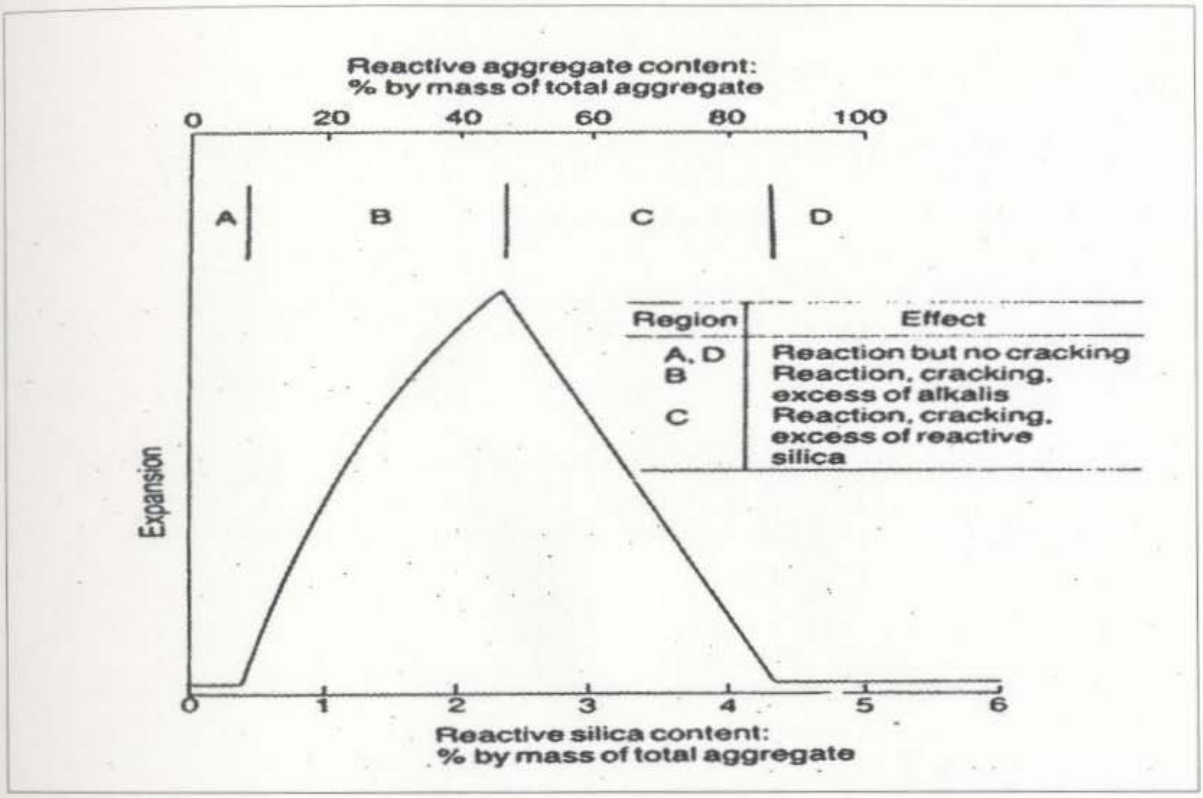

2.3.2.1 Evaluation of Aggregates

The first useful and efficient method for determining the reactivity of an aggregate is by petrographic examination (ASTM C295). Petrographic examination of potential construction aggregates begins with field investigations of the aggregate source. Many aspects of the deposit are recorded including the deposit type, the rock type(s), the degree of weathering and all noticeable geological features (eg. faults, folds, joints, dykes, fractures, cleavages, bedding thickness, grain size, mineralization, etc.) (Bragg, 1995). After determining the rock type,

texture, weathering, and hardness of the aggregate, a petrographic number (PN) is assigned. It is this petrographic number which is a measure of the potential of the aggregate to be used for construction purposes.

In addition, Bragg and Foster (1992) investigated the relationship between the results of petrography and the results of alkali-reactivity testing for many Newfoundland construction aggregates. After petrographic evaluation of the aggregates along with the standard chemical tests, it was determined that the rate of accuracy in determining the aggregates reactivity was quite high in all cases. Therefore, Bragg (1995) created a separate numbering system that, for the experienced petrographer, allows for the initial evaluation of the aggregate's reactivity, thus providing a simple and effective method for construction aggregate assessment.

As a result, the initial petrographic examination of the aggregate is mainly a screening test whereby if it is believed that the aggregate will cause premature deterioration of the concrete, or is believed to be reactive, then the aggregate source should probably not be used. However, regular mechanical properties testing (Abrasion testing, Freeze-thaw, Micro-Deval, soundness, etc.), as well as the methods available for identification of reactive aggregate should be carried out to verify the results.

By identifying the aggregate to be used in the mix design, it is possible to determine what tests for chemical reactivity are relevant. If after some assessment the aggregate type is still unknown, the age of the structure and the amount, if any, ASR visible, may give some

indication as to the reactivity of the aggregate, thereby narrowing down selection. If in the end, the aggregate has not been correctly identified, or if deleterious features of the aggregate go unnoticed, then the testing procedure used may not necessarily be the optimum procedure to be used in the determination of the aggregate's reactivity. This may result in inconsistent laboratory expansions (Rodgers, 1990).

The geology of a particular aggregate may have varying degrees of reactivity due to the wide range of polymorphic forms the aggregate can undertake. For example, some rhyolites, even though they tend to be reactive and experimentation may find the aggregate to be reactive, may show signs of little or no reactivity during field performance. The amount and order in the crystal structure is also a major factor influencing the reactivity (Palmer (1978), Hobbs (1989)).

It is also very important that the aggregate sample be representative of that being placed in the field. However, even for samples taken by an experienced petrographer, the sample can never represent more than the batch from which it was taken. Also, as with most quarries, there may be localized areas of reactive material, which may or may not be observed within the sample (Hammersely, 1992).

Selective quarrying of aggregates that have proven to be non-reactive in the field is probably the most efficient control measure of ASR, in regard of aggregates selection and use. However, the reactivity of the aggregate depends on the construction conditions, and will

probably be different for differing conditions (Swamy, 1992).

2.3.3 The Availability of Moisture

The availability of moisture from the environment, or residual mix water in mass concrete, is probably the most important of the required elements since without, the gel cannot imbibe any moisture, and thus cannot expand.

Stark (1990) investigated the effect of relative humidity (RH) on mortars mixed according to ASTM C227, containing 0.92% Na_2O equivalent cement with a known non-reactive aggregate. After subjecting the mortar bars to specific tests, it was concluded that at a RH exceeding 80% referenced to 21 °C to 24 °C, expansive ASR continued.

Samples taken by Stark (1990) from pavement slabs located in California (CA), New Mexico (NM), Georgia (GA), and Illinois(IL) during the summer period when it had not rained for at least a week showed that in samples, regardless of climate, at depths greater than 5 centimetres, the RH exceeded 80%. Therefore, conditions conducive to ASR likely exist regardless of the time of year. Even though moisture may not have been obtained from climatic wetting, subsurface moisture can maintain the relatively high RH levels required, even after 50 years of being in service. Stark (1990) concludes that this is a good reason for incorporation of superplasticers, to decrease the water-cement ratio, in the mix design. The following figure, as determined by Stark (1990) represents the threshold RH level required for AAR expansion to occur.

Figure 3 - Threshold Level for Expansion to Occur (Stark, 1990)

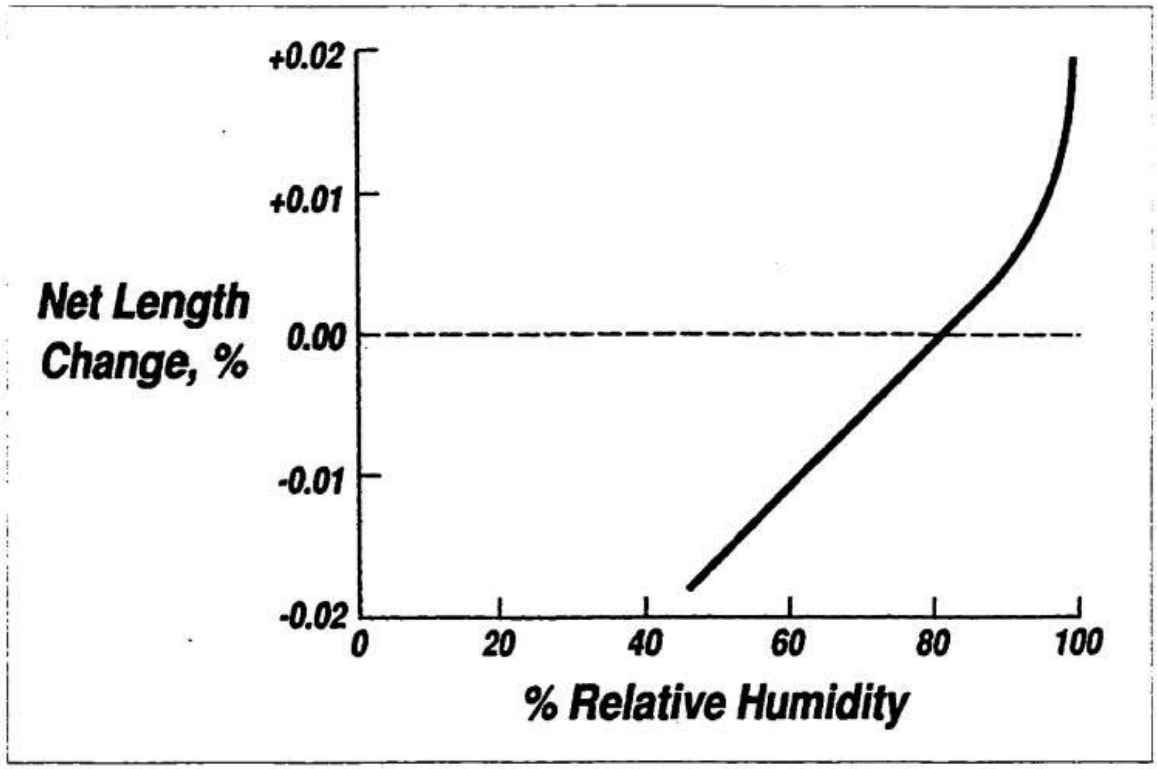

Many laboratory tests conducted by Arumugasaamy and Swamy (1978), Stark (1990) and Swamy (1995a, 1995b) have indicated that, even though there is usually enough residual mixing water to initiate an alkali-aggregate reaction, an external source is often necessary to sustain and accelerate the reactivity.

Swamy (1992) concluded from field and test data that the environment and the availability of moisture plays a very crucial role in the development of the rate of expansion and total expansion. For example, a particular concrete mass may have exhibited relatively low or no alkali-aggregate reaction at a certain age. However, as a result of the aforementioned

characteristics, favorable conditions may be provided whereby the reaction no longer remains dormant, but instead develops expansions that may become deleterious in the overall structural integrity. As a result, Swamy (1992) has added a fourth requirement, the environment / exposure conditions, in order for ASR to occur. From results of experimentation it is evident that variations in the local environmental conditions such as high temperatures, together with adequate availability of moisture (i.e. cyclic heating combined with wetting and drying), as well as the geometric configuration have a significant effect on whether a structure will crack and deteriorate due to an alkali-aggregate reaction (Swamy,1995a).

2.4 Additional Factors Influencing ASR

2.4.1 Applied or Induced Stress

Experimentation conducted by Clark (1990) , Hobbs (1989), Hobbs (1990), Jawed (1992), and Danay (1994) determined that applied or induced restraint can markedly decrease expansions of concrete specimens affected by ASR.

The following figures represent the effect of applied stress on the expansion of mortars subjected to a continuously applied stress (figure 4), and the expansion of mortars subjected to an applied stress after 112 days (figure 5). From the following figures it is quite clear that an applied stress of 0.35 N / mm^2 was sufficient in either reducing the expansion, or restricting further expansion.

Figure 4 - Behavior of mortars subjected continuously to an applied stress (Hobbs, 1989)

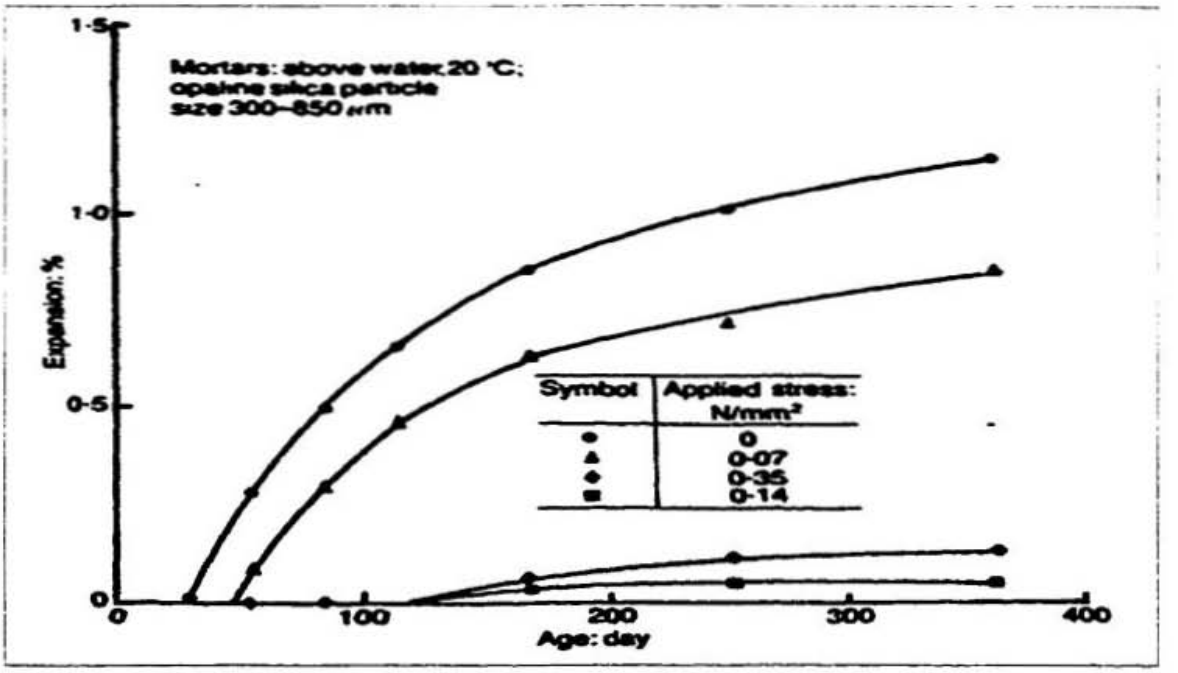

Figure 5 - Behavior of mortars subject to an applied stress at 112 days (Hobbs, 1989)

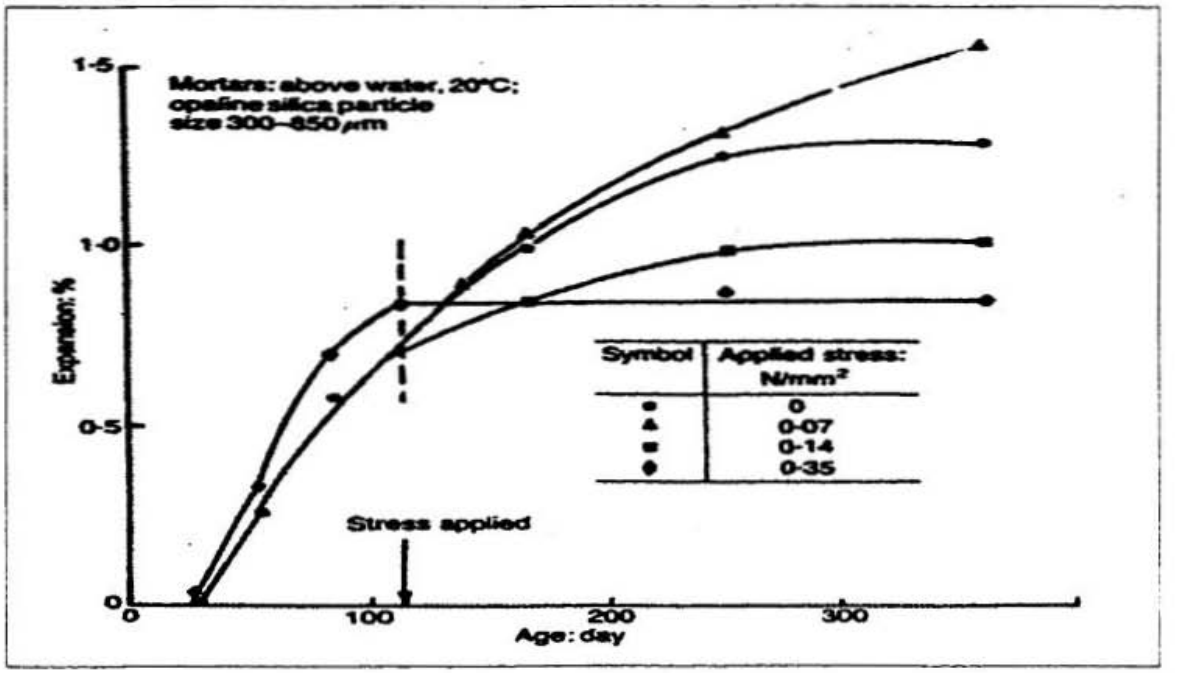

2.5 The Performance of Canadian Test Methods

The main purpose of the testing procedures are to identify potentially reactive aggregates that could cause abnormal expansion and cracking of concrete. There is no doubt that the most realistic and accurate way to assess the potential for ASR is by monitoring in-situ. However, this is often very time consuming as it may take several years for the structure to experience any type of reaction which can be quite costly, and often impossible given time restrictions.

The mortar bar test (ASTM C 227), the accelerated mortar bar test (NBRI, ASTM C9-P214), and the concrete prism test (CAN3-CSA A23.2-14A) are the most common and reliable testing methods for the identification of aggregate reactivity. In the past, correlation of results from different laboratories across Canada showed a coefficient of variation of 23% (Rodgers, 1990), however, new testing procedures were developed to bring the variation of results within 10%. This 10% variation can be attributed to the fact that many tests are sensitive to the testing procedures and any small variation that may take place by different technicians. In addition, there is always an component of subjectivity in carrying out the particular experiments and interpreting the results (Swamy, 1992). For example, expansions are affected by the storage conditions, temperature, and the environment in which the specimen is stored. Nonetheless, the 10% variation is considered adequate for universal comparison of results (Rodgers, 1990).

Expansions resulting from the Accelerated Mortar Bar test have been classified in the following manner. Expansions exceeding 0.15% at 14 days (in solution) are classified as

being potentially reactive. Experimentation conducted by Hooton (1992) proposed that expansions exceeding 0.33% at 28 days, and 0.48% at 56 days will cause the aggregate to also be classified as being potentially reactive. It is important to note that if the 28 day or the 56 days limit is not exceeded, whereas the 14 day expansion has been exceeded, the later test results will control in the rating of the aggregate.

Many other testing methods have been evaluated, however, they have not been accepted in North America. Several reasons why these other testing procedures have not been accepted include the fact that some of the tests are only applicable with highly reactive siliceous aggregates (Chatterji, 1989), other procedures do not have sufficient supporting evidence (Hooton, 1989), and some of the procedures may take longer than the NBRI testing methods, especially if slowly expanding aggregates are being used (Schmitt, 1989). The Duggan Test was also evaluated (Jones (1990), Heinz (1987)), however, it was determined that the measured expansions of the test cylinders had little to do with the reactivity of the aggregate, but instead with the SiO_3^- content of the cement.

Hooton and Rodgers (1989) evaluated all of the aforementioned tests and concluded that only the NBRI test was able to predict the reactivity of all aggregate samples evaluated. The Concrete Prism Test is also very reliable, however, due to the significantly larger amount of time required to obtain results, it is often not a practical alternative. As a result, the Accelerated Mortar Bar test is most commonly used since the reactivity of the aggregate can be obtained much faster than by the other testing methods. Presently, it takes 14 days to

conduct an accelerated mortar bar test, 6 months to conduct the mortar bar test, and 1 year to conduct the concrete prism test.

Shayan and Quick (1989) conducted research regarding the products of alkali-aggregate reactions using a known reactive aggregate. The aggregate was used in the concrete prism test, the accelerated mortar bar test, and was also found used in the field. From the experiments, it was concluded that the products formed were similar in all three cases, thereby demonstrating the accuracy of the different testing procedures. However, Vivian (1992) believed that the results obtained from accelerated testing at elevated temperatures should be interpreted with caution, as conditions experienced during the testing phase are much unlike that experienced in field conditions. As well, elevated temperatures may promote reactions that may not occur, or which proceed at very low rates at atmospheric temperatures.

2.6 Reducing ASR using Supplementary Cementing Materials

2.6.1 General

Most, if not all, researchers have concluded that it is impossible to be completely positive an alkali-aggregate reaction will not occur. However, research recently conducted as shown that certain additives can aid in minimizing the reaction. These include the use of a low alkali cement, the use of an aggregate proven to be non-reactive in the environment in which the structure is to be located, partial replacement of the cement by supplementary cementing materials (SCM's), as well as the use of chemical admixtures.

The extensive research conducted over the past few decades involving the use of SCM's and chemical admixtures can be attributed to several factors. Often it is the case that a non-reactive, high quality, aggregate source cannot always be found in close proximity to the construction site, and that cements containing varying degrees of Na_2O equivalent are very rarely easily accessible, especially as in Newfoundland.

Supplementary cementing materials enhance the pore structure, grain refinement, and thereby the permeability or water tightness of the mix which reduces the mobility of the aggressive agents. If used in the correct manner, and in the right proportions, supplementary cementing materials can help control strains and loss of engineering properties, but it cannot eliminate all deleterious effects (Swamy, 1992). However, some of the additives may contribute to the percentage of alkalis in the concrete which may increase the potential for alkali-aggregate reactivity.

The following is a brief overview of some of the more common mineral and chemical admixtures.

2.6.2 Mineral Admixtures

For the most part, it is believed that fly ash (i.e. pulverized fly ash (PFA)), blast furnace slag (BFS), condensed silica fume (CSF), and natural pozzolans are effective in controlling the deleterious expansions resulting from ASR. However, the effectiveness of the SCM depends on the chemical compositions of the cement, the percentage replacement, the mineralogy of

the aggregate, as well as the chemical composition and mineralogical aspects of the SCM itself.

Supplementary cementing materials help reduce the permeability of the mix, and thereby reduce the mobility of aggressive agents, and also provide additional calcium silicate hydrate which chemically "tie-up" alkalis in the concrete, thus lowering the pH of the pore water solution. However, determination of the optimum dosage is very important, and should be confirmed by experimentation. Laboratory investigations have shown that particular additives may increase the alkalinity of the concrete, thereby contributing to the reaction. Therefore, to prevent excessive expansion in the presence of potentially reactive aggregates, authorities in the field of alkali-aggregate reactivity suggest limiting the total available alkali content of concrete. Usually, 3 $kg/m^3$is often suggested as the limiting value, which should account for all the contributions from all the concrete components (cement, SCM, aggregates, mix water, chemical additives, etc.), provided the concrete is not exposed to external alkalis such as deicing salts, seawater, and brines (Duchesne (1994), Neville (1995)).

In addition ASTM - C441 and C-618 states that a mineral admixture is effective in reducing alkali-aggregate expansion if it is capable of reducing the control expansion at 14 days by 75%, and the reduced expansion is smaller than 0.02%" (Chen et al., 1990).

It must be remembered that these minerals are not added to the mix design solely for the purpose of controlling ASR. Several of the more common additives are investigated in the

following sections.

2.6.2.1 Fly Ash

Fly ash, a combustion by-product of carbon in thermal power stations, may have varying chemical compositions, depending on the coal used, and the combustion process. Fly ash influences the total hydroxyl ion concentration, setting time, entrapped air content, and strength development. In addition, the use of fly ash decreases the permeability of the concrete, increases the Modulus of Elasticity, and lowers the heat of hydration. However, the most important influence with respect to ASR is the effect on total available hydroxyl ion concentration as recommended by Hobbs (1989), and Rotter, (1995).

In some situations the replacement of cement with pulverized fly ash (PFA) (40% - 50% by mass) has proven successful in the reduction of the ASR (Chen et al. (1990), Alasali et al. (1990)). However, there has been pessimism as to the critical level of replacement of cement by PFA when the alkali content may increase (Hobbs, 1989). Research in this area is presently controversial due to the fact that the results are largely dependent on the methodology being used. Extensive testing and experimentation are required to draw definitive conclusions. Some of the more recent experimentation are reviewed in the following paragraphs.

Farbiarz et al. (1989) have conducted experimentation concerning the use of blended fly ash cement (IP cement) versus the use of fly ash added to the mix, and have concluded that the

blended mix is a more effective solution in controlling the expansion. At the present, it is thought that the reduction in reactivity is a result of the increased fineness of the IP cement.

Most of the other papers published concerning the use of fly ash as a preventative agent to ASR have concluded that the reaction is effectively controlled only when greater than 20% cement is replaced by fly ash. These papers include work by Okada (1989), Kawamura (1989), and Blackwell (1992). However, Kawamura et al. (1989) concluded that too little percentage of fly ash (approximately 5%) may in fact increase expansion. In addition, Blackwell et al. (1992) expresses the need for long term measurements of specimens that contain fly ash due to the fact that there are concerns the fly ash may be merely delaying the expansion by slowing down the diffusion of alkalis.

It is important to note that fly ash has been regularly used in concrete structures located in the United Kingdom, and to date none of these structures have reported damage due to ASR. However, since the actual role that fly ash plays in the development of the micro structural aspects of concrete, many researchers are still skeptical of its use (Thomas et al., 1992). Nonetheless, Thomas et al. (1992) investigated two mass concrete dams in the United Kingdom. Since only one of the structures contained fly ash it provided the means to determine if fly ash was effective in deterring the reaction. Visual examination, petrographic examination, along with testing of cores all indicated that partial replacement of cement with fly ash was effective as a means for suppressing ASR in field situations. In addition, recent research by Hooton (1989) on concrete containing a known reactive aggregate has shown that

a 30% replacement of the cement with fly ash was effective in preventing expansion for 30 years in a structure located in Ontario, Canada.

For concrete exposed to freeze-thaw conditions, ACI 318-89 limits the quantity of fly ash and other pozzolans to 25 % of the total cementitious material. At higher levels, excess deterioration is observed due to the increase in porosity of the cement paste (Neville, 1995).

2.6.2.2 Ground Granulated Blast Furnace Slag

Ground granulated blast furnace slag (GGBFS) is a non-metallic hydraulic by-product of the iron industry that consists mainly of silicates and calcium silico-aluminates, comparable to class C fly ash (Rotter, 1995). GGBFS is generally not used as an agent to control ASR, however, its ability to reduce expansions due to ASR is recognized worldwide (Rodgers (1990), Connell (1992), Sims (1992), Hobbs (1989)). However, Rodgers (1990) concluded that concrete made with significant amounts of BFS along with other supplementary materials tends to be more susceptible to freeze-thaw, especially in environments where deicer salts are used.

Connell (1992), and Sims (1992) state that 50% substitution levels are suitable to prevent expansion due to ASR if alkalis are not derived from other sources such as the supplementary cementing materials, or the cement itself. However, investigations using various laboratory salt-scaling tests (ASTM C 672) conducted by Rodgers (1990) indicated that at 50% substitution levels, the scaling loss from the surface became unacceptable. As a result, the

Ontario Ministry of Transportation now limits the substitution levels of BFS to a maximum level of 25% (Rodgers, 1990).

2.6.2.3 Silica Fume

Silica fume, a by-product of the silica and ferro-silicon industry, is often used in Portland Cements in Canada, but not necessarily for controlling ASR. They are most often used for advantages such as reduced cost, increased strength-producing properties, lower permeability, alkali dilution, portlandite consumption in the cement paste, alkali depletion in the pore solution due to the pozzolanic reaction, and lower heats of hydration (Rodgers (1986), Bérubé (1992)). Nonetheless, the silica readily reacts with the alkalis of the cement, causing the formation of a gel similar to that formed during the reaction between the alkalies and the silica of the reactive aggregate. However, due to the large surface area of the finely ground silica fume, the reaction does not result in expansion. Silica fume has been found to advantageous at percentages between 6% and 10% when using low water / cement ratios. (Neville, 1995).

Oberholster (1989) has conducted significant research regarding the use of silica fume as a reduction agent to ASR. Oberholster's experimentation (1989) has concluded a 5% replacement of cement with SF was not effective in reducing the expansion of concrete cubes which were stored in the outside environment. However, a 10% replacement was effective in 350 kg OPC mixes, but not with 450 kg OPC mixes (Hobbs, 1989).

Wang and Gillott (1992) determined that after ten months of testing specimens mortar bars containing 6 % and 12 % silica fume, the expansion was decreased by 20% and 40%, respectively. The silica fume also delayed the onset of the reaction which was attributed to the pozzolanic reaction which competes with the alkali-silica reaction for available alkalies.

2.6.3 Chemical Admixtures

The use of chemical admixtures to reduce the possibility of the occurrence of an alkali-aggregate reaction has been investigated throughout the past few years. While some of the results seem positive, many believe that minimization of the reaction can be more easily controlled by other means. The following presents a brief review of some experimentation involving the use of chemical admixtures in controlling ASR.

According to Jawed (1992) two types of chemical admixtures have been successful in suppression of ASR in highway structures. These include high molecular weight metacrylate treatments to pavements, and saline application to bridge slabs. In addition, Jawed (1992) states that lithium hydroxides have also proven to be useful in the mitigation of ASR with in-service structures.

Hudec and Labri (1989) have conducted experimentation with acidified calcium phosphate being added to both the aggregate (prior to its use) and the concrete. Their results have shown that the addition of this chemical has reduced the ASR expansion. Lithium salts have also been found to be effective in reducing the expansion due to ASR. Sakaguchi et al.

(1989) confirmed that the use of lithium salts, although very expensive, are quite effective in suppressing ASR. Nonetheless, there is a need for large scale in service experimentation to determine the true effectiveness of a chemical admixture with concrete.

2.7 Mechanical Properties of Concrete Affected by ASR

2.7.1 General

Since the commencement of research regarding ASR, most, if not all investigations have been concerned with how the reaction may effect the engineering properties of structural members. The following sections provide an extensive review of recently published literature.

2.7.2 Plain Concrete

2.7.2.1 General

The detrimental effects of ASR are much more pronounced in plain concrete, and under laboratory conditions. In addition, laboratory investigations involving unreinforced concrete affected by ASR have shown a markedly larger decreases in mechanical properties such as in direct and indirect tensile strength, modulus of rupture, modulus of elasticity, and dynamic modulus of elasticity, than with compressive strength.

However, losses in engineering properties do not all occur at the same rate or in proportion to the expansion undergone by ASR affected concrete (Swamy, 1988). "It is doubtful, therefore, if the same values of critical harmful expansive limits can be specified for all types of structures without regard to either their effect on engineering properties or the type of

reactive aggregate that gives rise to the rate of loss in these properties" (Swamy, 1988, p.372).

Most of the literature concerning ASR is derived from laboratory samples containing no reinforcement that have been conditioned under constant conditions that do not represent the actual field environment. Therefore, the results obtained are not directly useful to the design engineer (Swamy, 1988).

Clayton et al. (1990) discovered that cores taken from field samples affected by ASR showed approximately half the tensile strength loss of conditioned laboratory specimens. However, cores, upon removal of the three-dimensional restraint may exhibit expansion after removal, and decreases in strength and stiffness that is not indicative of the actual situation of the internal concrete. Therefore, actual in-service massive concrete may exhibit even lower reductions in strength. (Chana (1992), Clayton et al. (1990)).

Any strength test conducted on a specimen quantifies the performance of the material in relation to that method of test only and does not necessarily reflect the performance of the material in its structural context. Therefore, for structures subject to disruption, very little , if any reliance, should be placed on values obtained from any one test and that commonly accepted procedures, such as the cube crushing test, may not indicate the value to be used in a normal design check (Clayton et al., 1990). Therefore, in recent years, research is being carried out involving laboratory conditioned reinforced concrete or samples that have been in-service for a number of years to determine the structural implications of ASR. In this

manner, the results obtained will be more useful to the design engineer.

2.7.2.2 Compressive Strength

Compressive strength of concrete affected by ASR has been seen to decrease as damage due to ASR increases (Ono (1990), Clark (1990), Pleau et al. (1989), Swamy and Al-Asali (1988), and Hobbs (1989)). Even though the actual decrease in compressive strength may be as much as 65 % (Hobbs, 1989), the actual decrease is proportional to the expansion of the concrete, with a 20% reduction being common place for reactions that are likely to occur in practice (Rotter, 1995).

However, Swamy and Al-Asali (1988) determined that the compressive strength was not a good indicator of the onset of ASR, nor the progress of the reaction. However, due to the simplicity of the testing procedure, monitoring of compressive strength is often used in concrete monitoring.

2.7.2.3 Tensile Strength

At present, there is no CSA Standard developed for the determination of the direct tensile strength of concrete. In the past, the tensile strength has been assessed by an indirect tensile test, either being the splitting cylinder test or the indirect tension test involving concrete prisms.

When determining losses in tensile strength using the splitting cylinder test, reductions in

tensile strength of concrete usually do not exceed 40 % (Clark 1990). However, Swamy and Al-Asali (1988) determined that losses in tensile strength observed using the splitting tensile test for samples containing fused silica were approximately 65% when expansions of specimens were on the order of 6mm/m.

The ratio of compressive strength to tensile strength seems to be a good indicator of deterioration due to ASR, with the tensile strength being more sensitive with time (Swamy and Al-Asali 1988).

2.7.2.4 Pulse Velocity and Dynamic Modulus of Elasticity

A number of non-destructive tests (NDT) have been used to evaluate the properties of AAR affected concrete. For example, the use of pulse velocity and dynamic modulus techniques have been used to monitor the initial and progress of concrete deterioration, while resonance frequency methods have been used to monitor the effectiveness of mineral admixtures to contravene expansive strains (Swamy, 1995).

Results of the experimentation by Swamy (1995) indicate that both the pulse velocity and the dynamic modulus are highly affected by the presence of AAR. Swamy (1995) determined that as the percent expansion increases the percentage loss in the pulse velocity also increases, that the increase in the expansion substantially decreases the percentage loss in the dynamic modulus, and that these properties are significantly affected long before any deleterious expansion takes place (i.e. long before any cracks will become visible on the exterior of the

affected concrete). These results also indicate that the percentage in loss of the dynamic modulus is much larger than for the pulse velocity. This indicates that the effects of AAR are more critical on the stiffness of concrete rather than the effects of micro cracking (Swamy, 1995).

However, it is important to realize that the pulse velocity test is only a spot test (one small location on the structure at a time), and the pulse velocity relationships are exponential. Therefore, without special calibration, one cannot directly assess the overall strength of the structure. In order to obtain the true picture of the structural implications, continuous NDT monitoring of structures, and evaluation of cores for material damage and structural integrity is required.

2.7.2.5 Modulus of Elasticity

The Modulus of Elasticity of concrete is more sensitive to deterioration resulting from ASR than compressive or tensile strength (Habita et al. 1992; Swamy and Alasali 1988). Reports by the Institution of Structural Engineers (1988) have indicated that specimens become more ductile with increasing deterioration, thus decreasing the Modulus of Elasticity. Investigations by Habita et al. (1992), and Hobbs (1989) indicate that the Young's Modulus decreased in some specimens by approximately 40 to 50%. However, the actual decrease that will be experienced during any one series of tests is a direct function of the mix design constituents, storing conditions, and testing procedures.

2.8 Reinforced Concrete

A limited amount of research was initially conducted regarding the effects of ASR on reinforced and prestressed concrete beams. However, in the past few years, several investigations have taken place involving reinforced concrete elements that have been conditioned in a controlled environment, and with those that have been subjected to natural in-service conditions.

Swamy (1989) investigated the effects of ASR on beams involving an highly reactive, and less rapidly reactive aggregate. These beams, which were singly reinforced and contained shear links, were subjected to an environment that was favourable to ASR for a period of two years. During the conditioning period, the specimens were left unloaded while the time dependent strains were monitored at various locations throughout the depth of the beam. In addition, a control beam was also examined. The result obtained from the investigations can be observed in the following figures.

Figure 6 - Expansive Steel Strains in Beam with Highly Reactive Aggregate (Swamy, 1989)

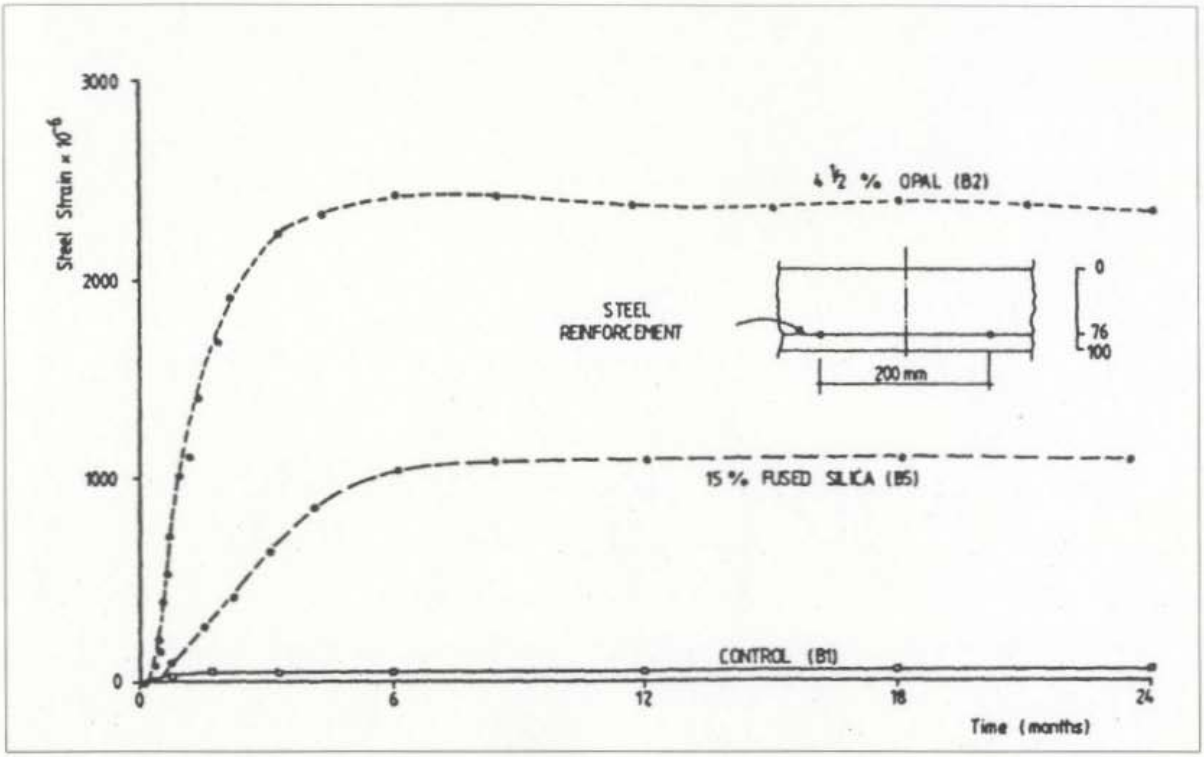

Figure 7 - Concrete Strains in Beam with Opal as Reactive Aggregate (Swamy, 1989)

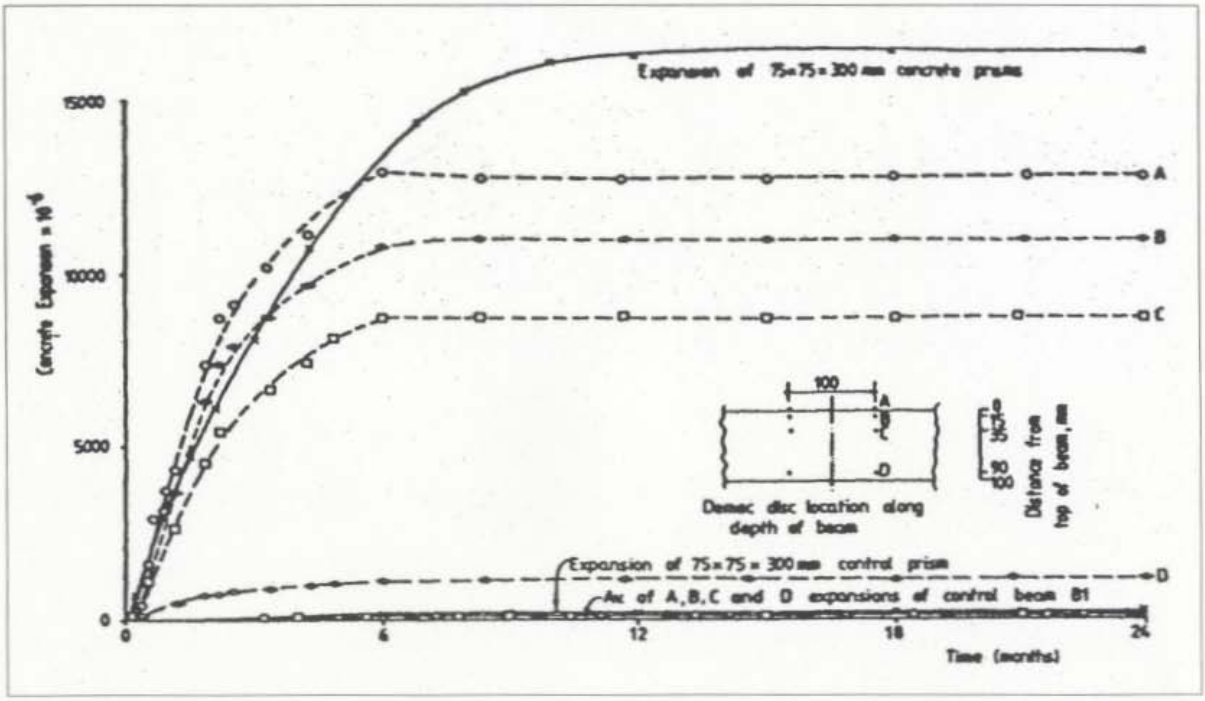

Figure 8 - Concrete Strains in Beam with Fused Silica as Reactive Aggregate (Swamy, 1989)

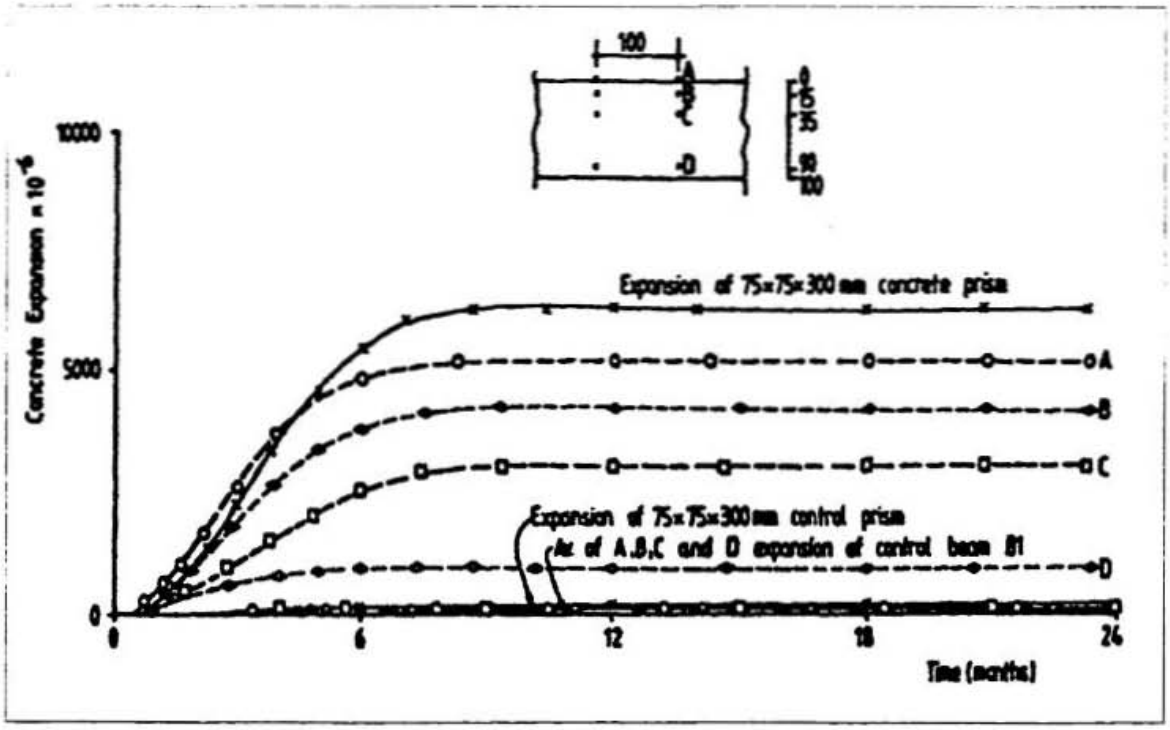

The beam containing the highly reactive aggregate (Figure 7), after a period of 6 months, produced strains of approximately 13,000$\mu\epsilon$ in the top fibre, while in the vicinity of the reinforcement, strains were reduced to approximately 1200$\mu\epsilon$. For the less rapidly reactive aggregate (Figure 8), after a conditioning period of 2 years, strains at the top fibre were recorded as being 5200$\mu\epsilon$, while strains in the area near the reinforcement were reduced to 850$\mu\epsilon$. From the preceding figures it can be seen that the difference in the induced strains over the depth of the beams is clearly influenced by the aggregate used, and the presence of reinforcement (Swamy, 1989).

In addition, the beams investigated by Swamy (1989) showed a certain degree of hogging which resulted from the tension face expansion being restrained by the reinforcement, while the compression face was left free to expand. "This induced prestressing condition will have a beneficial effect in enabling the beams to carry ultimate loads higher than would be expected otherwise. It is unlikely that a doubly reinforced beam would show similar hogging and prestressing effects; thus, while a well designed flexural member is unlikely to show serious structural deformations due to ASR in practice, it is unlikely to benefit from the favourable effects of the prestressing condition induced by hogging due to ASR" (Swamy, 1989, p.455). Nonetheless, the strains induced by ASR far exceed the tensile capacity of concrete used in practice. Therefore, the in-service concrete affected by ASR can definitely develop cracks that may cause serviceability problems and also initiate corrosion of reinforcement (Swamy, 1989).

Swamy (1989) upon testing the beams to failure while recording the load and deflection discovered that all beams affected by ASR showed a markedly larger decrease in the stiffness of the beams. However, the deflections recorded at failure did not show any additional sagging due to the beneficial effect of the hogging produced by the reaction. Furthermore, none of the beams showed any shear, bond, or anchorage distress prior to failure. The following figure represents the effect of hogging on the load-rotation of beams affected by ASR.

Figure 9 - Load Rotation curves of ASR-affected and control beams (Swamy, 1989)

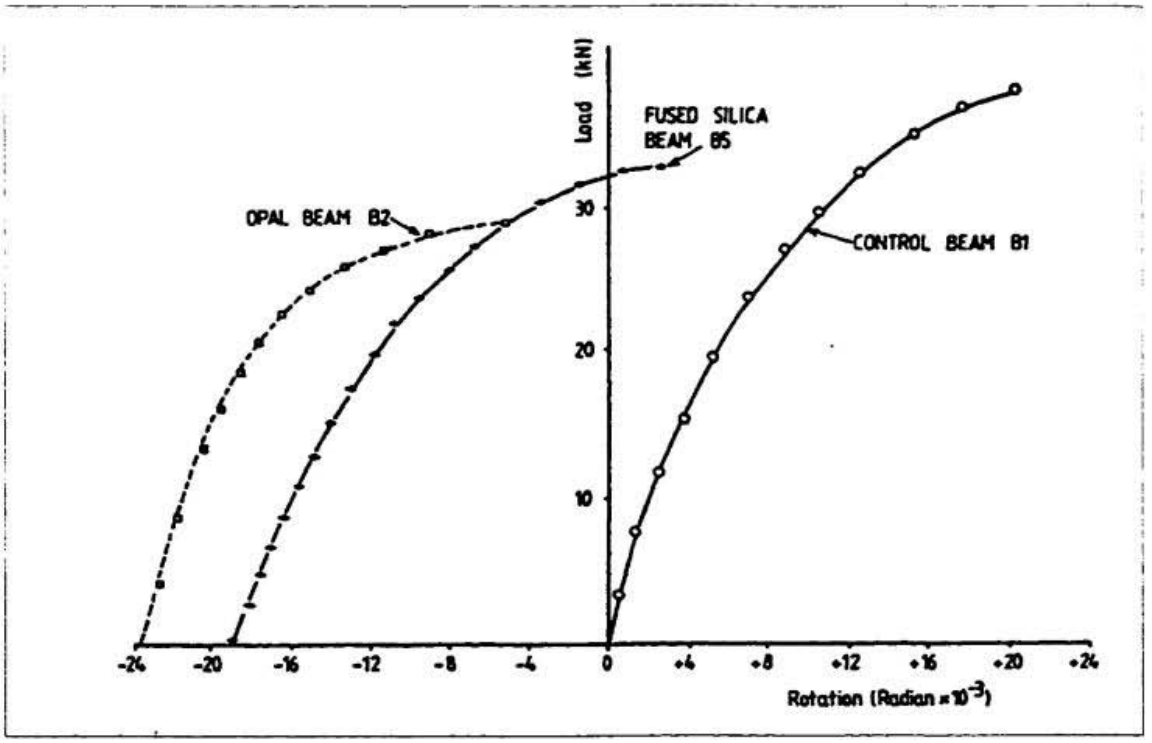

An assessment of seven in-service prestressed concrete bridges known to be suffering from alkali-aggregate reactivity was recently conducted in England to determine if there were possible problems with durability. Prior to testing, a visible examination of the specimens was administered. Each specimen showed the distinctive map-cracking along with hairline cracks of which some contained products of the reaction, however, no more than might be expected after 15 years of service (Turdoff, 1990). The results indicated that ASR cracking does not have a significant effect on the stiffness or strength of well reinforced and prestressed concrete members. In some of the tests the strength of the member actually increased relative to the control. (Turdoff, 1990). In addition, Turdoff (1990) observed that there was no loss

of concrete section, no unexpected deflection at midspan and that none of the cracking suggested structural distress. These factors indicated that the bending moment capacity of the beams has not been impaired. Research conducted in Denmark and England confirmed these results that while the strengths of unreinforced specimens were reduced, well reinforced concrete showed no adverse effects to ASR (Turdoff (1990), Koyangi et al. (1992), Clayton et al. (1990)). Most structures with visible evidence of ASR are under-reinforced and overstressed by today's design standards, and most structures that have undergone remedial work fall within this category (Wood, 1989).

In experiments conducted by Koyangi et al. (1992), the pulse velocity of specimens subjected to ASR was proportional to the reinforcement ratio. The dynamic modulus decreased as the reinforcement ratio decreased due to the lack of restriction to expansive forces of ASR (Koyangi et al, 1992). In addition, the surface cracking (map-cracking) that is often associated with ASR is modified by the presence of reinforcement. The additional reinforcement produces restraint of the expansion in the plane of the reinforced direction, thereby forcing the cracks to predominately follow parallel to the reinforcement (Clayton et al. (1990), Koyangi et al. (1992), Clayton et al. (1990)).

Investigations have also been conducted regarding the flexural strength of members affected by ASR with regard to the reinforcement ratio. Koyangi et al. (1992) discovered that although the flexural strength of members without reinforcement affected by ASR decreased by approximately 60%, the cracking load of ASR affected concrete exceeded the cracking

load of unaffected concrete when the reinforcement ratio was greater than 0.1%. In specimens where the reinforcement ratio exceeded 0.7%, the flexural capacity of ASR affected concrete was found to be greater than that of unaffected concrete at the same reinforcement ratio. Specimens tested with a reinforcement ratio exceeding 2% experienced loads nearly twice as large as the cracking loads of unaffected concrete. "This seems to be caused by the internal compressive stress which was induced as a reaction force by the retainment of expansion due to ASR by the reinforcement" (Koyangi et al., 1992, p.559).

Bach et al. (1992) conducted a series of tests with reactive aggregates using a 0.8% Na_2O equivalent cement in order to examine the effects of ASR on the shear strength on beams and slabs. From the experimentation, it was concluded even in beams without shear reinforcement, neither the shear strength, nor the punching shear strength was reduced even when serious ASR deterioration was visible. However, Chana et al. (1992) determined that for beams with no links and poor end anchorage (5 times the bar diameter, d_b, past the centre line of the support), the maximum shear strength decreased by 30% for plain bars, and 23% for ribbed bars. These reductions were considered to be modest for beams with poor anchorages. Clayton et al. (1990) investigated the effects of ASR on the shear capacity of prestressed concrete I-beams tested with added salts along with a reactive aggregate that was stored at 38 °C for a period of 5 months. Although the shear capacity was decreased by 20% when first cracking was observed, beams having shear reinforcement recovered this loss when the concrete continued to expand.

However, Habita et al. (1992) conducted several experiments in order to determine the expansive strains developed in reinforced concrete beams that were conditioned with NaOH in order to accelerate an alkali-aggregate reaction. Figure 10 represents the beam subjected to NaOH, as well as the strains developed from the reaction only. "These results show higher strain values in the central part of the beam compared with the lower and upper parts. The strain is therefore restrained by longitudinal rebars" (Habita et al., p.404, 1992).

As a result, in recent years, far more importance has been given to reinforcement detailing of concrete structures. Wood (1992) believes that people who detail their reinforcement for earthquake loading can be less concerned with ASR than those who live on a more stable geology.

Clark (1990) has investigated the effects of applied stress on specimens subjected to alkali-aggregate reactivity, as is similar to that found in the field. From the investigations, Clark (1990) determined that, under an applied load, the specimens showed and increase in the stiffness, resistance to cracking, and shear resistance. For concrete, it was determined that a compressive stress of 1 - 4 MPa is required to prevent expansion due to ASR. In the field, compressive or restrictive stresses of this magnitude are almost inherent in every part of a structure. In addition, this emphasizes the need for dead load simulation in ASR models, otherwise, expansions may be substantially overestimated.

Figure 10 - X section of Beam Strains Resulting from ASR (Habita et al., 1992)

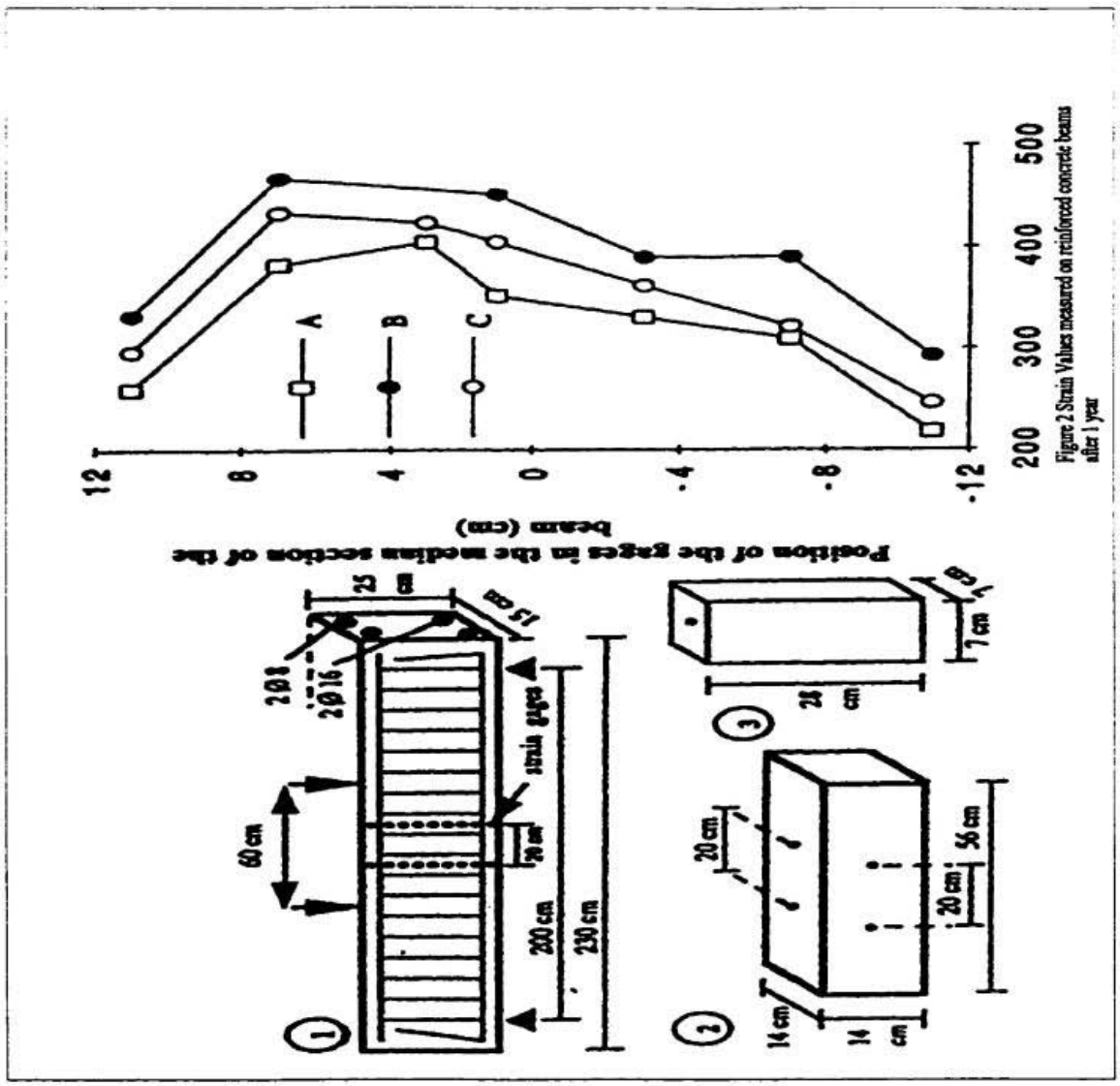

2.9 Concrete and the Marine Environment

Concrete exposed to the marine environment is subjected to various chemical and physical processes which can substantially decrease its useful life. For example, abrasion by ice, sand, or water, along with the ingress of sodium ions which increase the alkali content, chloride ions which may corrode the reinforcement, and freeze-thaw can affect the structural integrity of the concrete to the point where premature failure may be possible (Neville (1995), Mehta (1988)).

Concrete that is continuously submerged in sea water is not at the same level of risk to deterioration as to concrete located in the splash zone. Concrete continually immersed in water is unlikely to show large expansions because, although water is readily available for absorption by ASR gel, this is counteracted by the loss of alkalis through leaching (Swamy (1994), Stark (1990)). However, when concrete is exposed to alternating wetting and drying cycles, salts build up in the mix due to the evaporation of pore water. Alternating cycles of wetting and drying thus enhance ASR, and thereby induces micro cracking in the external faces of the structure. Davies and Oberholster (1989) conducted experimentation which has shown that concrete exposed to the application of sea spray experienced expansions much greater than concrete which is submerged.

Concrete exposed to the marine environments must be very durable. The conditions to which the concrete are exposed are such that problem areas are not easily accessible for remedial work, and as a result can be quite expensive. Therefore, it is often the case that stringent

regulations are implemented during the construction phase so that the end product is as free from flaws as possible. It is the goal to produce a resulting concrete that is maintenance free throughout the service life of the structure, which may be between 50 and 70 years.

In concrete structures exposed to the marine environment, the permeability is the most important factor affecting the long-time durability. In order to ensure the durability of such concrete, Mehta (1988) proposes that the following conditions must be met. These include using a concrete mixture that will almost become impermeable upon curing (as in an high strength concrete), to adopt a good concrete practice (excellent quality assurance and quality control techniques), and to take measures to prevent excessive concrete cracking in service.

Mehta (1988) has confirmed again that the interaction of seawater and the constituents of normal strength hydrated cements can have deleterious reactions such as carbonation, sulfate attack, and magnesium ion attack. However, when high strength concrete are used (60 MPa or higher, such as often used in offshore concrete structures) the permeabilities are often of a lower rate ($<10^{-14}$ kg/MPa. m.s.) that the otherwise destructive reactions are combatted. High strength concretes (HSC) have a greater cement content (>400 kg/m^3), a very low water cement ratio (max. 0.40), a high quality coarse aggregate (max. 20mm), a water reducing agent (usually a superplasticer), a mineral admixture (usually silica fume), and an air-entraining agent to aid in the protection against frost attack. It is the result of the preceding constituents that HSC has improved micro structures which provide for the larger increases in strength and durability, and thus is likely to be less susceptible to ASR.

2.10 Assessment and Rehabilitation of ASR Affected Structures

Diagnostic methods for the assessment of ASR in concrete structures include visual inspections, measurement of crack widths, ultrasonic pulse velocity measurements, coring and evaluation of residual strength and expansion potential of cores from structures, and load tests on the structures, and petrographic examination. However, these procedures are often very expensive and time consuming, and rarely, if ever, occur until severe visible signs of ASR are observed during regular field maintenance operations.

Alkali-aggregate reactivity is usually first noticed on large exposed surfaces such as end blocks on bridges, retaining walls, or dams. The "map-cracking" observed on large exposed surfaces such as end blocks, retaining walls, or dams is mainly caused by high stresses due to shrinkage and temperature gradients quite early in the life of the structure. As a result, other deleterious agents such as freeze-thaw, and the ingress of moisture and other deleterious ions, can begin to augment the reaction, and cause premature deterioration of the structure. Sometimes it may be difficult to determine if the cracking in the structure is only the result of ASR or if other external forces have been the major contributor. Therefore, in order to be sure that a reaction has taken place it is necessary to look for aggregates that have been surrounded by reaction rims, or aggregates that have been split into several pieces by the expansive gel. The effects will be more noticeable if the structure is located in a marine environment or if deicing salts are frequently used (Swamy, 1992).

Many believe that cracks generated by ASR should be injected with epoxy resin so as to prevent the ingress of any additional contaminants. However, gels formed by ASR have a natural tendency to resist external attack, and resisting the further expansion of the gel may increase internal pressures within the concrete, and result in the increase in crack widths. Therefore, it is believed to be more suitable to fill existing cracks with a flexible product so as to allow the gel formed to expand if suitable conditions exist (Turdoff, 1990).

In order to control the damaging effects ASR can have on the structure, one must be sure of the visible signs of ASR, the internal characteristics as a result of the ASR, and also realize the structural implications that may result in the future. Swamy (1995) also states that the limitations of all testing procedures must be known, as well as the implications of the subsequent results. Unless the examiner is sure of what is being examined (eg. aggregate type, environmental conditions, etc.) the resulting rehabilitation may not be effective, or only provide short term relief of the problem.

Another major concern of ASR and structural integrity of the system results from the fact that ASR forces are expansive, and these expansive forces are superimposed on areas that have already been stressed or cracked. The end result is that additional stresses are induced on the concrete and steel embedded in the structure (Swamy, 1995). It is also known that while structural design techniques can restrict expansion, it cannot counteract the effects of alkali-aggregate expansion, nor can the expansion be completely controlled by jointing. However, even if the induced stresses are high, it is very unlikely, almost impossible that the system

will experience immediate failure as a result of ASR alone. Nonetheless, as a result of the reaction, other deleterious elements may cause deterioration to the system which may affect the overall safety and stability of the structure (Swamy, 1992).

2.11 Analytical Models

2.11.1 General

Extensive physio-chemical research regarding ASR during the past few decades, has resulted in several researchers exploring the use of finite element and numerical techniques to model the effects of the reaction on field structures (Diab and Prin (1992), Goltermann (1994), Leger et al. (1990), Nielsen et al. (1993), May et al. (1992), etc.). However, due to the fact that most of the research available has been conducted on unreinforced specimens, the characterization of the reaction is so complex, and the numerous other factors involved, many of the models have been regarded as being too simplistic, and thus not especially useful to the design engineer.

The majority of the problems associated with modelling field distress from laboratory condition samples can be explained by the following. The gel formed from ASR behaves as a mobile viscous fluid which is dependent on temperature and on the proportion of the chemical constituents. The rate of flow of the gel is dependent on pressure, viscosity, and size of the conduit. However, with accelerated testing techniques, the conditions created in the laboratory are very dissimilar to those found for structures in service. Most laboratory testing is conducted with specimens held under constant temperature, with either the addition

of alkalis to the mix or either the specimens being submerged in a solution bath, as well as being left unloaded until the reaction has been well advanced, and then loaded within a period of minutes to failure. Therefore, since the parameters determined from laboratory testing are not applicable to field situations, the parameters determined are also not a good indication of those found in field structures.

Micromodels focus on the physio-chemical principles of ASR reaction kinetics. However, the link between the physio-chemical principles, and the resulting expansion is made by way of many simplifying assumptions regarding the external environment (the effects of restraints, external climate, loading, etc.) and thus are less attractive for use in civil engineering applications. Most of the micromodels, as seen in Table 1, do involve thermodynamics of irreversible processes, and are often very mathematically intense (Rotter, 1995)

Macromodels focus on structural level parameters, and have been developed in an attempt to provide a useful tool to the design engineer. Most of the models follow simple empirical rules which relate expansions to local environmental factors such as humidity, temperature, etc. In addition, these models are based upon in-situ measurements which allow for estimated assessments of future durability, serviceability, and safety without becoming concerned with the underlying chemical processes. Several macromodels that have been recently developed can be seen in Table 2.

Table 1: Micromodels Developed for ASR Modelling (Rotter, 1995)

	Seiller et al. (1994)	Furusawa et al. (1994)	Hobbs I (1981)	Hobbs II (1993)	Neilsen et al. (1993)
Model Type	Local probabilistic model	Diffusion model	Chemical knietics model	Chemical kinetics model	Spherical cell damage model
AAR Expansion	Fraction of volume occupied by cracks	Porportional to gel quantity exceeding absorption capacity of pores	Porportional to gel volume increase after critical time threshold	Porportional to gel volume increase after critical time threshold	Calculated from strain tensor
Chemical process	Chemical balance by Dent Glasser and Kataoka (1981a)	n / a	Chemical rate equations for two stage ASR process	Chemical rate equations for ASR single stage process	n / a
Temperature	n / a	Arrhenius law of diffusion coefficient	n / a	Empirical temperature history function	n / a
Moisture	n / a	n / a	n / a	n / a	Coupling to FE moisture Calculation, multilinear expansion-humidity relationship
Random Distribution of reactive sites	Presence probability defined as concentration average over volume elements	n / a	n / a	n / a	n / a
Grain Size Distribution	Monte Carlo simulation	Summation over all grain size fractions	n / a	n / a	n / a
Diffusion of ions into reactive grain	Equivalent diffusion constant	Simplified Fick's equation, diffusion characteristic of aggregates determined by leaching tests (ASTM C-289)	n / a	n / a	n / a
Diffussion of ions within concrete	Combination of chemical balance and Fick Equation solution	n / a	n / a	n / a	n / a
Pressure exerted by gel	Capillary pressure equation combined with pore size distribution	n / a	n / a	n / a	Input value estimated from pressures necessary for pop out formation
Applied / Induced Stress, reinforcement	Induced Stresses	n / a	n / a	n / a	Applied and induced stresses derived from spherical shell model with internal pressure

continued ...	Seiller et al. (1994)	Furusawa et al. (1994)	Hobbs I (1981)	Hobbs II (1993)	Neilsen et al. (1993)
Cracks/damage due to AAR	Scalar damage variable, classical energy based crack propagation criterion	n / a	n / a	n / a	Matrix tensile strength permits calculation of radial crack extensions
Time Implementation	time step iteration	time step iteration	analytical dependance (kinetics equations)	analytical dependance (kinetics equations)	No explicit time implementation

Note: n/a in the above table indicates that the corresponding feature is not taken into account

Table 2: Macromodels Developed for ASR Modelling (Rotter, 1995)

	Cervera et al. (1994)	Mounzer et al. (1993)	Charlwood et al. (1992)	Courtier (1990)	May et al. (1992)	Castro et al. (1991)	Kladek et al. (1995)
Model Type	Nonlinear FE Model	FE-model using CTMR-rule	Restrained Expansion Calculation	Restrained Expansion Calculation	Restrained Expansion Calculation	FE-model using identification techniques	Elasto-plastic FE model
AAR Expansion	governed by water pressure	equals maximum expansion encountered in the structure modulated with CTMR-function	Linear relationship between log (stress) and restrained expansion	Linear stress-restrained expansion relationship, line slope related to reinforcement percentage	Differential equation relating restrained expansion to free expansion with linear solution	in-situ measured values for model calibration, calculated behaviour obtained by minimizing error function containing temperature and expansion distribution	in-situ measurement used for estimation of the model parameters
Chemical process	n/a	Approximated by normalized expansion factor, F_R, relating reactivity and expansion	n/a	n/a	n/a	n/a	n/a
Temperature	taken into account	Normalized expansion factor, F_T, relating temperature and expansion bilinearly	n/a	n/a	n/a	nonlinearity introduced by temperature dependant sensitivity matrix I.	n/a
Moisture	water enters structure only through cracks	Normalized expansion factor, F_M, relating expansion and moisture bilinearly	n/a	n/a	n/a	n/a	n/a
Random Distribution of reactive sites	n/a	n/a	n/a	n/a	n/a	n/a	n/a
Grain Size Distribution	n/a	n/a	n/a	n/a	n/a	n/a	n/a
Diffusion of ions into reactive grain	n/a	n/a	n/a	n/a	n/a	n/a	n/a
Diffusion of ions within concrete	n/a	n/a	n/a	n/a	n/a	n/a	n/a
Pressure exerted by gel	n/a	n/a	n/a	n/a	n/a	n/a	n/a

continued ...	Cervera et al. (1994)	Mounzer et al. (1993)	Charlwood et al. (1992)	Courtier (1990)	May et al. (1992)	Castro et al. (1991)	Kladek et al. (1995)
Applied / Induced Stresses, reinforcement	Applied and induced stresses	Applied and induced stresses, logarithmic stress-expansion relationship by Charlwood (1992), F_c	Applied or induced stresses, FE - implementation	Applied or induced stresses, FE - implementation	Applied or induced stresses, FE - implementation, non-linear stress-strain curves can be used (incremental technique)	Applied and induced stresses	Applied and induced stresses
Cracks/damage due to AAR	tensile criterion for principal stresses	Nonlinear FE Analysis	n/a	n/a	n/a	n/a	Scalar damage parameter calculated from the stress deviator invariants
Time Implementation	time step technique	Use of time dependant temperature distributions	No explicit time implementation	No explicit time implementation	No explicit time implementation	time steps	time steps

Note: n/a in the above table indicates that the corresponding feature is not taken into account

3.0 Experimental Investigation

3.1 Introduction

This chapter summarizes the procedure used in the determination of the aggregate sources to be used in the study, as well as mix designs, the testing procedures and methods of data acquisition carried out on the different specimens.

3.2 Petrographic Examination

Initially, before the experimental phase of the project could commence, the aggregate sources for the study had to be chosen. It was realized that the experimental testing could be much more easily carried out if the material suitable for the testing could be obtained from local concrete ready mix plants. Otherwise, all of the fine and coarse aggregates would have to be manually crushed which would be too labour intensive. Therefore, samples of fine aggregate were obtained from 7 different ready mix suppliers and tested according to ASTM C295.

Petrographic examination is an initial screening process by which the potential reactivity of an aggregate source may be assessed. As well, the petrographic examination is used to determine the composition of the aggregate, and if it contains specific minerals or rocks that have been known to be reactive in concrete, the aggregate may be rejected.

Petrographic analysis uses microscopic techniques described in CSA Test Method A23.2-23C. Some of the items that can be reviewed by a petrographic examination include paste, cement type, micro cracks, porosity, gel, aggregate, supplementary cementing materials, alkali-aggregate reactivity, and several other aspects.

Engineering judgement and geological knowledge is needed when interpreting the results of a petrographic analysis. Caution must be exercised due to the variability in the tests, and the difficulties encountered in the interpretation of the results when not carried out by an experienced researcher.

In addition to the composition of the aggregate samples, a rating system, based on the petrographic analysis as established by the American Society for Testing and Materials (ASTM), and the Ontario Ministry of Transportation (MTO), was used. This rating system was expanded recently in Newfoundland by Bragg (1995). In completing this new rating system, 7100 samples were examined over a 15 year period, and of those, 600 were used in the formation this approach. This rating system allows the experienced petrographer to assess the potential of the aggregate to be involved in an alkali-aggregate reaction. It should be

noted that this particular test method is not yet adopted by the Canadian Standards Association. However, it was used as an aid in determining potential alkali-aggregate reactivity of the samples collected. The petrographic examination of the aggregate sources are contained in Table 3.

Table 3 - Petrographic Analysis of Aggregate Samples

Aggregate Source	Composition	% per Sample	Petrographic Rating
Sample A	Granite Diorite Siltstone	35 50 15	FAIR
Sample B	Granite Sandstone Basalt Felsic Tuff	75 15 5 5	LOW
Sample C	Greywacke Siltstone Diorite Mafic Volcanic (Basalt)	60 25 5 10	HIGH
Sample D	Green Siltstone Red Siltstone	98 2	HIGH
Sample E	Granite Sandstone Diorite Basalt Rhyolite Tuff	50 25 5 10 5 5	HIGH
Sample F	Gabbro Granite Diorite Micaceous Sandstone Mafic Volcanics Felsic Volcanics	40 5 15 20 15 5	FAIR TO LOW
Sample G	Limestone	100 %	VERY LOW

3.3 Accelerated Mortar Bar Testing

After the initial assessment of the aggregate sources by petrographic examination, an Accelerated Mortar Bar Test (CSA A23.2-25A) was conducted on each sample in order to substantiate its potential reactivity. This particular testing procedure was chosen due to the fact that the test procedure can be carried out in 14 days, whereas, as previously stated, other applicable testing procedures required a much longer testing time. The results for each sample after 14 days are given in the following table.

Table 4 - A.M.B. Rating of the Different Ready Mix Suppliers

Aggregate Sample	A.M.B. Rating
Sample A	0.081 %
Sample B	0.081 %
Sample C	0.366 %
Sample D	0.298 %
Sample E	0.502 %
Sample F	0.164 %

As previously stated, expansions exceeding 0.15% at 14 days, 0.33% at 28 days, and 0.48% at 56 days will cause the aggregate to be classified as being potentially reactive. It is important to note that the Accelerated Mortar Bar Test results are normally not used as a basis for aggregate acceptance or rejection without first determining its expansivity in the concrete prism test. However, once again, time did not permit such testing, and therefore, the appropriate aggregates were chosen based on AMB rating only.

It was initially hoped to conduct the testing regime on a highly reactive, moderately reactive, and non-reactive aggregate. The potentially non - reactive aggregate was Sample G, the potentially marginally reactive aggregate was Sample B, and the potentially reactive aggregate was Sample E. However, on arriving at the non-reactive source, it was determined that the fine aggregate did not have the gradation required. Therefore, it would have been necessary to pulverize the required amount of sample to the correct gradation at Memorial University of Newfoundland. This proved to be too labour intensive, and therefore it was dismissed. The experiments were conducted without the non-reactive aggregate.

It was ensured that the fine and coarse aggregate be from the same source, thereby, having the same reactivity.

3.4 Concrete Aggregates

3.4.1 General

In addition to the determination of a potentially moderately reactive aggregate, as well as a potentially highly reactive aggregate, the properties of the aggregate sources had to be determined. Since fine and coarse aggregate usually represent 70% to 85% of the concrete's mass, it was important to ensure that both sources were of similar quality. Both aggregate sources were tested in order to determine the various properties of the aggregates. These tests and the results are contained in the following table as conducted at the Provincial Department of Works, Services, and Transportation.

Table 5 - Results of Aggregate Testing (Sample E - Potentially High Reactivity)

Description of Test	*Test Method*	*Result*	*Unit*	*Specified Minimum*	*Specified Maximum*
Los Angeles Abrasion	*CSA A23.2 - 16A*	*18.1*	*%*		*35 (50)*
Absorption					
Fine Aggregate	*CSA A23.2 - 6A*	*0.160*	*%*		
Coarse Aggregate	*CSA A23.2 - 12A*	*0.524*			
Bulk Specific Gravity O.D.					
Fine aggregate	*CSA A23.2 - 6A*	*2.632*			
Coarse Aggregate	*CSA A23.2 - 12A*	*2.606*			
Petrographic Number	*CSA A23.2 - 15A*	*121.3*			*135 (Agg.)*
Material Finer than 80μm					
Fine Aggregate	*CSA A23.2 - 5A*	*5.3*	*%*		
Coarse Aggregate		*1.2*			
Fineness Modulus		*2.638*			*3.1*
Freezing and Thawing	*CSA A23.2 - 24A*	*1.284*	*%*		*6 %*
Accelerated Mortar Bar Test	*CSA A23.2 - 25A*	*0.081*	*%*		*0.15 % (14 d)*
Micro Deval - Fine Aggregate	*CSA A23.2 - 23A*	*5.28*	*%*		*20 %*
Micro Deval - Coarse Aggregate	*MTO (Draft)*	*2.65*	*%*		

Table 6 - Results of Aggregate Testing (Sample B - Potentially Marginal Reactivity)

Description of Test	*Test Method*	*Result*	*Unit*	*Specified Minimum*	*Specified Maximum*
Los Angeles Abrasion	*CSA A23.2 - 16A*	*16.6*	*%*		*35 (50)*
Absorption					
Fine Aggregate	*CSA A23.2 - 6A*	*0.766*	*%*		
Coarse Aggregate	*CSA A23.2 - 12A*	*0.664*			
Bulk Specific Gravity O.D.					
Fine aggregate	*CSA A23.2 - 6A*	*2.677*			
Coarse Aggregate	*CSA A23.2 - 12A*	*2.691*			
Petrographic Number	*CSA A23.2 - 15A*	*114.5*			*135 (Agg.)*
Material Finer than 80μm					
Fine Aggregate	*CSA A23.2 - 5A*	*2.7*	*%*		
Coarse Aggregate		*0.5*			
Fineness Modulus		*2.75*			*3.1*
Freezing and Thawing	*CSA A23.2 - 24A*	*1.49*	*%*		*6 %*
Accelerated Mortar Bar Test	*CSA A23.2 - 25A*	*0.502*	*%*		*0.15 % (14 d)*
Micro Deval - Fine Aggregate	*CSA A23.2 - 23A*	*7.64*	*%*		*20 %*
Micro Deval - Coarse Aggregate	*MTO (Draft)*	*4.6*	*%*		

After determining that both aggregate sources were satisfactory for the study, and obtaining the required amount of sample from each supplier, it was necessary to guarantee that both coarse and fine aggregate samples have the same gradation, to provide uniformity in the testing regime. A sieve analysis was conducted on both samples, with the different aggregate

sizes being separated in individual bins. The grading of the coarse aggregate samples, for both the normal and high strength mix designs is as follows:

Table 7 - Coarse Aggregate Gradation

Sieve Opening	Percent of Total Required Mass
19.5 mm	50 %
9.5 mm	35%
4.75 mm	15%

To ensure that both coarse aggregate samples were free of silts, coatings of clay, or other fine materials that may affect the hydration and bond of the cementing material paste, both samples were 'hand-washed' and air-dried.

3.4.2 Aggregate Geology

The geology of Newfoundland is complex and is best illustrated with reference Figure 11, as complied by Hayes (1990). In Eastern Newfoundland the geology is composed mainly of sedimentary and volcanic rocks with sporadic occurrences of granitic rocks. In Central Newfoundland, volcanic, sedimentary and granitic rocks with some occurrences of metamorphic rocks and ultramafic rocks are found to be common place.

The geology of the Avalon Peninsula, where alkali-aggregate reactivity is most severe, consists of Precambrian-Cambrian sedimentary rocks (shale, siltstone, argillite, sandstone, and conglomerate), extrusive igneous volcanic rocks (basalt, rhyolite, andesite, and their

associated tuffs), and intrusive igneous plutonic rocks (granite, diorite, and gabbro). The rocks on the Avalon Peninsula which have proven to be show alkali-aggregate reactivity are siliceous siltstone, argillites, sandstones, rhyolite, andesite, and their associated tuffs (Bragg, 1995). Referring to Figure 11, these rock types are of the Conception, Harbour Main, and Connecting Point groups, as well as the Bull Arm Formation.

Figure 11 - Newfoundland Geological Map (compiled by Hayes, 1990)

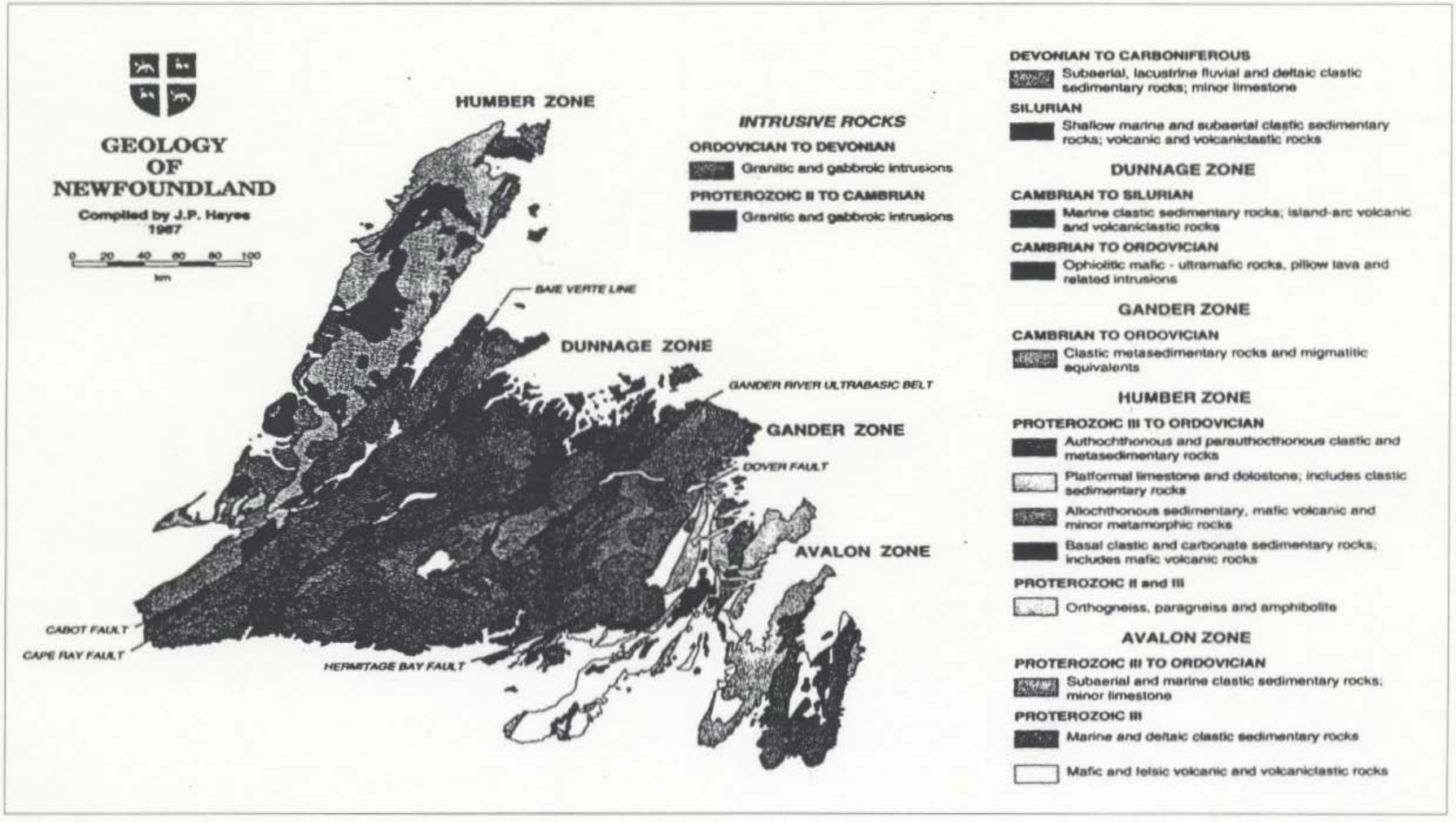

The reactive rocks of the Conception Group consist of siliceous siltstone, argillite, and sandstone, while the reactive rocks of the Harbour Main Group consist of rhyolite, andesite, and their associated tuffs. The reactive rocks of the Connecting Point Group consist of siliceous siltstone and sandstones, while reactive rocks from the Bull Arm Formation are known to be rhyolite, and their associated tuffs.

The two aggregate sources investigated were chosen based on their potential for alkali-aggregate reactivity. The two sites were gravel deposits on the Avalon Peninsula, the potentially marginally reactive aggregate being located in the Western Avalon Region, while the potentially reactive aggregate being located in the Eastern Avalon region.

The Eastern Avalon sample consists of granite, sandstone, basalt, and felsic tuff. The sandstone and the felsic tuffs are the reactive constituents of this sample.

The Western Avalon sample consists of granite, sandstone, diorite, basalt, rhyolite, and rhyolitic tuffs. The reactive constituents of this sample are the rhyolite, and the associated tuffs.

3.5 Mix Designs

For both the normal and high strength mixes, extreme care was taken to ensure that the aggregate sources were the only variation in mix design constituents. The following table

outlines the normal and high strength mix designs used in the experimental phase of the thesis.

Table 8 - Normal and High Strength Mix Designs (per 0.1 m^3)

Constituent	Normal Strength	High Strength
Cement	35.5 kg	45.0 kg
Fine aggregate	79.0 kg	65.0 kg
Coarse Aggregate	104.0 kg	107.0 kg
Water	16.1 litres	15.4 litres
Superplasticer	111.0 ml	550.0 ml
Air-entraining agent	18.0 ml	
Silica Fume		6.0 kg
Retarder		230 ml
Water / Cement Ratio	0.45	0.342
Slump	95 mm	180 mm
Air %	7 %	1.8 %
Density	2300 kg / m^3	2410 kg / m^3

In the mix, the ordinary portland cement (Type 10) CSA3-A55 with modified C3A content of approximately 6% as produced in Newfoundland, was used. The following table contains the portland cement constituents as provided by North Star Cement.

Table 9 - Cement Test Report (courtesy of North Star Cement, 1998)

Chemical	
Loss of Ignition (LOI)	3.39 %
Sulphur (SO_3)	4.15 %
C_3A	6.83 %
Silica (SiO_2)	20.28 %
Iron (Fe_2O_3)	3.18 %
Alumina (Al_2O_3)	4.61 %
Total Calcium	61.41 %
Free Calcium	1.15 %
Magnesium (MgO)	3.44 %
Total Alkalies (Na_2O equiv.)	1.05 %
Physical	
Blaine	415 m^2 / kg
Fineness (45 μ)	97.5 % pass
Autoclave	0.26 %
Sulphate Expansion	0.004 %
Initial Setting Time	145 minutes

For the mix designs, the air-entraining agent used was a neutralized vinsol resin, a water reducing agent was of a polyhydroxycarboxylic base. A superplasticizer of sulfonated naphthalene formaldehyde base was also included in the mix to yield desirable concrete workability.

3.6 Testing Regime

3.6.1 General

Due to the fact that the effects of AAR on concrete in Newfoundland have not been throughly investigated, it was decided to test most of the mechanical properties of concrete. The following section briefly describes the testing procedures.

3.6.2 Compression Testing

3.6.2.1 General

This method determines the compressive strength of the specimen according to ASTM C39 - 86. All cylinders were loaded to failure at the same loading rate.

The compression cylinders used in the experimentation were 76.2 mm x 152.4 mm. The size of the specimens was kept small due to the fact that larger cylinders would have required a substantially larger amount of concrete, and thereby were not feasible. However, during the 28 day testing, an additional three 152.4mm x 304.8 mm cylinders were tested and compared with the smaller cylinders.

The device used in the testing of the concrete cylinders was a CSA certified CT - 782 Soil Test Incorporated compression testing machine. A high strength (15,000 psi) capping compound was used on all cylinders. At the particular time of testing, all samples were placed in a simple cage that was equipped with 2 mechanical dial gauges, accurate to 1.27 x 10^{-3} mm, in order that the stress-strain relationship of the cylinders could be determined.

The accuracy of the mechanical dial gauges was proven several times using strain gauges mounted to the specimens, in conjunction with the mechanical dial gauges. Each mounting screw of the apparatus was held in place on the specimen using epoxy resin that was allowed to cure on each sample to negate any slippage of screws.

3.6.3 Tension Testing

3.6.3.1 General

There are basically three test methods used to determine the tensile strength of plain concrete, which can be divided into two categories. These are the direct tension test, and the indirect tension tests which include the beam flexure test and the splitting cylinder test (Chen, 1993). In the experimentation conducted, both the indirect beam flexure test, and the direct tension test were conducted in order to study the effects of ASR on high and normal strength concrete.

3.6.3.2 Direct Tension Testing

At present there is no standard testing procedure developed to determine the direct tensile strength of concrete. This is due to the fact that there are many difficulties associated with applying a pure tensile force on the specimen. However, in previous research conducted at Memorial University of Newfoundland, Chen (1993) was able to determine the direct tensile strength of concrete.

Approximately 150 specimens, 37.5 mm x75 mm x 300 mm long were cast for the high and normal strength mixes using the two different aggregates. Prior to testing, each specimen was notched on both the 37.5 mm sides, near the centre, in order to induce failure in a specific zone. A representative sample and corresponding test setup used in the determination of the tensile strength can be seen in Figure 12.

Only the 28 day specimens and the final 12 weeks specimens from both the water and the solution were instrumented with strain gauges to determine the stress strain response. During other tests, the failure load, and notched area were the only parameters recorded.

3.6.3.3 Direct Tension Test Set-Up

The testing system used in the determination of the required parameters for the direct tension tests was a closed-loop servo hydraulic universal testing machine, and a high-speed data acquisition system, along with a rigid frame loading system. The system consisted of an hydraulic actuator and a load cell with a maximum capacity of 100 kN and 91 kN, respectively.

The test set-up consisted of a MTS 850 structure test system, a digital function generator, an MTS 403 Controller, along with a computer that was instrumented with 10 additional data acquisition channels used for the recording of results.

Figure 12 - Direct Tension Testing Apparatus

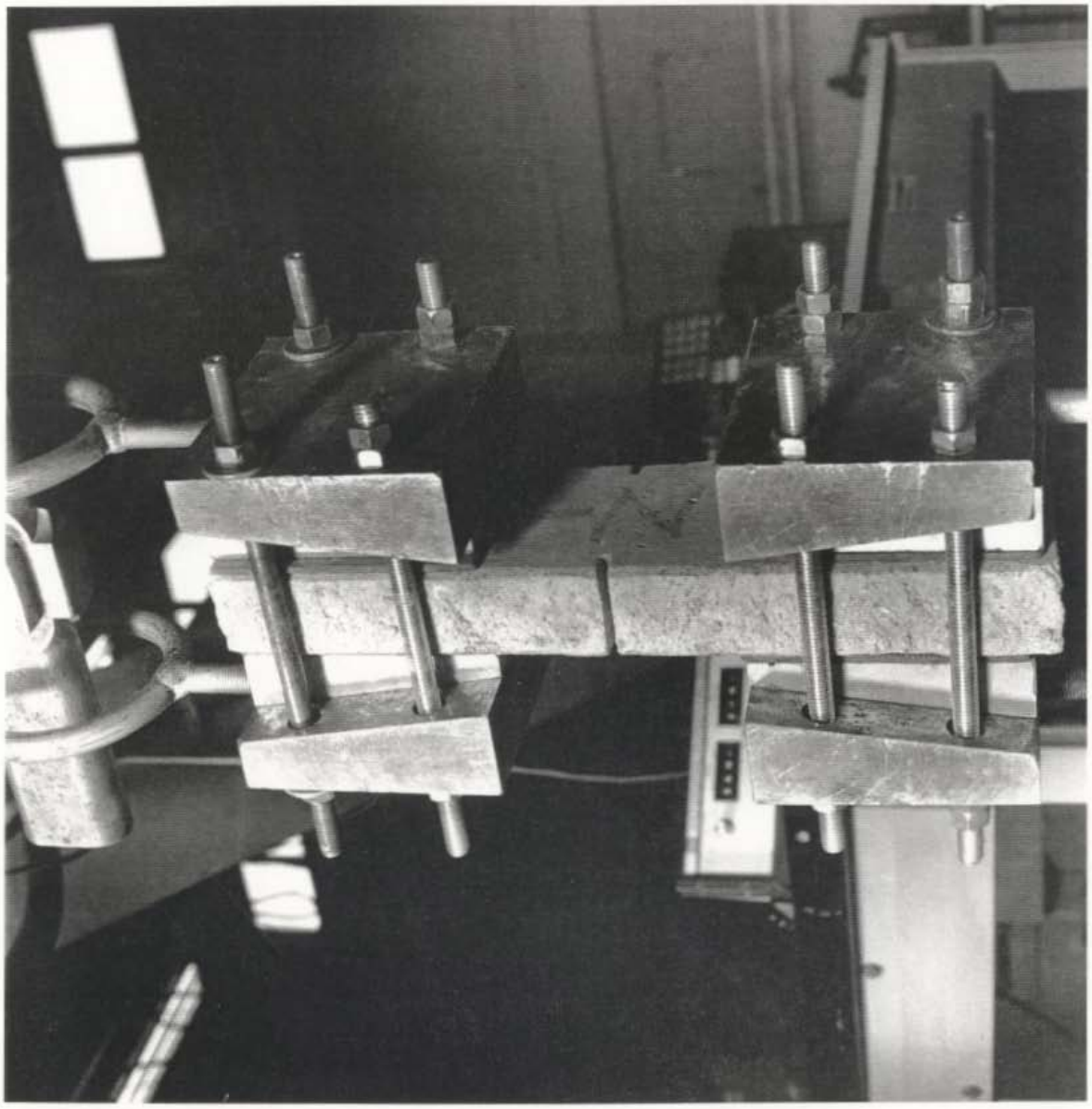

The digital function generator allowed for the control of the loading ram. For all tests, the loading ram was controlled to move 75 mm in 3600 seconds, thereby having the loading ram in stroke control. The data acquisition system along with *Labtech Notebook*, a computer program designed by Labtech Technologies Corporation, was used in recording the digital load and strain of the test specimens. A data acquiring frequency of 5 Hz was used for each test in recording the load, and the corresponding strain, when required.

For the experimental testing phase of this thesis, only the ascending portion of the curve was recorded. This is due to the high number of test specimens, as well as the substantially increased amount of time required for testing when the descending portion of the curve is required. Testing of samples that would otherwise take hours to complete could now be completed within 20 minutes.

A special test set-up was used by Chen (1993) for the testing of concrete specimens in direct tension. Wedge type frictional grips are designed to ensure that the fracture of the specimens occurs away from the grips, along the area in which the specimen had been notched. The grips consisted of self-clamping steel and aluminum wedges and a universal joint connection to the loading machine. This allowed freedom of rotation along the coordinate axes and eliminated the possibility of inducing end moments in the specimens. The wedge action was provided by the sliding of soft aluminum wedges over complementary angled steel wedges. A 5 mm thick layer of gasket rubber with double serrated surfaces was introduced between the specimen and the aluminum wedges in order to enhance the friction, and thus allow for

uniform transfer of shear stresses between the specimen and the wedges. The steel wedges were held in place with an arrangement of four bolts, which were torqued with a moderate amount of pressure, adequate enough to hold the specimen until it experienced failure. Figure 13 shows a typical direct tension set-up.

3.6.3.4 Indirect Tension Testing

ASTM C293 - 79 allows for the determination of the modulus of rupture, a measure of tensile strength, by testing a plain concrete prism in flexure. This was accomplished using centre-point loading. In the placing of the specimens in the frame, careful consideration was taken to ensure that the loading ram, and the specimen were such so that any induced moments or eccentricity were minimized

All samples tested under this procedure were approximately 75 mm x 75 mm, and tested over a span of 254 mm. However, more accurate measurements for each sample were determined with a digital vernier caliper (accurate to 0.05mm) at the time of testing. A representative sample and corresponding test setup used in the determination of the tensile strength can be seen in Figure 14.

Figure 13 - Direct Tension Test Set-up

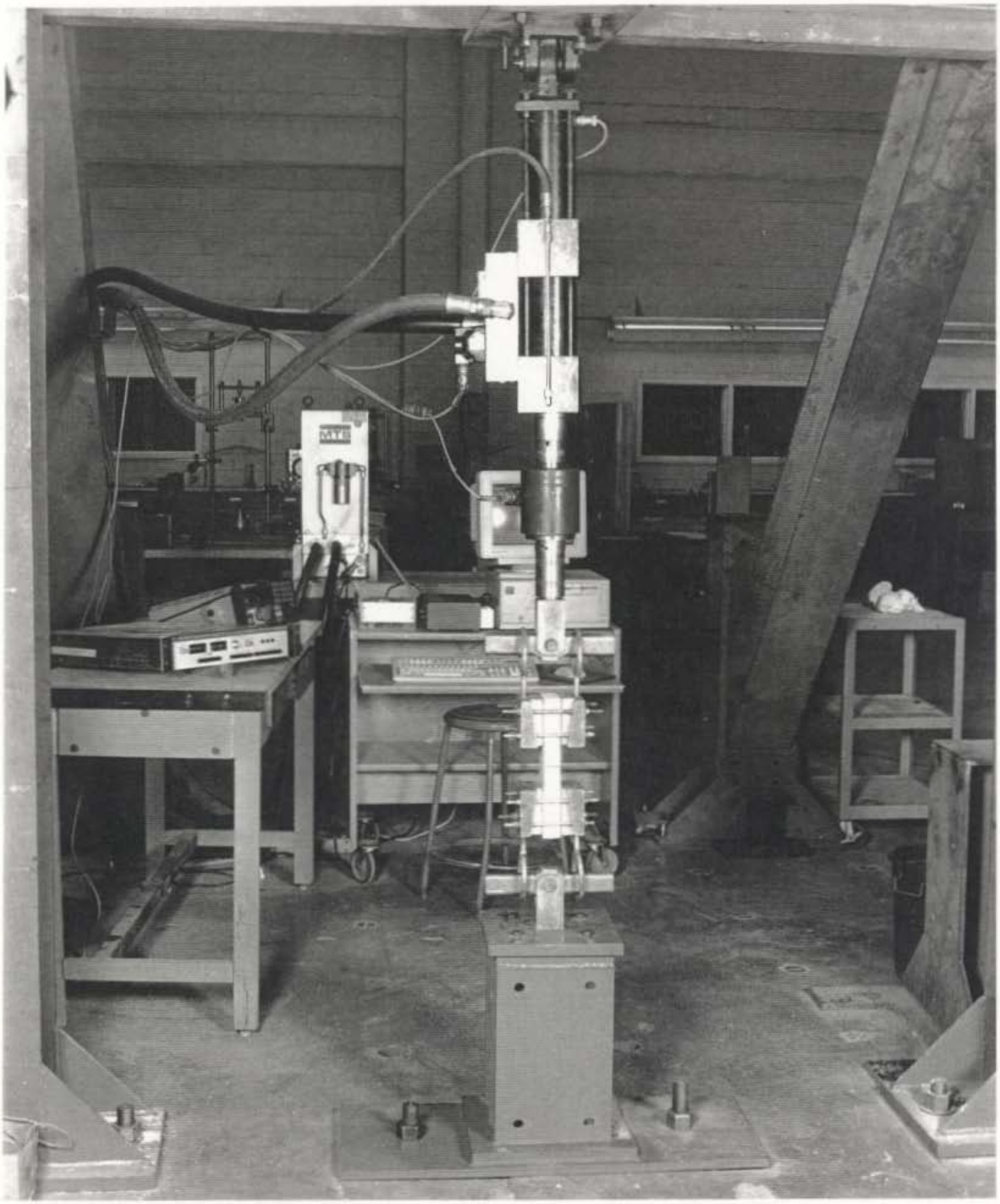

Figure 14 - Indirect Tension Set-up

3.6.3.4.1 Indirect Tension Test Set-Up

The method of data acquisition, loading rate, and instrumentation for samples were identical subjected to indirect tension, as to those for specimens subjected to direct tension, with the only exception being that the signal of the digital function generator was inverted. This allowed for controlling the loading ram's direction of travel.

3.6.4 Freeze and Thaw Testing

The effects of freezing and thawing of concrete is especially of interest in cold climates due to the effects it may have on the overall durability of the structure. Most researchers explain the phenomenon of freezing and thawing in the following manner.

As the temperature of the hardened concrete is lowered, the water held in the capillary pores in the cement paste freezes and the expansion of the concrete takes place. Upon thawing, followed by re-freezing, further expansion takes place so that the repeated cycles have a cumulative effect. This action takes place mainly in the hardened cement paste. If the pressure generated by the freezing of the concrete is greater than the tensile strength of the concrete, it results in damage, which can vary from surface scaling to complete internal disintegration.

The cumulative damaging effect of the freezing and thawing of concrete results from the fact that during freezing, the excess water is forced to locations where it can freeze. The locations include fine cracks, which progressively become larger as the water expands during freezing.

These cracks remain enlarged during the thawing process because they become filled with water. Additional cycles of freezing and thawing follow the same pattern, resulting in progressive deterioration.

The objective of this testing was to compare the resistance of high strength and normal strength concrete specimens consisting of the two different aggregate sources to repeated rapid cycles of freezing and thawing using samples located in water and 1 molar NaOH solution for a period of 6 weeks, after the initial 28 day curing period at approximately 98% relative humidity (RH), and 23 °C ± 2 °C. All of the testing was carried out in accordance with the associated standards regarding resistance of concrete to freezing a thawing (ASTM C 666-84), Ultrasonic Pulse Velocity (ASTM C 597-83), and Resonance Method (ASTM C 215-60). Swamy (1992) confirmed that both the pulse velocity and dynamic modulus are highly sensitive to changes in the overall internal structure of specimens experiencing damage as a result of AAR. In addition, both the pulse velocity, and resonance test method can detect measurable losses long before external evidence of any damage resulting from the reaction is visible.

3.6.4.1 Freeze and Thaw Testing Machine

The Soiltest Freeze-Thaw Tester (CT-110) as developed by Solitest Incorporated (1970) was used to subject the specimens to accelerated environmental effects of freezing and thawing in accordance with ASTM C 290. Under regular operating conditions, and operating between 5 °F and 75 °F, the Freeze-Thaw Tester underwent approximately 5 freeze-thaw cycles per

day. Temperature is accurately controlled with the use of a thermistor embedded in a control specimen, while freeze-thaw cycles are recorded on appropriate freeze-thaw cycling paper.

3.6.4.2 Dynamic Testing Apparatus (E-Meter)

This method conforms to ASTM 215 - 85 and involves the measurement of the fundamental longitudinal frequency of concrete prisms, 75 mm x 75 mm x 300 mm, in order to calculate the dynamic modulus of elasticity.

As can be seen from the following figure, the specimen is clamped at the centre with an electromagnetic exciter unit placed against one end face of the specimen and a pick-up against the other.

Figure 15 - Test Arrangement for E-Meter Testing

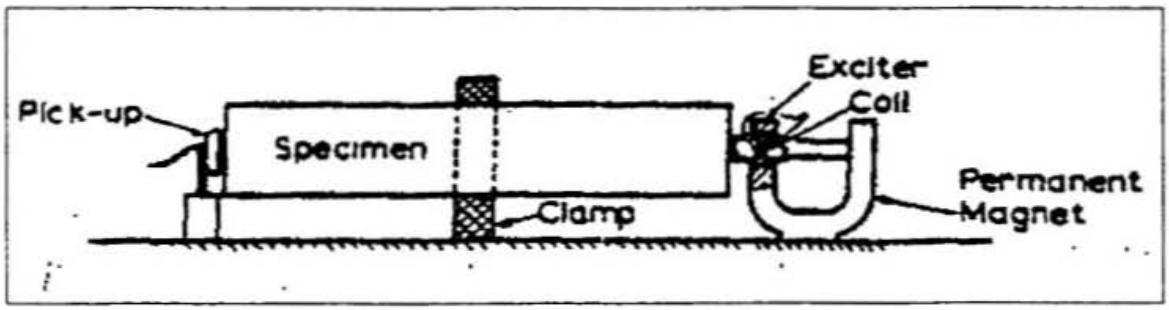

The exciter is driven by a variable frequency oscillator with a range of 100 to 10,000 Hz. The vibrations propagated within the specimen are received by the pick-up, and amplified in order to be measured by an indicator. The frequency of the excitation is varied until resonance is obtained at the fundamental frequency of the specimen. The dynamic modulus of the specimen can be calculated from the fundamental frequency, specimen length, and specimen density.

From the testing, it should become apparent that specimens subjected to the solution, will experience substantial decreases in the dynamic modulus of elasticity when compared to specimens subjected to de-ionized water. However, the decrease in the dynamic modulus of elasticity is assumed to be less for the high strength concrete mixes due to the increase in material properties. In addition, it is believed that the more reactive aggregate will experience larger losses in material properties.

3.6.4.3 Ultrasonic Pulse Velocity (V-Meter)

This test method conforms to ASTM C 597-83 and involves the determination of the pulse velocity of propagation of compression waves in concrete. The velocity of ultrasonic pulses travelling in a solid material depends on the density and elastic properties of the material. The ultrasonic pulse velocity apparatus provides the time required for the pulse to travel through the medium. Upon accurately measuring the specimen, the pulse velocity of longitudinal ultrasonic vibrations travelling in an elastic solid can be calculated by dividing

the overall specimen length by the time required for the pulse velocity to travel the length of the specimen. The following is a schematic representation of the V-Meter Test set-up.

Figure 16 - Test Arrangement for V-Meter Testing

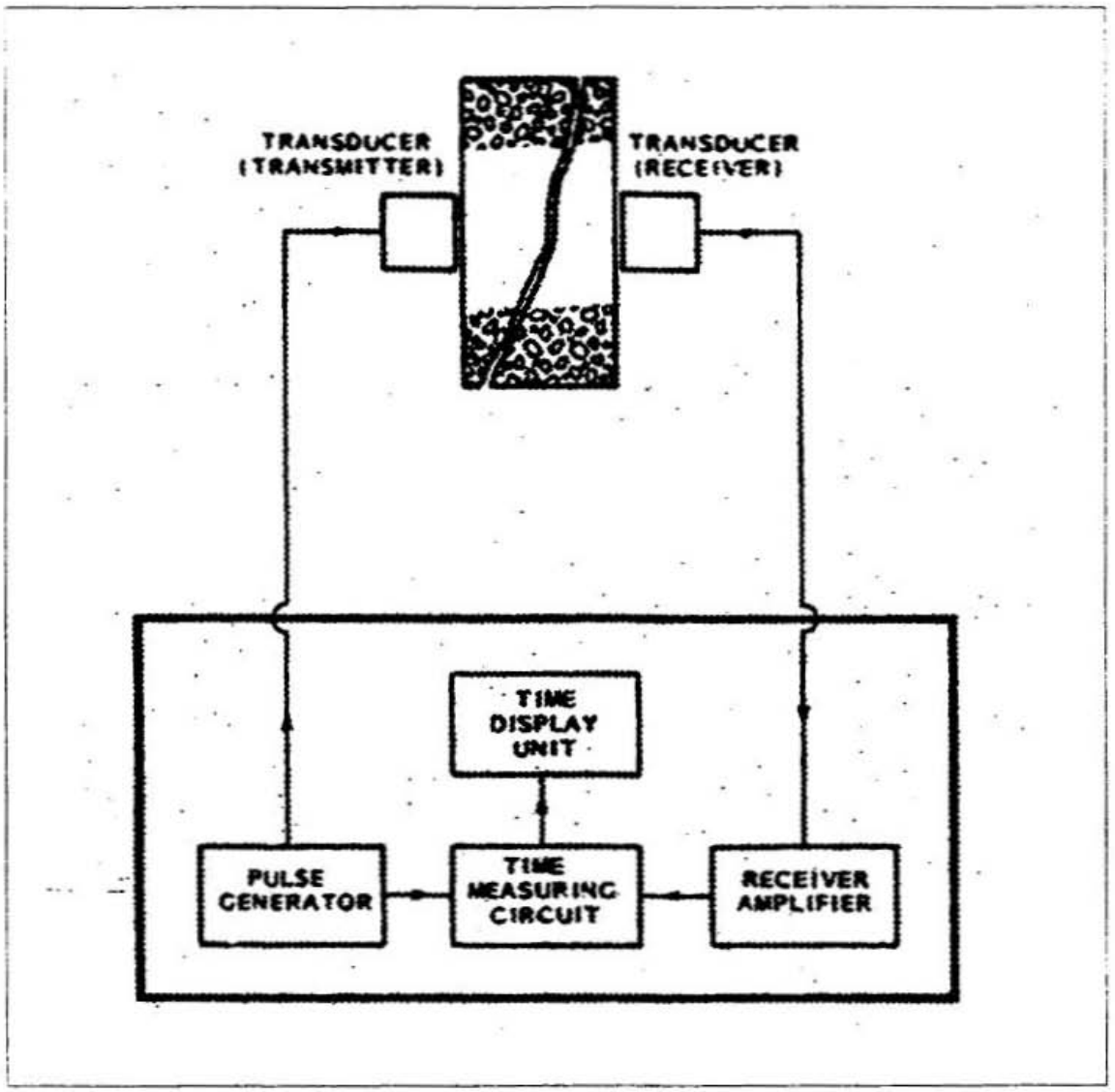

3.6.5 Creep of Concrete in Compression

The test method involves the determination of the creep properties of concrete under a sustained load in accordance with ASTM C 512 - 82. In this method, the load-induced time-dependant compressive strain is recorded at pre-selected ages under controlled environmental conditions.

The testing regime for the creep tests is somewhat different from the other test methods. During the time of casting, a total of 6 specimens were cast for both the high and normal strength mixes. After allowing the specimens to cure under 100% relative humidity (RH) at 23 °C ± 2 °C for 28 days, half of the specimens were placed in heated water, while the other half were placed in heated solution. It was decided initially, that both sets of specimens be allowed to remain in the tanks for a period of 6 weeks, and then loaded to 50% of the 28 day compressive strength (f 'c). After the specimens were loaded in the loading frames, and torqued, the initial readings, as well as the instantaneous strain reading was measured. Thereafter, the specimens were placed back in the curing room, so that shrinkage would not become a factor. The distance between each of the pins were then measured at 2, 7, 28, 56, 90 days respectively.

For each specimen, the strain for each of the pins was determined at each of the pre-determined dates. The average value for each specimen was then plotted.

3.6.6 Testing Procedure

Samples used for each of the aforementioned tests were evaluated initially after a 28 day curing period at 98% RH, and 23 °C ± 2 °C. The 28 day testing of the samples provided the reference properties to which all other data would be compared. Next, the samples remaining were equally divided, with half of the samples being placed into tanks containing de-ionized water, while the other half were placed into a solution of 1 molar NaOH. Each tank was then heated to 80°C using a stainless steel submersion heater.

Both sets of specimens were then contained in the tanks for an extended period of time, with samples from both tanks being tested at 6, 9, and 12 weeks, respectively, for the compression, direct tension, and indirect tension samples. At each testing date, a minimum of 4 samples were tested.

However, for the freeze-thaw specimens, the samples were only placed in the corresponding tanks for a period of 6 weeks. After this time, the samples were taken from the tanks, the required material properties were recorded, then the samples were placed in the freeze-thaw machine until they underwent 300 freeze-thaw cycles. The samples were then tested at approximately every 50 freeze-thaw cycles, with all the relevant data being recorded.

A similar procedure was used in the testing of the creep specimens. All samples were initially placed in the corresponding tanks for a period of 6 weeks, then 3 specimens from each tank were extracted and loaded in a creeping frame. However, all creep specimens, after being

loaded in the frames, were placed in the curing room at 98% RH in order that shrinkage could be excluded from the resulting analysis of the results.

3.7 Testing Rationale

A thorough review of the literature has shown that for normal strength concrete, the mechanical properties such as compressive strength, tensile strength (direct and indirect), Modulus of Elasticity (dynamic and static), as well as pulse velocity decrease as the specimens are subjected to extended periods of the aggressive 1 molar NaOH solution. As for the specimens subjected to the de-ionized water, none of the samples mechanical properties should decrease or deteriorate with time. However, the approximate loss in mechanical properties is dependant on a multitude of factors, as previously discussed in the literature review, and therefore, is very difficult to accurately predict. However, the Modulus of Elasticity (dynamic and static), as well as tensile strength, seem to be the properties most affected.

In addition, it is believed that the highly reactive aggregate will experience a greater percentage loss of the properties than that of the marginally reactive aggregate. However, again, this premise may not necessarily hold true. There is some combination of the alkalies available from the aggregates, as well as those contained in the other constituents of the mix design that will produce a maximum reaction. However, if the combination is such that it is below or above this optimum, then the testing procedure used in this study may not show the

extreme maximum possible loss in material properties of concrete using the different aggregate sources.

However, initially, before the testing of the concrete specimens began, several 75 mm mortar cubes were prepared using the same aggregates and testing conditions chosen for this study, and subjected to both a water, and 1M sodium hydroxide solution at 80 °C for a period of 4 weeks. After being subjected to the solution for the four week period, the highly reactive aggregate showed a decrease in compressive strength of approximately 15 % with respect to reference specimens, whereas the compressive strength of the moderately reactive aggregate remained unchanged with reference specimens. In addition, mortar cubes containing the highly reactive aggregate showed evidence of gel surrounding aggregate particles resulting from the alkali-aggregate reaction. As a result of the aforementioned investigation, it was decided that a submergence period of 12 weeks in a 1M NaOH solution, after the initial curing period, would provide ample time for an alkali-aggregate reaction to take place.

3.8 Submersion Tanks and Solution Concentration

Due to the size and number of samples required for the testing phase, it was required to build a holding facility that was 4 feet long, three feet wide, and three feet high. Initially, stainless steel tanks were investigated, and were determined to be more than adequate to meet all requirements. However, the cost for materials and labour in construction of two such tanks proved to be high. As a result, it was decided to construct the tanks from regular, mild steel, and to coat the inner surface that would be exposed to the aggressive solution with an inert

epoxy coating. The coating, an all weather DTR Pitt-Guard epoxy obtained from Pittsburg Paints, was applied to the tanks that had been sand blasted to ensure optimum product performance. The coating as provided by Pittsburg Paints was ensured to withstand the 80°C NaOH solution without any material breakdown. To ensure product performance, visual inspections, as well as titrations of the solution were carried out on a regular basis.

In addition, two Cole - Palmer stainless steel coiled element submersion heaters (model # 492-6) were mounted to the side of each tank, and used to concentrate heat near the bottom of the tanks. The heaters were equipped with a stepless calibrated automatic temperature control dial, having sensitivity as low as ± 2 °F, and a range of 70 °F to 250 °F. The heating element was made using a 316 stainless steel that was known to be non-reactive with the 1M NaOH solution. The coil had a radius of 350 mm, and the stem was 400 mm high.

Both tanks were covered with two layers of Styrofoam SM so that heat loss would be minimal. This allowed for easy retrieval of specimens. Figure 17 is a photograph of the typical holding tank set-up.

Figure 17 - Holding Tank and Submersion Heater Set-up

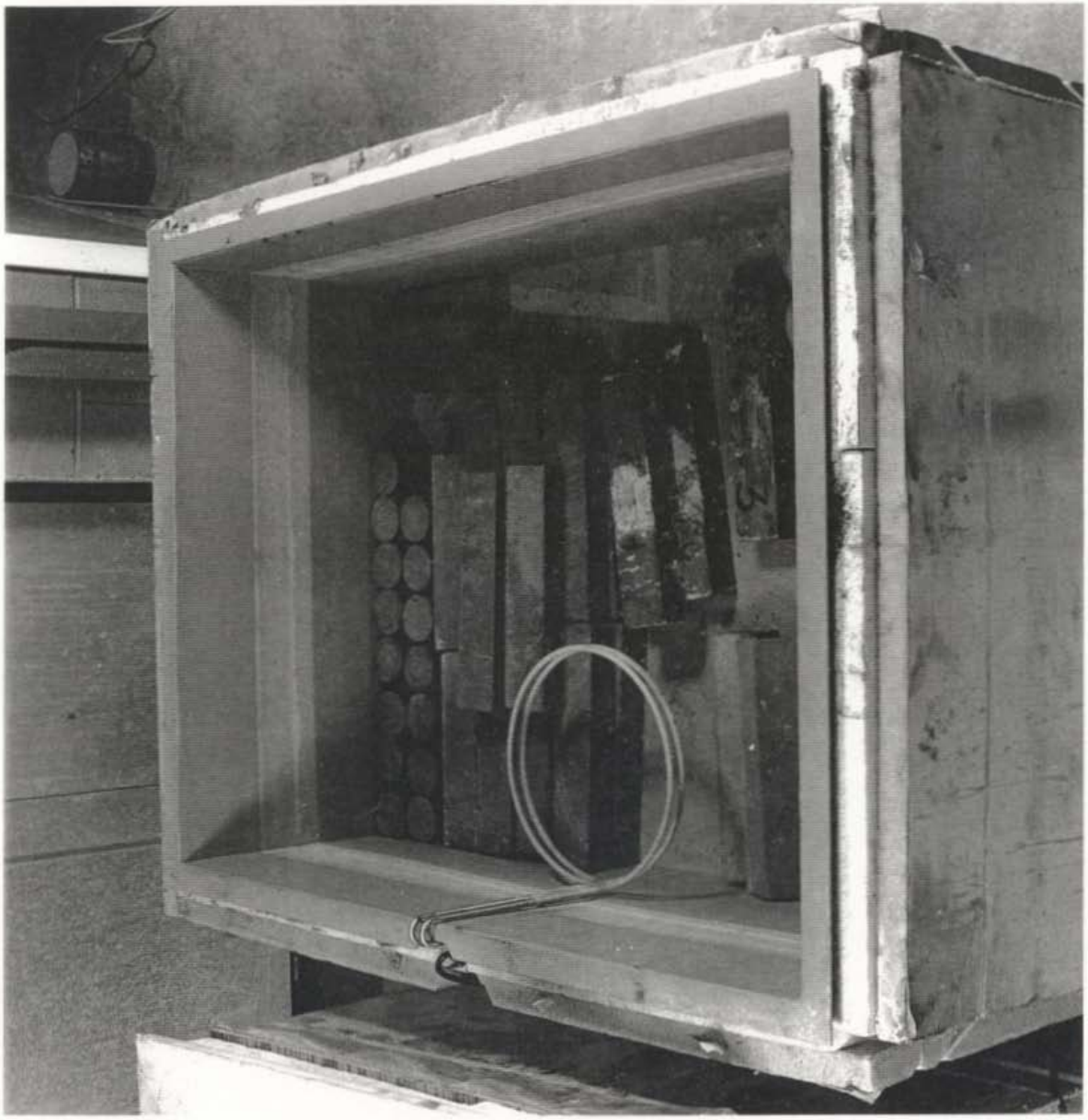

4.0 Results and Discussion

4.1 General

The formation of the non-linear region in the stress strain curve of concrete is a direct result of the interfaces between the aggregate and the cement paste, as well as the development of bond micro cracks at those interfaces. As the first micro cracks begin formation, the stored strain energy becomes transformed into the surface energy of these new crack faces. Then, as the load is continually increased, it results in the progressive development of micro cracks, which results in a progressive increase in stress intensity and the magnitude of the strain. As a result of the micro crack development, the effective area resisting the applied load is reduced, resulting in larger local stresses than the nominally applied external stress. This results in the strain of the specimens increasing at a much faster rate than the nominal stress, which results in the generation of the non-linear portion of the stress-strain curve. As the load is continually increased, these micro cracks grow to cause the formation of macro cracks, which eventually result in the overall failure of the specimen.

In concrete elements, if the strains developed due to an alkali-aggregate reaction exceed the ultimate tensile strain of the surrounding concrete (usually determined to be between 150 and 200 $\mu\epsilon$, and rarely exceeding 500 $\mu\epsilon$), then micro cracks will develop in the hydrated cement paste, and sometimes in the aggregate itself. Therefore, it is quite reasonable to understand that if crack growth is initiated before the application of any load, from any test, that a decrease in overall strength, and increased compressibility will be observed. However, for the samples subjected to the de-ionized water, there should be no loss in mechanical properties. If anything, a gain in the overall properties should be observed from samples located in solution baths. This is attributed to high temperatures resulting in a secondary pozzolanic reaction

For the high strength concretes (HSC), it has been determined that such concrete develops a smaller amount of cracking than the normal strength concrete (NSC), at all ages of loading. This results in the ascending portion of the stress-strain curve being much steeper, and linear up to higher proportions of the ultimate strength. In addition, it is known that the high strength concrete is much more brittle than normal strength concrete, often resulting in an explosive failure upon reaching ultimate strength. Furthermore, high strength concrete usually undergoes an increase in strength, even after the 28 day curing period, often continuing for a period of approximately 6 months. This phenomenon can be explained considering calcium hydroxide, a by-product of the cement hydration, reacts at room temperature with the silica fume and fly ash to form tobermorite gel, which has a very stable

and strong cementing quality. This pozzolanic reaction contributes to the increase in strength of high strength concrete for the first six months.

Therefore, since high strength concrete specimens experience an improvement in material properties with time, the results observed from testing specimens subjected to the NaOH solution will be a 'net effect' reaction. A 'net effect' reaction refers to the fact that as the material properties of the concrete specimens are being reduced, if at all, by the alkali-aggregate reaction, the specimens will also be experiencing a gain in material properties due to the secondary pozzolanic reaction. For normal strength concrete specimens subjected to the NaOH solution, the loss in mechanical properties will also be a 'net effect' reaction. However, the increase, or improvement, in mechanical properties will be less, as the normal strength specimens will have attained most of its strength within the initial 28 day curing period.

Losses in the material properties tested will not occur in direct relation to expansion. Therefore, from all previous investigations, it is still very difficult to prescribe limiting values of mechanical properties. The following sections will investigate the differences resulting in the mechanical properties determined from samples subjected to the different testing regimes.

4.2 Compression Results

4.2.1 General

The compressive strength of ASR-affected concrete is a function of time, and has been found to decrease as damage due to the reaction increases on the micro-structural level. Most researchers (Pleau et al. (1989), Swamy and Al-Asali (1988), Ono (1990), and Clark (1990)) determined that losses in compressive strength can be as high as 40% to 60%, with a reduction of 20% being likely to occur for expansions found in practice. However, a direct comparison between the works of other researchers, and the work carried out here is virtually impossible. The losses in compressive strength from each experiment depends greatly on numerous parameters such as mix design, aggregate type, and storage conditions; none of which have been duplicated by all the investigations. However, the general trends observed are applicable.

Throughout this laboratory investigation, very similar trends were found in reduction of compressive strength for normal strength concrete specimens consisting of the potentially highly reactive aggregate. In addition, for normal strength concrete specimens made using the marginally reactive aggregate, very little, if any, strength reduction was observed. These findings were initially anticipated, and agree quite well with those observed from research conducted by other observers.

To the author's knowledge, no compressive strength testing, or any other mechanical property investigation, has included high strength concrete specimens that have been subjected to

alkali-aggregate reactivity. However, since high strength concrete has a much improved micro-structure than normal strength concrete, it is reasonable to assume that the formation of gel pressures due to the alkali-aggregate reaction will have little, if any effect, on the overall strength, and compressibility of these specimens. In addition, due to the decreased permeability of the high strength concrete specimens, it is reasonable to assume that alkalies from the 1 molar NaOH solution bath will not penetrate these specimens as easily, and thereby will not be able to initiate an alkali-aggregate reaction.

However, over the past decade, the Portland Cement Association has conducted extensive research on the mechanical properties of high strength concrete, without the inclusion of any alkali-aggregate reactivity. Research has confirmed that for all high strength concretes, regardless of aggregate type combinations, the ultimate stress occurred at strains in the range of 2×10^{-3} to 4×10^{-3}. In addition, the modulus of elasticity is usually in the range of 31 to 45 GPa (Farny et al., 1994).

Furthermore, Wee et al. (1996) confirmed from testing that the strain at ultimate strength of high strength concrete varied between 2E-3 and 3E-3, whereas the modulus of elasticity was on the order of 40GPa. From these experiments, it was also concluded that as long as the strength remains approximately the same, the method in achieving the strength by varying a combination of factors (eg. the admixtures used to achieve the strength, and the different water/cement rations) have little effect on the ascending portion of the curve. Therefore, the

results obtained for specimens after the initial 28 day curing period should resemble those determined from this investigation.

The following sections present the mechanical properties determined from testing of all specimens, normal and high strength mix designs using a potentially highly reactive aggregate, as well as a potentially marginally reactive aggregate, in compression.

4.2.2 Compression (NSC - Highly Reactive)

The mechanical properties determined from the potentially highly reactive aggregate used in the normal strength mix design showed the greatest reduction. The stress - strain results of samples subjected to solution and water can be viewed in Figure 18, and Figure 19, respectively. For specimens subjected to the NaOH solution, an overall reduction in strength of 28% was observed after a period of twelve weeks, whereas, for specimens subjected to the de-ionized water, an overall increase in strength of 14% was observed after the same time frame (Refer to figure 20 and 21 for plots of average strength versus time, as well as, Tables 10 and 11 for compression results of all samples). The increase in strength for specimens subjected to the de-ionized water is attributed to the elevated storage temperatures which forced the completion of cement hydration, and thus improved material properties.

In addition, the stress - strain curves of normal strength concrete consisting of the highly reactive aggregate were used to investigate the effects of the alkali-aggregate reaction on the strain at ultimate stress, as well as its effects on the secant modulus of elasticity for the

material. For the samples subjected to the NaOH solution, a reduction in the secant modulus of approximately 80% was observed, as well as an increase in strain at ultimate stress of approximately 180% (Refer to Tables 12 and 13). As for the specimens that were subjected to the de-ionized water, the variance in mechanical properties determined is not nearly as drastic. These results are consistent with what was initially expected, as well as those observed by other researchers conducting compressive strength tests on similar materials.

Figure 18 - Normal Strength Concrete in Solution (Highly Reactive)

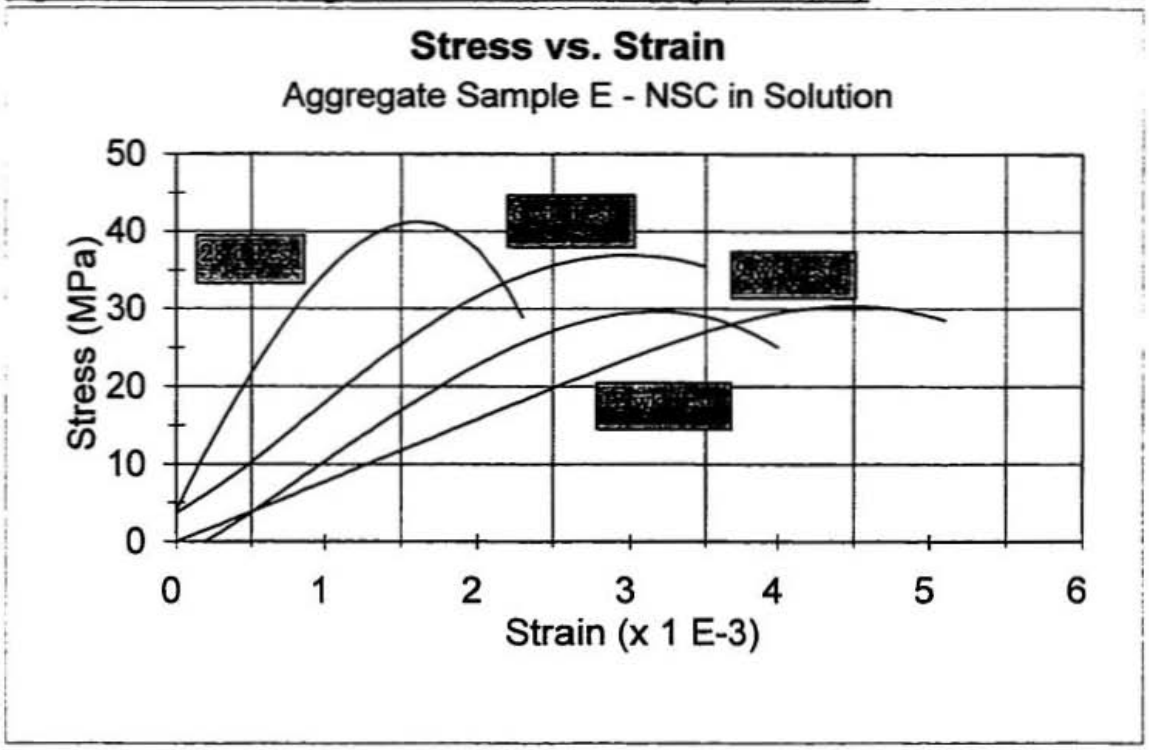

Figure 19 - Normal Strength Concrete in Water (Highly Reactive)

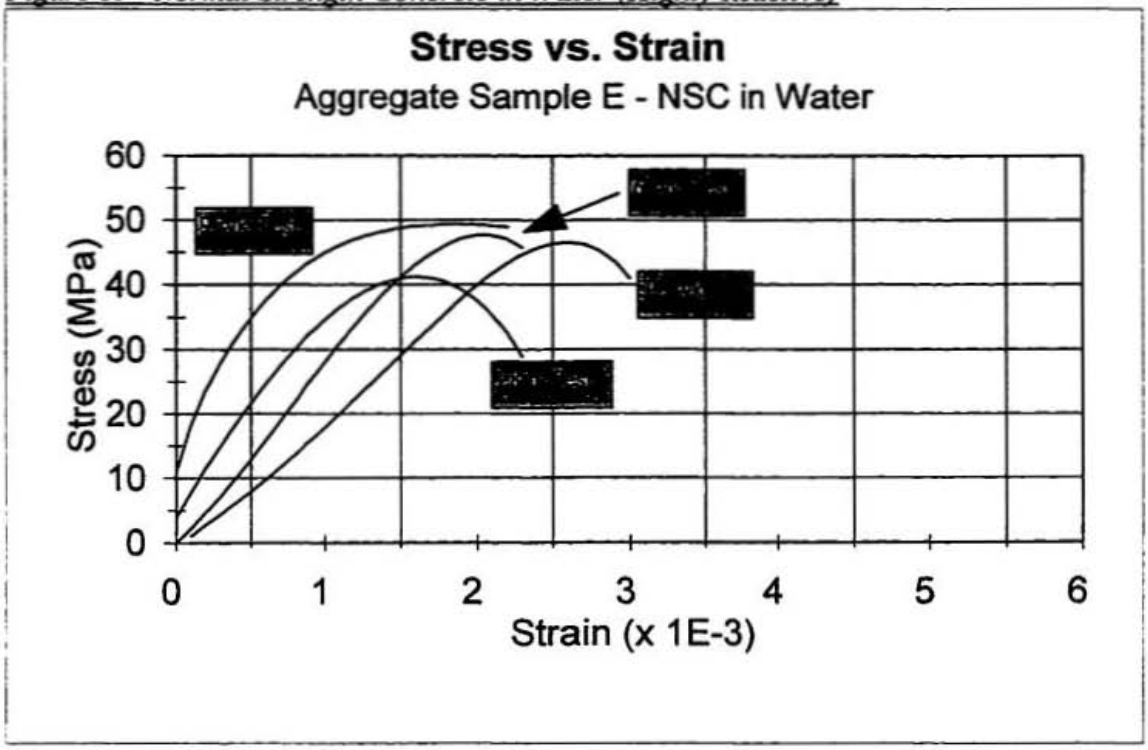

Figure 20 - Mean Strength vs. Time: NSC in Solution (Highly Reactive)

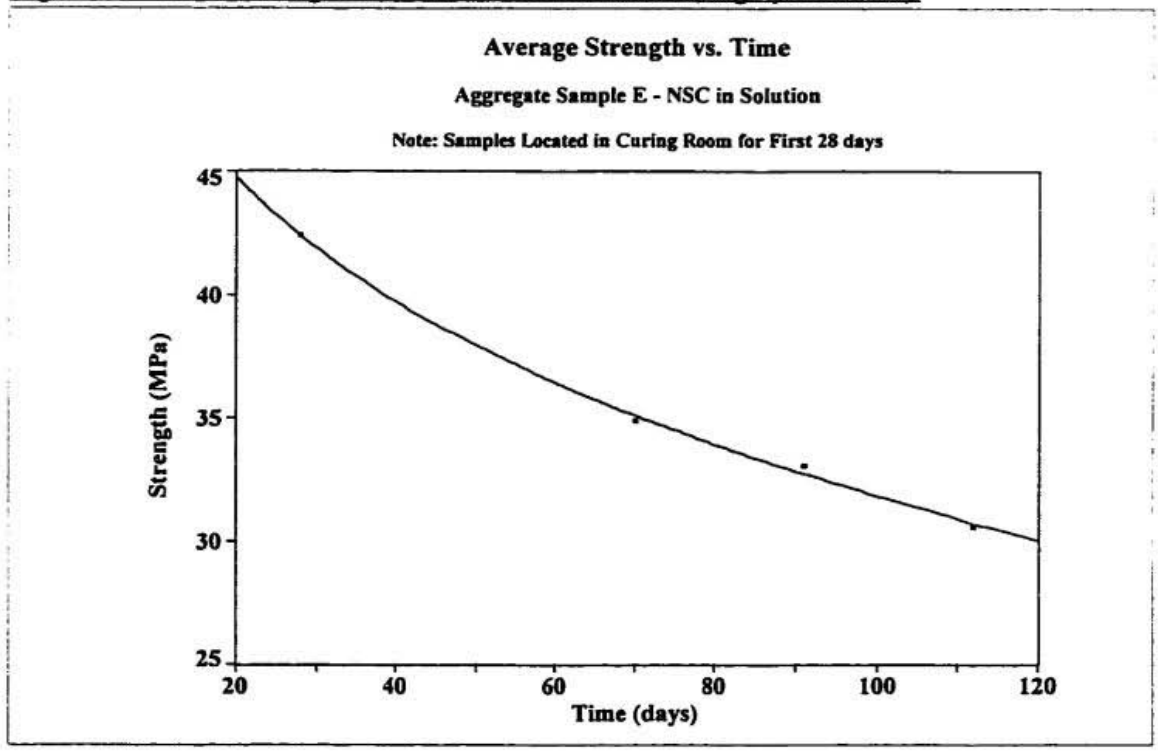

Figure 21 - Mean Strength vs. Time: NSC in Water (Highly Reactive)

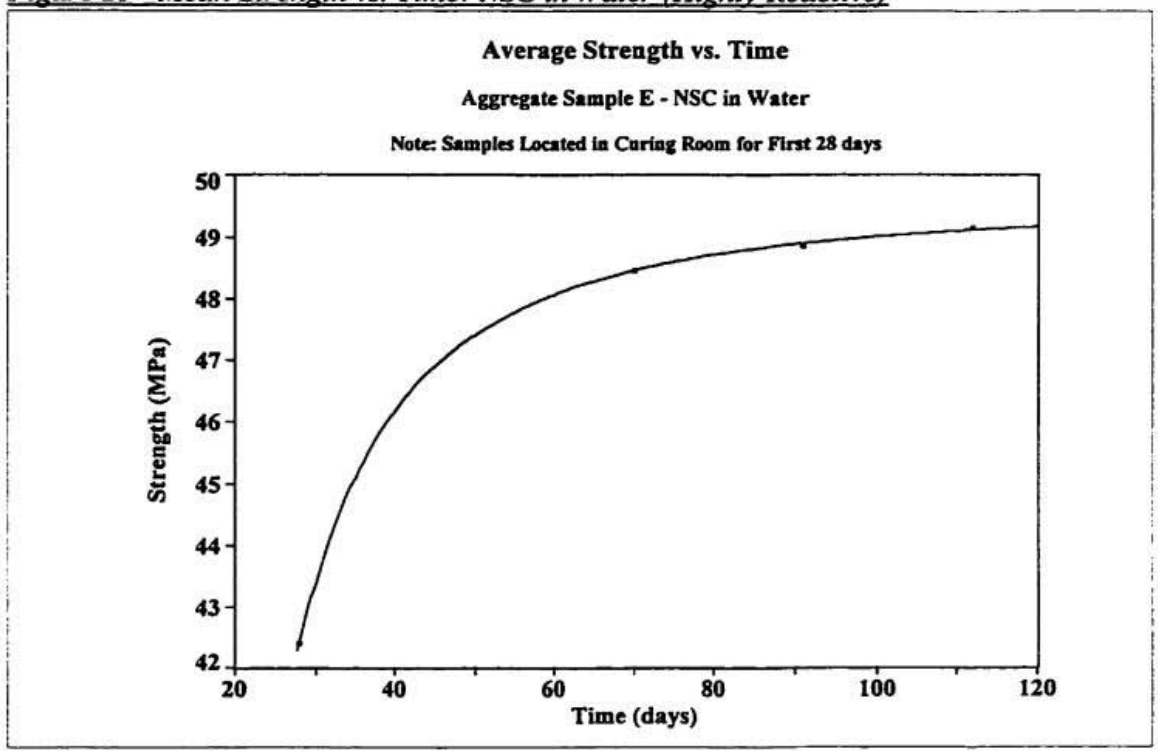

Table 10 - Compression Results - NSC in Solution (Highly Reactive)

Time (days)	Sample #	f'c MPa	Mean f'c Solution MPa	Std. Dev. Solution MPa	Avg. % of MAX f'c Solution	Coefficient of Variation
28 days	1 2 3	41.10 45.60 40.47	42.39	2.8	1	5.22 %
6 wk	1 2 3	32.77 35.21 36.67	34.88	1.97	0.82	2.59 %
9 wk	1 2 3	29.46 34.72 34.91	33.03	3.09	0.78	6.38 %
12 wk	1 2 3	31.01 30.04 30.62	30.56	0.49	0.72	0.16 %

Table 11 - Compression Results - NSC in Water (Highly Reactive)

Time (days)	Sample #	f'c MPa	Mean f'c Water MPa	Std. Dev. Water MPa	Avg. % of MAX f'c Water	Coefficient of Variation
28 days	1 2 3	41.10 45.60 40.47	42.39	2.8	0.86	5.22 %
6 wk	1 2 3	48.77 48.57 47.99	48.44	0.41	0.99	0.11 %
9 wk	1 2 3	48.57 49.16 48.77	48.83	0.3	0.99	0.06 %
12 wk	1 2 3	50.23 47.21 49.95	49.13	1.67	1	1.86 %

Table 12 - Analysis of Compression Results (NSC in Water - Highly Reactive)

Time	f'c (MPa)	0.5 f'c (MPa)	ϵ @ 0.5 f'c (x 1E-3)	ϵ 'c (x 1E-3)	Secant Modulus GPa
28 days	41.25	20.625	0.527	1.6	39.136
6 wk	47.71	23.86	0.8564	2	27.856
9 wk	49.4	24.7	0.222	1.9	111.16
12 wk	46.6	23.3	1.2407	2.6	18.781

Table 13 -Analysis of Compression Results (NSC in Solution - Highly Reactive)

Time	f'c (MPa)	0.5 f'c (MPa)	ϵ @ 0.5 f'c (x 1E-3)	ϵ 'c (x 1E-3)	Secant Modulus GPa
28 days	41.25	20.625	0.527	1.6	39.136
6 wk	36.98	18.49	1.028	2.6	17.94
9 wk	29.7	14.84	1.33	3.2	11.152
12 wk	30.42	15.21	2.024	4.5	7.514

4.2.3 Compression (NSC - Moderately Reactive)

Compressive testing on the normal strength concrete containing the potentially marginally reactive aggregate showed little, if any changes for specimens subjected to the solution to accelerate an alkali-aggregate reaction, or for specimens subjected to the de-ionized water solution. The stress- strain curves for specimens tested over a period of 12 weeks after the initial 28 day curing period can be viewed in Figures 22 and 23. For specimens subjected to the solution, the ultimate strength of the specimens after a period of 12 weeks stayed virtually

the same, while specimens subjected to the de-ionized water experienced an increase in strength of approximately 23 % (Refer to Figures 24 and 25, and Tables 14, through 17 for compression results of the specimens).

The stress - strain curves of the normal strength concrete consisting of the marginally reactive aggregate were also used to investigate the effects, if any, on the strain at ultimate stress, as well as on the secant modulus of elasticity. Mechanical properties of specimens subjected to the solution, as well as specimens subjected to the de-ionized water did not change appreciably in either instance, especially when compared to data acquired from normal strength specimens consisting of aggregate E, the highly reactive aggregate.

Once again, it was initially suspected that the normal strength concrete consisting of the potentially marginally reactive aggregate would not experience the same level of reduction in mechanical properties as experienced by the normal strength concrete consisting of the potentially highly reactive aggregate. The results obtained are indeed consistent with those expected, as well as those determined by previous researchers.

Figure 22 - Normal Strength Concrete in Solution (Moderately Reactive)

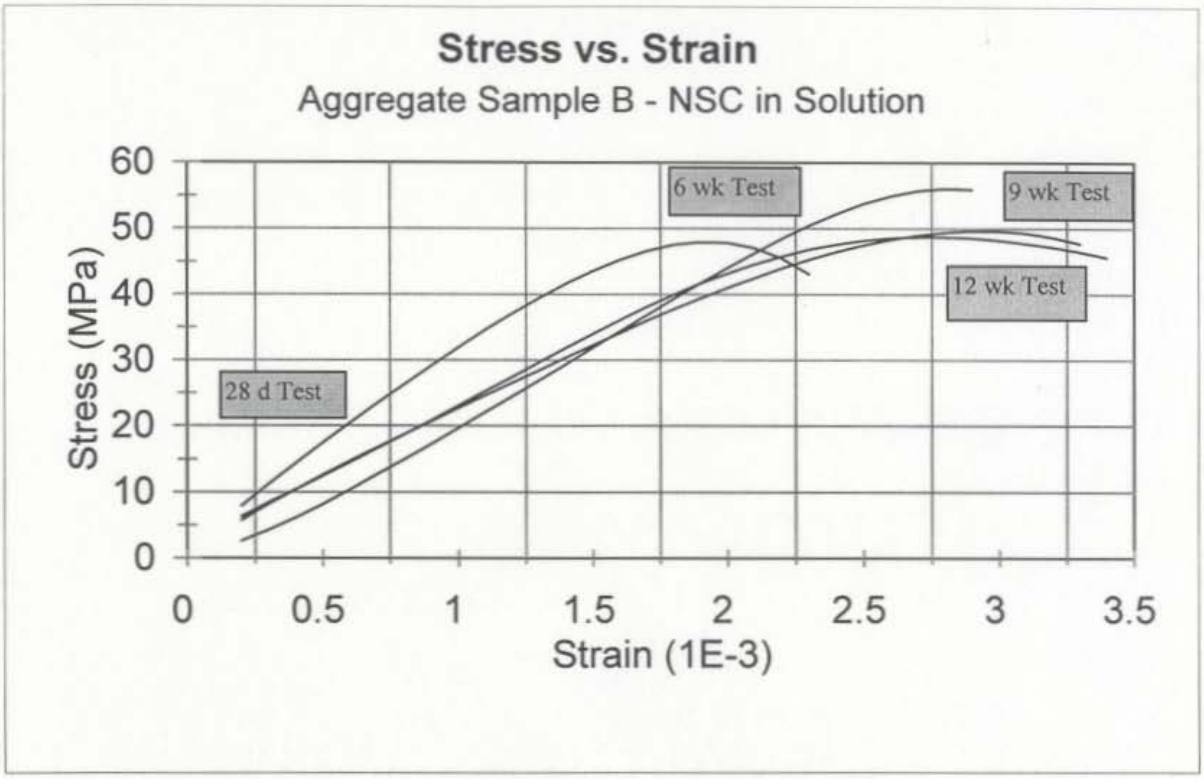

Figure 23 - Normal Strength Concrete in Water (Moderately Reactive)

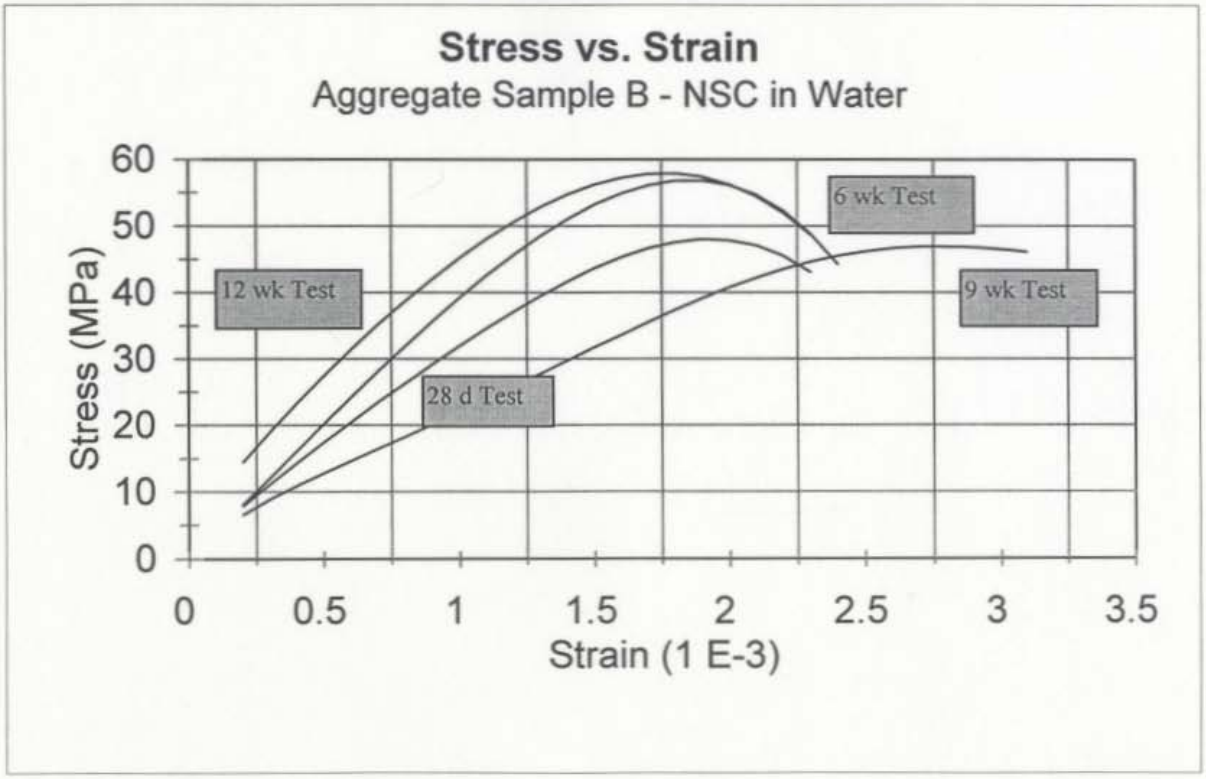

Figure 24 - Mean Strength vs. Time: NSC in Solution (Moderately Reactive)

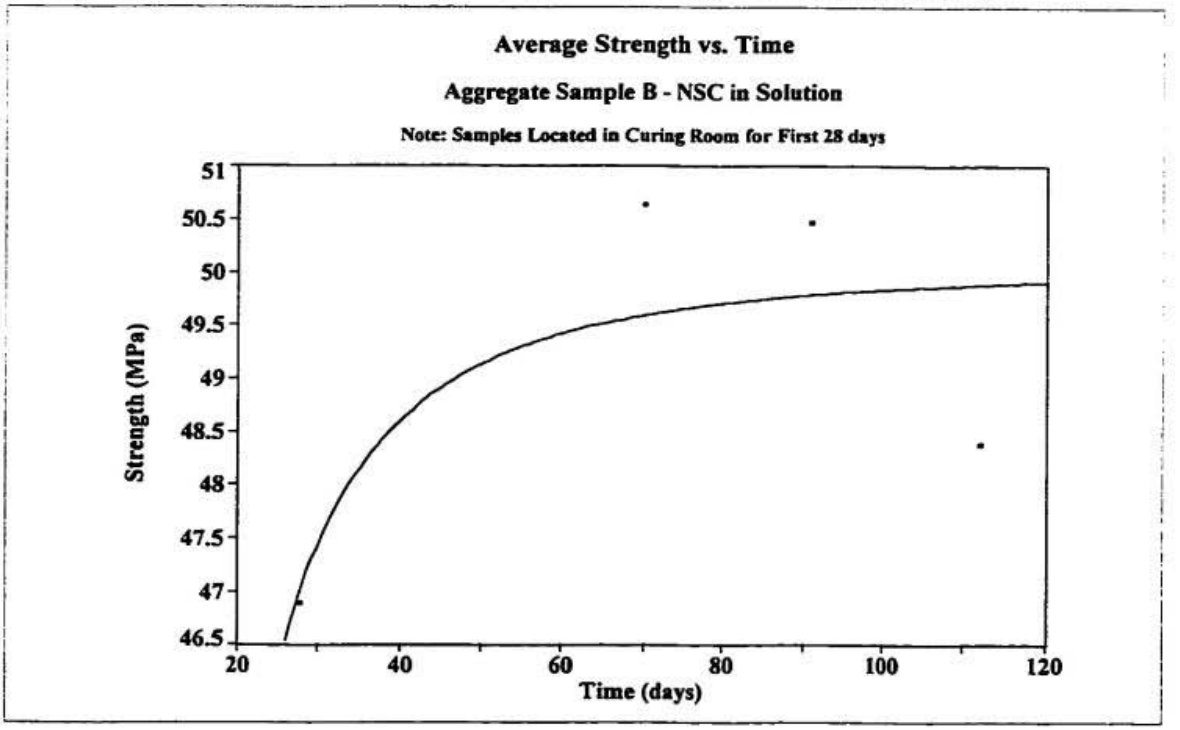

Figure 25 - Mean Strength vs. Time: NSC in Water (Moderately Reactive)

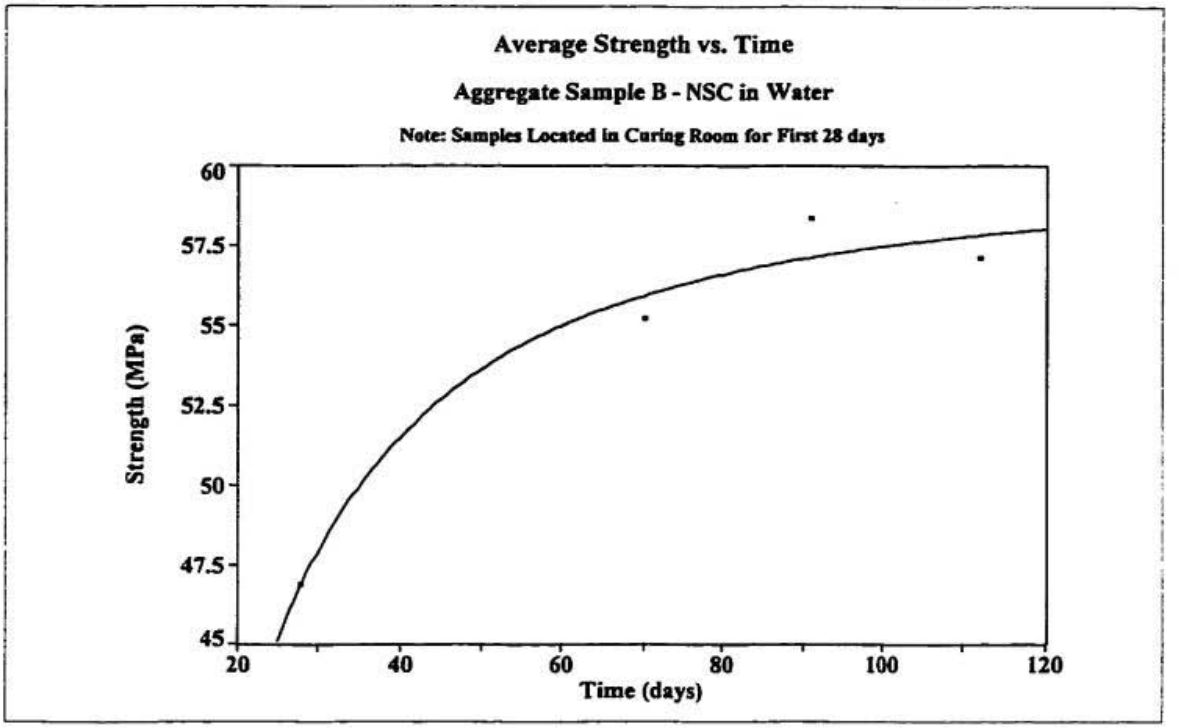

Table 14 - Compression Results - NSC in Solution (Moderately Reactive)

Time (days)	Sample #	f'c MPa	Mean f'c Solution MPa	Std. Dev. Solution MPa	Avg. % of MAX f'c Solution	Coefficient of Variation
28 days	1 2 3	46.62 47.21 46.82	46.88	0.3	0.93	0.09
6 wk	1 2 3	54.62 51.65 45.65	50.64	4.57	1	20.88
9 wk	1 2 3	49.36 50.33 51.70	50.46	1.18	1	1.38
12 wk	1 2 3	48.77 47.80 48.56	48.38	0.51	0.96	0.26

Table 15 - Compression Results - NSC in Water (Moderately Reactive)

Time (days)	Sample #	f'c MPa	Mean f'c Water MPa	Std. Dev. Water MPa	Avg. % of MAX f'c Water	Coefficient of Variation
28 days	1 2 3	46.62 47.21 46.82	46.88	0.3	0.8	0.09
6 wk	1 2 3	56.77 55.60 53.28	53.28	1.78	0.95	3.16
9 wk	1 2 3	59.98 60.28 54.82	60.28	3.05	1	9.28
12 wk	1 2 3	57.55 57.74 55.99	57.74	0.96	0.98	0.92

Table 16 - Analysis of Compression Results (NSC in Water - Moderately Reactive)

Time	f'c (MPa)	0.5 f'c (MPa)	ϵ @ 0.5 f'c (x 1E-3)	ϵ 'c (x 1E-3)	Secant Modulus GPa
28 days	47.98	23.99	0.717	1.9	33.46
6 wk	56.87	28.435	0.707	1.9	40.28
9 wk	46.94	23.47	1.076	2.8	21.81
12 wk	57.93	28.97	0.537	1.8	53.95

Table 17 - Analysis of Compression Results (NSC in Solution - Moderately Reactive)

Time	f'c (MPa)	0.5 f'c (MPa)	ϵ @ 0.5 f'c (x 1E-3)	ϵ 'c (x 1E-3)	Secant Modulus GPa
28 days	47.98	23.99	0.717	1.9	33.46
6 wk	56.15	28.08	1.343	2.8	20.9
9 wk	49.68	24.84	1.109	2.9	22.4
12 wk	48.78	24.39	1.059	2.8	23.04

4.2.4 Compression (HSC - Highly Reactive)

As previously stated, to the best of the author's knowledge, no effects of alkali-aggregate reactivity on the compressive strength of high strength concrete have been previously reported. However, due to the improved properties of high strength concrete, it is believed that the effects on material properties of specimens subjected to the aggressive NaOH solution will be minimal, if any, for specimens subjected to the de-ionized water, as well as those contained in the NaOH solution.

The stress - strain curves for the high strength concrete specimens subjected to the NaOH solution and the de-ionized water can be viewed in Figures 26 and 27, respectively. For the specimens subjected to solution, the stress-strain curve becomes much steeper after the 28 day period, experiencing an increase in strength of 18% during this time period, as well as decrease in strain at ultimate capacity of approximately 20%. These improvements in mechanical properties are again attributed to the secondary pozzolanic reaction, as mentioned in the preceding section, as well as the decreased permeability of the high strength specimens which resist the intrusion of the aggressive NaOH solution to initiate an alkali-aggregate reaction. However, as time in the NaOH solution bath increases, the strain at ultimate capacity increases slightly, even though the average strength of specimens stays nearly the same, increasing only by 6%. Refer to Tables 18 through 21 for results of high strength concrete compression testing using potentially highly reactive aggregate, aggregate E, and Figures 28 and 29, for plots containing the average strengths of specimens subjected to the NaOH solution, as well as de-ionized water.

All high strength concrete specimens subjected to the de-ionized water experienced a significant increase in overall strength after the initial 28 day curing period, with the average increase in strength being almost 21% after a period of 12 weeks. In addition, the strain of these concrete specimens at ultimate capacity remained, for the most part, equal to that determined during the 28 day testing. The only exception was the stress-strain curve of the six week test specimens. For some unknown reason, the 6 week stress - strain curve followed a trend unlike that seen with the 9, and 12 week test specimens, in that the strain experienced

at ultimate load increased by approximately 70%. Since reasons as to the generation of this stress - strain curve cannot be explained, it has been deemed an anomaly.

Figure 26 - High Strength Concrete in Solution (Highly Reactive)

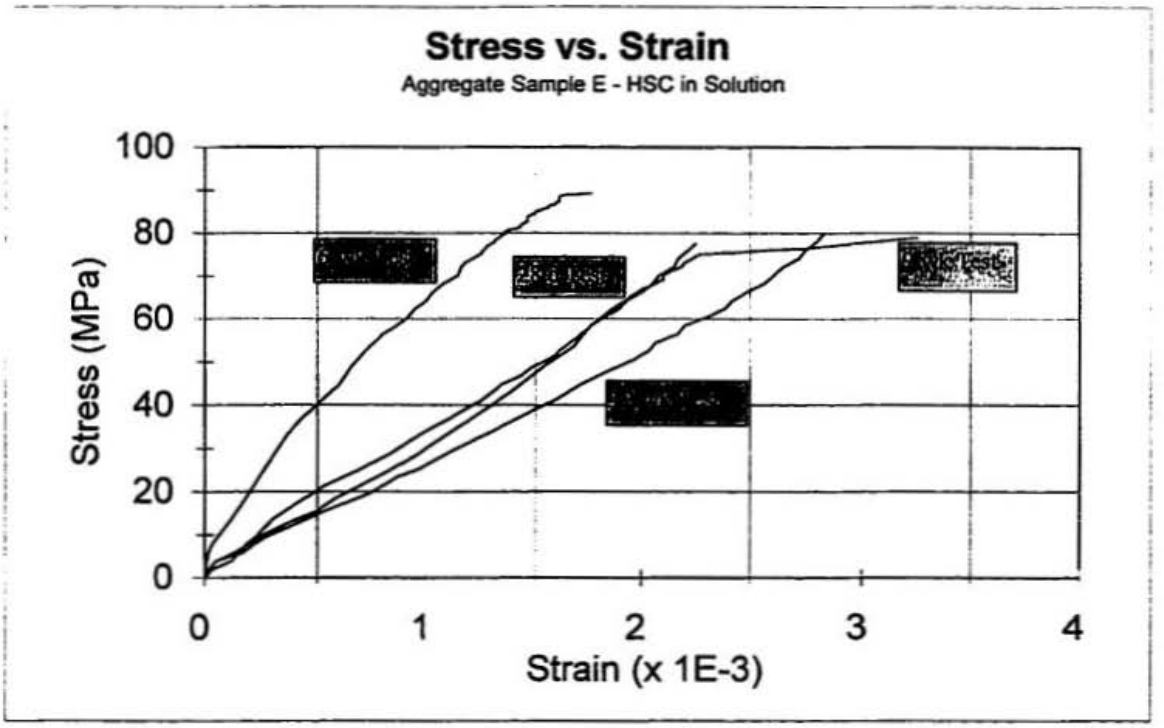

Figure 27 - High Strength Concrete in Water (Highly Reactive)

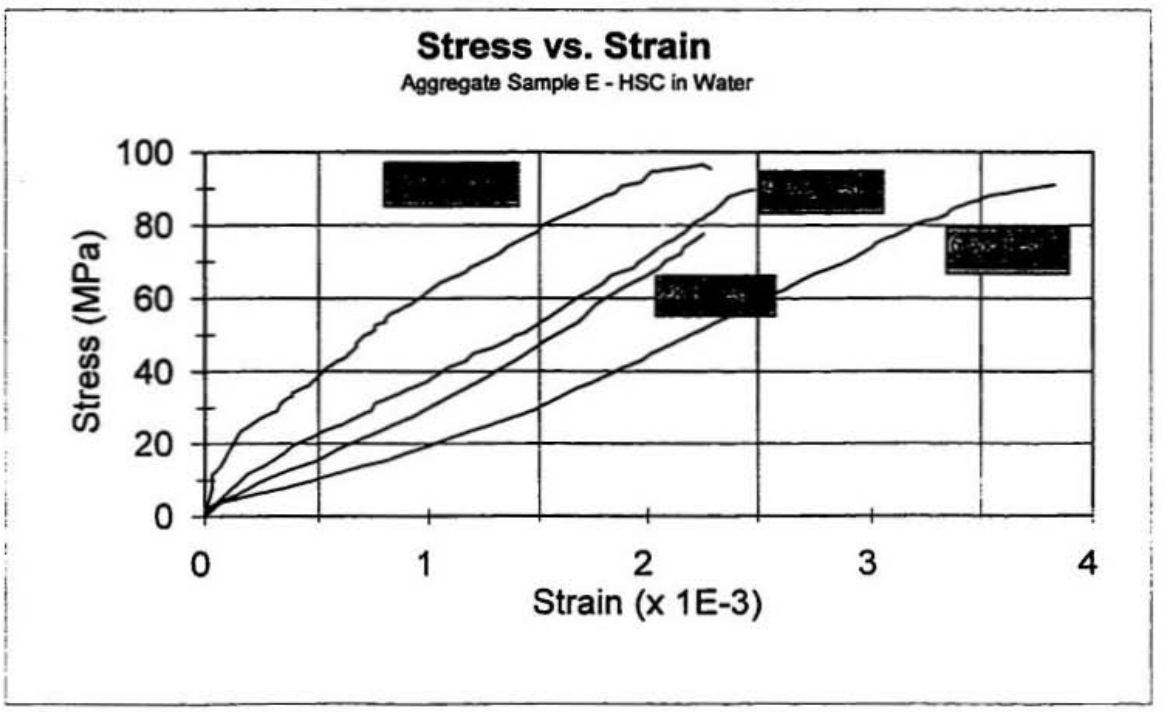

Figure 28 - Mean Strength vs. Time: HSC in Solution (Highly Reactive)

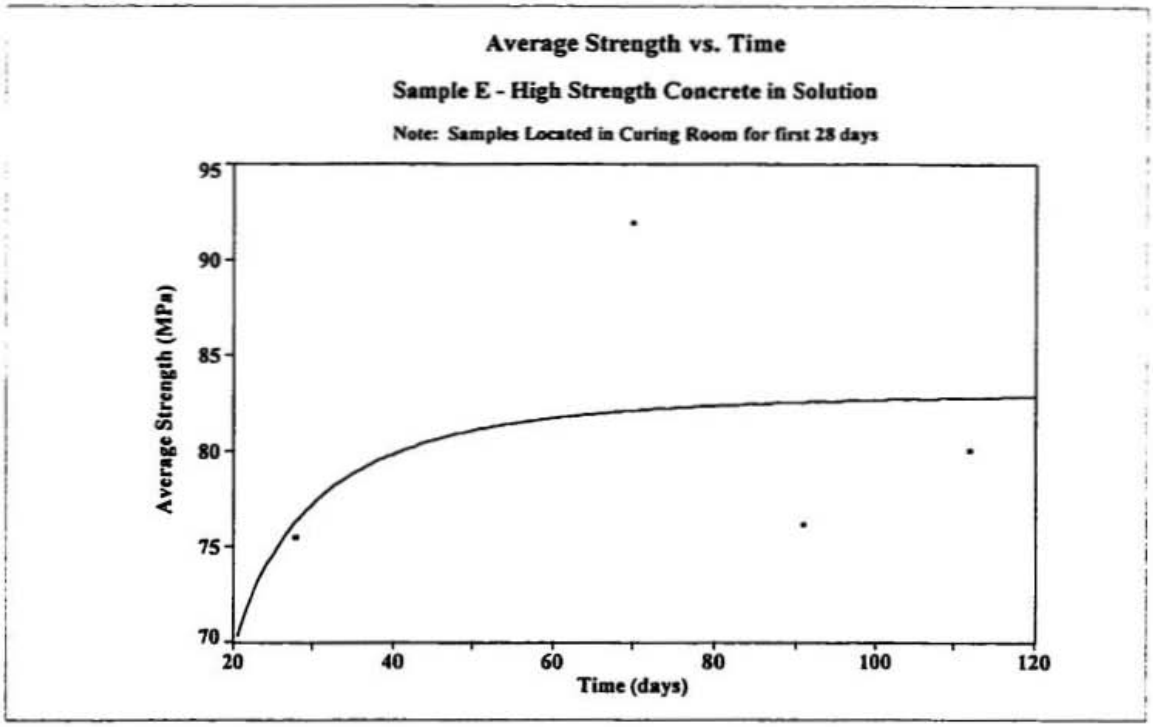

Figure 29 - Mean Strength vs. Time: HSC in Water (Highly Reactive)

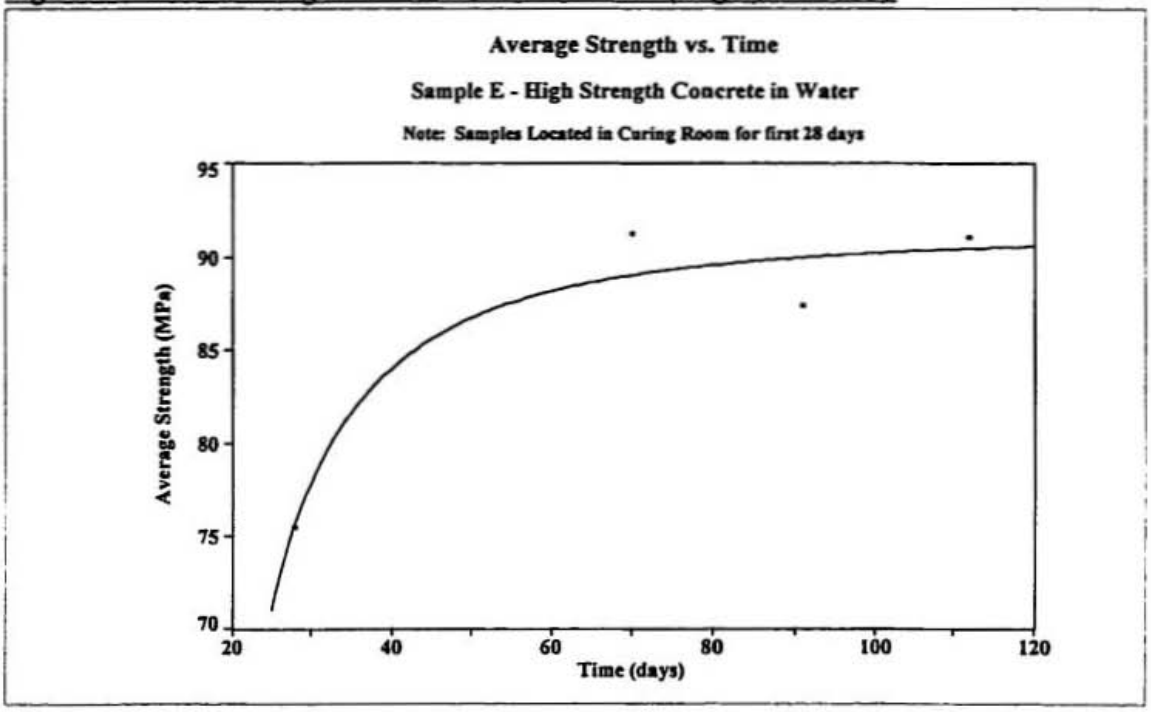

Table 18 - Compression Results - HSC in Solution (Highly Reactive)

Time (days)	Sample #	f'c MPa	Mean f'c Solution MPa	Std. Dev. Solution MPa	Avg. % of MAX f'c Solution	Coefficient of Variation
28 days	1 2 3	72.16 77.70 76.40	75.42	2.9	0.82 %	5.6
6 wk	1 2 3	96.12 90.32 89.35	91.93	3.66	1.00 %	8.93
9 wk	1 2 3	78.03 82.17 68.27	76.16	7.14	0.83 %	33.96
12 wk	1 2 3	79.98 79.01 80.96	79.98	0.98	0.87 %	0.63

Table 19 - Compression Results - HSC in Water (Highly Reactive)

Time (days)	Sample #	f'c MPa	Mean f'c Water MPa	Std. Dev. Water MPa	Avg. % of MAX f'c Water	Coefficient of Variation
28 days	1 2 3	72.16 77.70 76.40	75.42	2.9	0.83 %	5.6
6 wk	1 2 3	91.88 91.10 90.82	91.27	0.55	1.00 %	0.2
9 wk	1 2 3	89.73 86.23 86.16	87.37	2.04	0.96 %	2.78
12 wk	1 2 3	96.56 89.74 86.81	91.04	5	1.00 %	16.68

Table 20 - Compression Results - HSC in Water (Highly Reactive)

Time	f 'c (MPa)	0.5 f 'c (MPa)	∈ @ 0.5 f 'c (x 1E-3)	∈ 'c (x 1E-3)	Secant Modulus GPa
28 days	77.7	38.85	1.27	2.25	30.59
6 wk	89.35	44.675	0.6	1.77	74.46
9 wk	89.74	44.87	1.17	2.48	38.35
12 wk	95.59	47.8	0.67	2.28	71.34

Table 21 -Compression Results - HSC in Solution (Highly Reactive)

Time	f 'c (MPa)	0.5 f 'c (MPa)	∈ @ 0.5 f 'c (x 1E-3)	∈ 'c (x 1E-3)	Secant Modulus GPa
28 days	77.7	38.85	1.27	2.25	30.59
6 wk	91.1	45.55	2.04	3.83	22.33
9 wk	79.01	39.51	1.21	1.21	32.65
12 wk	79.98	39.99	1.54	1.54	25.97

4.2.5 Compression (HSC - Marginally Reactive)

The stress - strain curves for high strength concrete specimens subjected to water and solution after the initial 28 day curing period, as well as after being submerged in the respective baths for 6, 9, and 12 weeks, respectively, can be viewed in Figures 30 and 31. From these graphs, it is clear that the aggressive NaOH solution had little effect on the material properties determined from the compression testing. In fact, samples from both the de-ionized water, and the NaOH solution experienced the same trends. For instance, the ultimate strength of

samples subjected to the solution increased approximately 26% from the initial average 28 day ultimate strength with respect to samples submerged in the NaOH solution for a period of 12 weeks. For specimens subjected to the de-ionized water, the average ultimate strength of high strength concrete samples increased 30% from the initial ultimate strength observed after the initial 28 day testing to ultimate strengths recorded after being submerged in the de-ionized water for a period of 12 weeks. Refer to Tables 22 and 23 for ultimate strength results of all specimens, as well as, Figures 32 and 33 for plots of average ultimate strength of high strength concrete consisting of the potentially marginally reactive aggregate versus time.

Tables 24 and 25 indicate that the strains of both samples remained quite similar at the testing periods. Even though both samples show a moderate increase in strain at ultimate strength, the strains experienced are well within the acceptable range for high strength specimens (between 2E-3 and 3E-3) determined by Wee et al. (1996), and Farny et al.(1994), for specimens tested after an initial 28 day curing period.

These results indicate that the high strength concrete samples consisting of the potentially marginally reactive aggregate were not affected by an alkali-aggregate reaction.

Figure 30 - High Strength Concrete in Solution (Marginally Reactive)

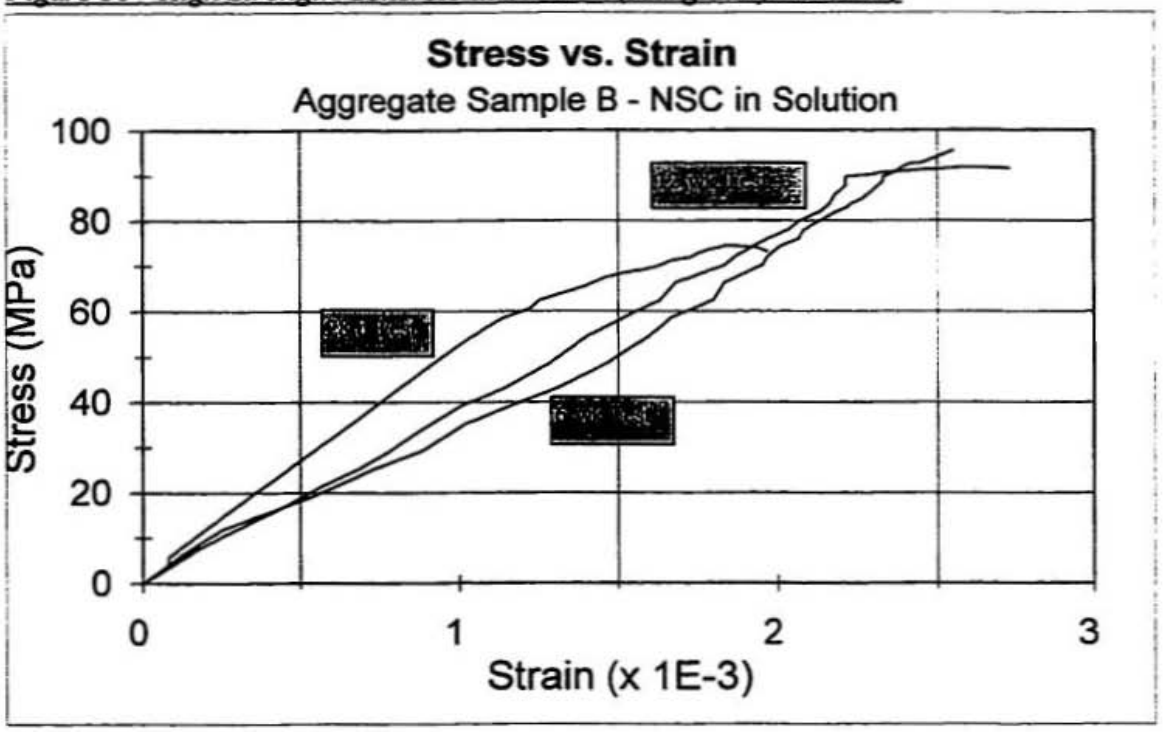

Figure 31 - High Strength Concrete in Water (Marginally Reactive)

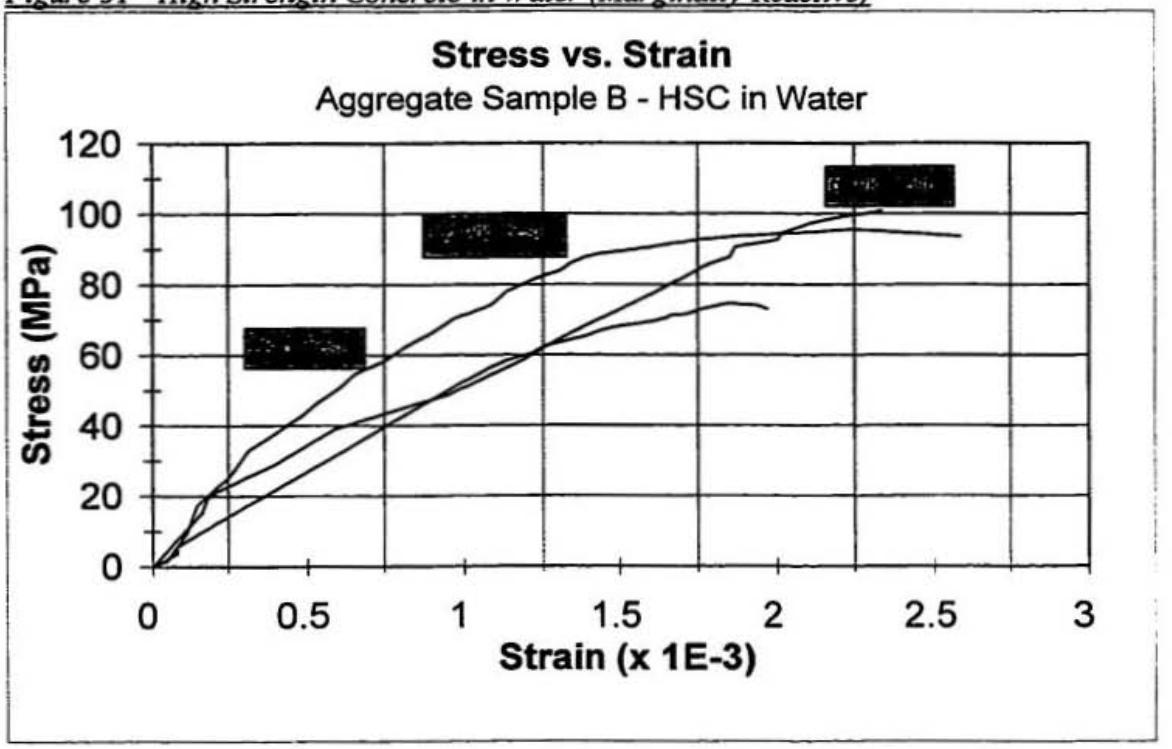

Figure 32 - Mean Strength vs. Time: HSC in Solution (Marginally Reactive)

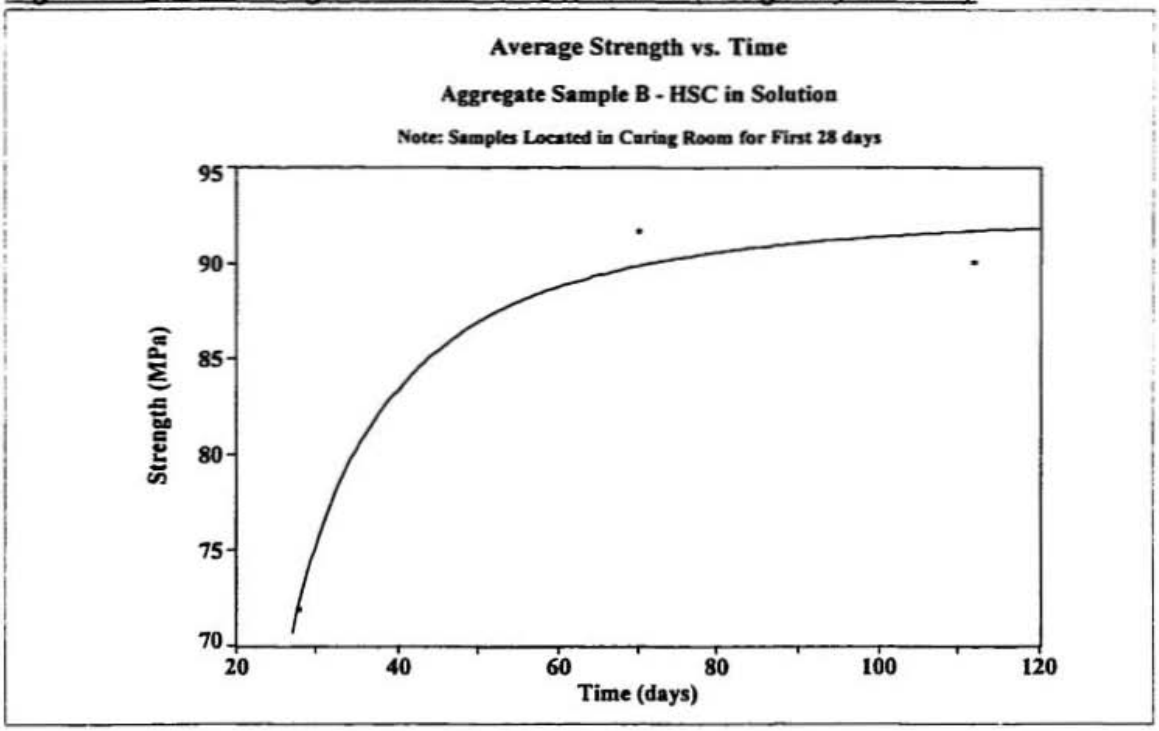

Figure 33 - Mean Strength vs. Time: HSC in Water (Marginally Reactive)

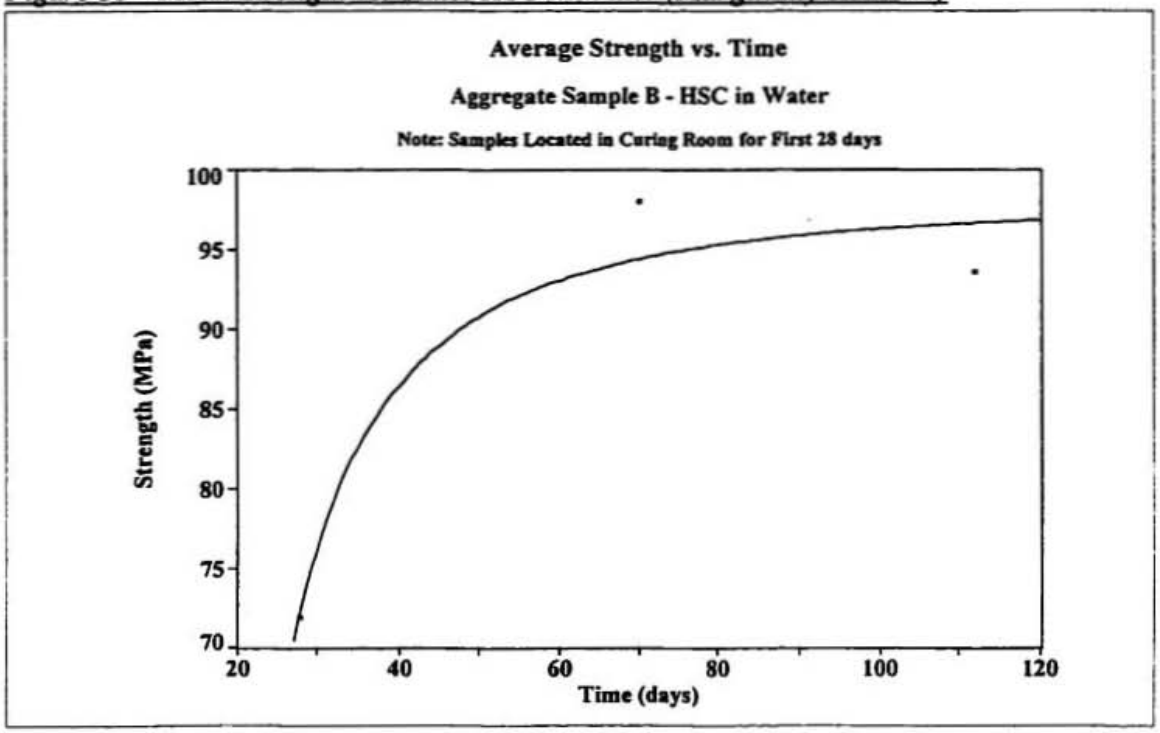

Table 22 - Compression Results - HSC in Solution (Moderately Reactive)

Time (days)	Sample #	f'c MPa	Mean f'c Solution MPa	Avg. % of MAX f'c Solution	Std. Dev. Solution MPa	Coefficient of Variation
28 days	1 2 3	74.52 69.06 72.18	71.92	0.78	2.74	7.51
6 wk	1 2 3	95.59 94.62 84.86	91.69	1	5.93	35.2
12 wk	1 2 3	85.84 92.66 91.69	90.69	0.98	3.69	13.64

Table 23 - Compression Results - HSC in Water (Moderately Reactive)

Time (days)	Sample #	f'c MPa	Mean f'c Water MPa	Avg. % of MAX f'c Water	Std. Dev. Water MPa	Coefficient of Variation
28 days	1 2 3	74.52 69.06 72.18	71.92	0.73	0.73	7.51
6 wk	1 2 3	102.42 100.96 90.71	98.03	1	1	40.67
12 wk	1 2 3	94.62 93.64 92.66	93.64	0.96	0.96	0.95

Table 24 - Analysis of Compression Results (HSC in Water - Moderately Reactive)

Time	f'c (MPa)	0.5 f'c (MPa)	ϵ @ 0.5 f'c (x 1E-3)	ϵ 'c (x 1E-3)	Secant Modulus GPa
28 days	74.52	37.26	0.36	1.85	103.5
6 wk	100.95	50.48	0.98	2.33	51.51
12 wk	93.64	46.82	0.53	2.58	88.34

Table 25 - Analysis of Compression Results (HSC in Solution - Moderately Reactive)

Time	f'c (MPa)	0.5 f'c (MPa)	ϵ @ 0.5 f'c (x 1E-3)	ϵ 'c (x 1E-3)	Secant Modulus GPa
28 days	74.52	37.26	0.36	1.85	103.5
6 wk	95.59	47.8	1.45	2.55	32.97
12 wk	91.69	45.85	1.23	2.73	37.28

4.3 Direct Tension Test Results

4.3.1 General

In has been only in recent years that the tensile strength of concrete has become a design parameter. Before this, the main parameter of concern was the ultimate strength of concrete after an initial 28 day curing period. However, not only is the compressive strength of concrete important, but also the behaviour of concrete under tensile stresses. In addition, cracking is a very important feature of concrete that is governed by its tensile properties.

To date, no test has been certified by the Canadian Standards Association (CSA) for the testing of concrete in direct tension. In the past, the tensile properties of concrete were investigated using indirect tension testing methods. However, Zhen-hai and Xiu-qin (1987), Philips and Binsheng (1993), as well as, Marzouk and Chen (1995) have investigated the response of normal and high strength concrete specimens in direct tension. Philips and Binsheng (1993) stated that uniaxial tests are the most direct experimental method of obtaining the stress-strain relationship, and better reflects the mechanical behaviour of concrete in tension than indirect tension tests.

The relationship between stress and strain of concrete specimens in direct tension has been described by Philips and Binsheng (1993) as follows. Stress of concrete specimens increases linearly with increasing strain, developing micro-cracks along the cement aggregate interface, at a point of approximately 70-80% f_t, which has both the effect of reducing the net effective area resisting the stress and increases the contribution of the cracks to the overall

strain. At this point, the concrete begins to behave in a non-linear fashion until the ultimate strength of the sample is reached. During the transition of the curve from the linear portion to the point at which ultimate stress is reached, the interfacial cracks propagate into the cement matrix, bridging aggregate particles. At the time of peak stress, the micro cracks begin to localize and form discrete macroscopic cracks, which in turn, cause the failure of the specimen.

Zhen-hai and Xiu-qin (1987) conducted direct tension test on plain normal strength concrete specimens of various water cement ratios arriving at very similar conclusions. It was concluded that the stress and strain of un-reinforced, normal strength concrete specimens, are proportional up to the elastic limit, which is usually at 40-60% of the ultimate stress. Subsequently, the strain of the concrete specimen increases quickly, resulting is the formation of a convex curve. From the specimens tested involving a similar mix design as to that conducted in this research, after the initial 28 day curing period, an average ultimate tensile stress of 2.43 MPa, and an average strain at ultimate stress of approximately 103 $\mu\epsilon$. This average value of ultimate tensile stress was determined to be approximately 6.65% of the compressive strength.

These results have been substantiated by Guo and Zhang (1987) who determined the average ultimate tensile stress of normal strength un-reinforced concrete specimens subjected to tension to be approximately 2.38 MPa, with an average strain at ultimate tensile stress to be approximately 106 $\mu\epsilon$ after an initial 28 day curing period. This average value of ultimate

tensile stress was determined to be approximately 5.92% of the corresponding compressive strength after an initial 28 day curing period.

Marzouk and Chen (1995) developed a testing procedure that allowed for the testing of normal and high strength concrete specimens in uniaxial or direct tension, and also arrived at very useful conclusions. After testing over 50 specimens, Marzouk and Chen (1995) determined that the strain of these high strength specimens at maximum tensile stress, tested after the initial 28 day testing period, measured between 100.5 and 136.9 $\mu\epsilon$. Furthermore, Marzouk and Chen (1995) determined that the direct tensile strength was recorded as being 4.8% of f 'c , where f 'c was the average ultimate stress of high strength concrete cylinders measured after the initial 28 day curing period. Testing of the normal strength specimens revealed that the direct tensile strength was determined to be approximately 8 % of f 'c.

It is important to note that the aforementioned research was conducted on normal and high strength specimens after the 28 day curing period, and that the research was being conducted to determine the stress - strain response of specimens only, and not the effect of an alkali - aggregate reaction on the specimens mechanical properties. However, these investigations do provide for a very meaningful starting point for the evaluation of the 28 day stress- strain response of all specimens, and provides a basis on which to analyse the response of specimens subjected to the de-ionized water and aggressive NaOH solution after a period of 12 weeks.

4.3.2 Direct Tensile Strength (NSC - Highly Reactive)

Results of normal strength concrete specimens tested in direct tension consisting of the potentially highly reactive aggregate, sample E, indicate that the tensile properties of specimens after the initial 28 day curing period agree quite well with the material properties as determined by Zhen-hai and Xiu-qin (1987), Philips and Binsheng (1993). For instance, the average ultimate tensile strength, f_t, was determined to be 2.85 MPa, with the strain at ultimate capacity being approximately 115 $\mu\epsilon$. This ultimate strength was determined to be 6.72 % of the compressive strength of cylinders tested of the same mix design after the initial 28 day curing period. Refer to Figures 34, 35, and 36, for plots of stress versus strain, and average percent of ultimate strength at 28 days versus time, respectively. In addition, Tables 26 and 27 include data regarding the tension testing results for specimens contained in both the water and solution.

Samples submerged in the de-ionized water were determined to approximately maintain the ultimate strength level for all other periods of testing. It was reasoned that since the de-ionized water would not initiate an alkali-aggregate reaction that there would be not change in material properties. However, samples subjected to the NaOH solution show a significant 40% decrease in the ultimate tensile strength over a period of 12 weeks. The ultimate strain of specimens after being submerged in the respective solutions did not show a difference at the 12 week testing period.

Figure 34 - Direct Tensile Stress vs. Strain (NSC - Highly Reactive)

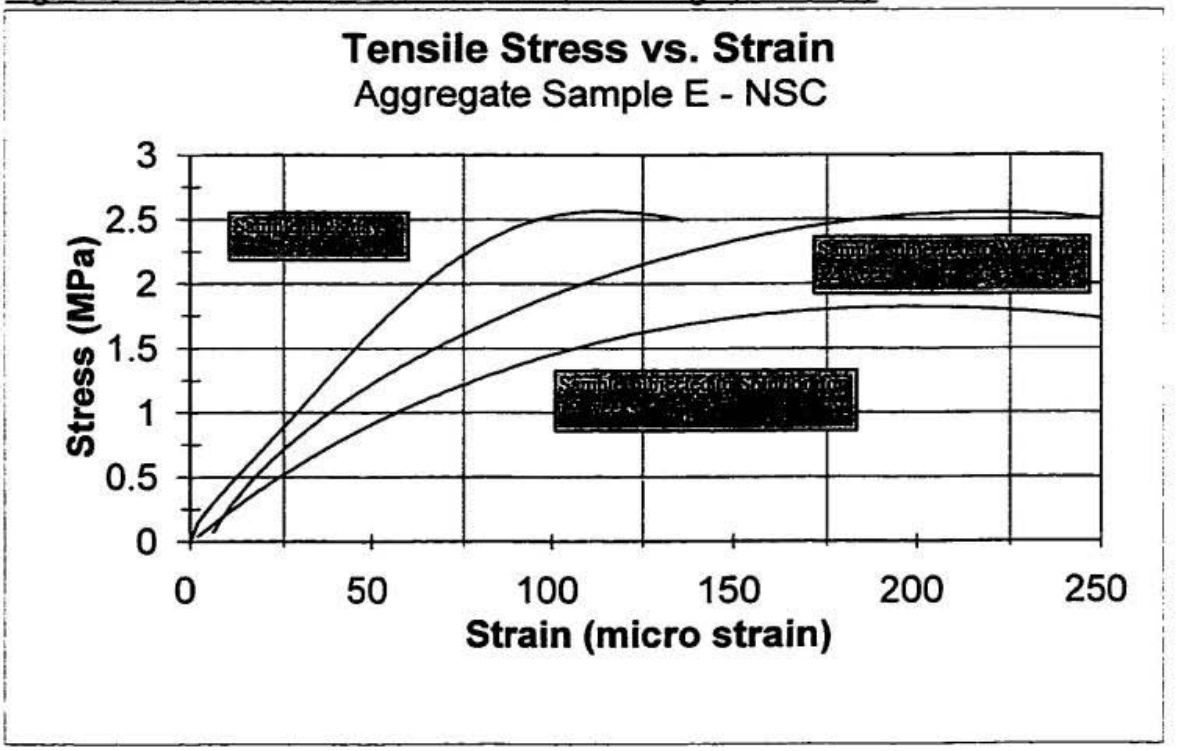

Figure 35 - Average % of f 'c (NSC in Solution - Highly Reactive)

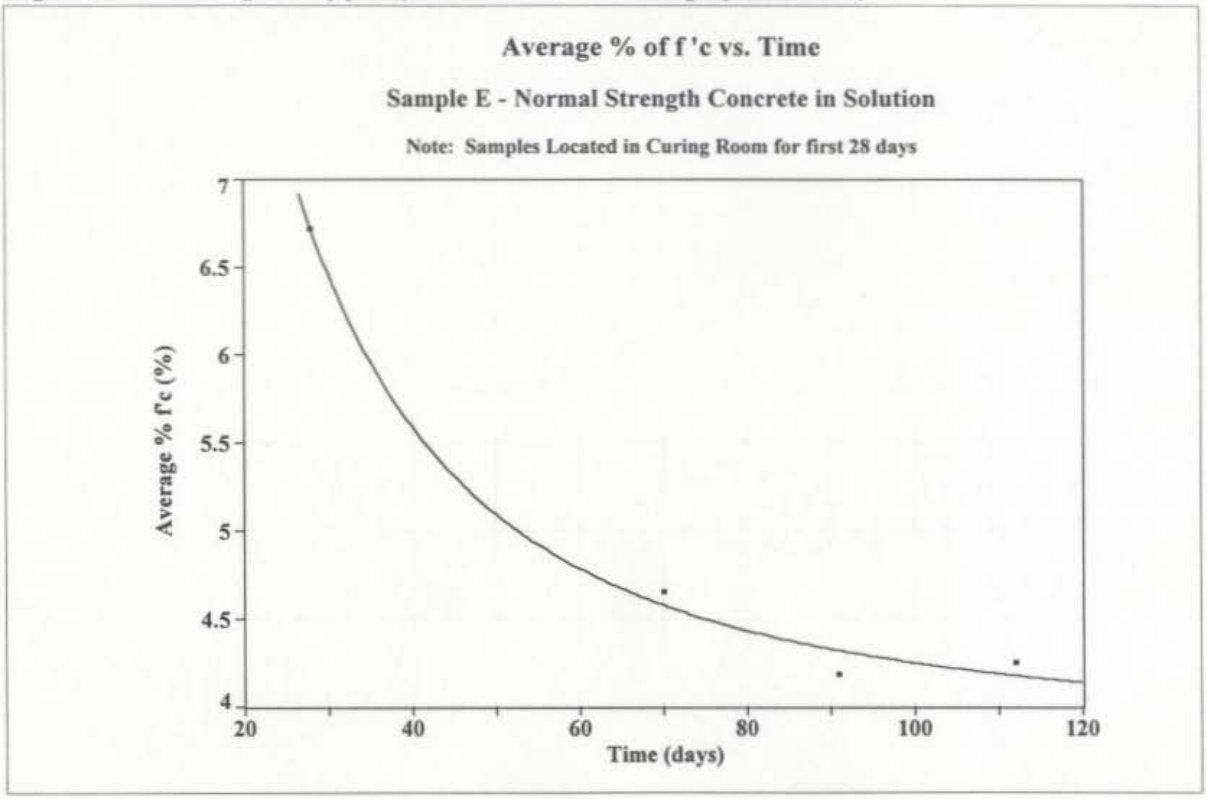

Figure 36 - Average % of f 'c (NSC in Water - Highly Reactive)

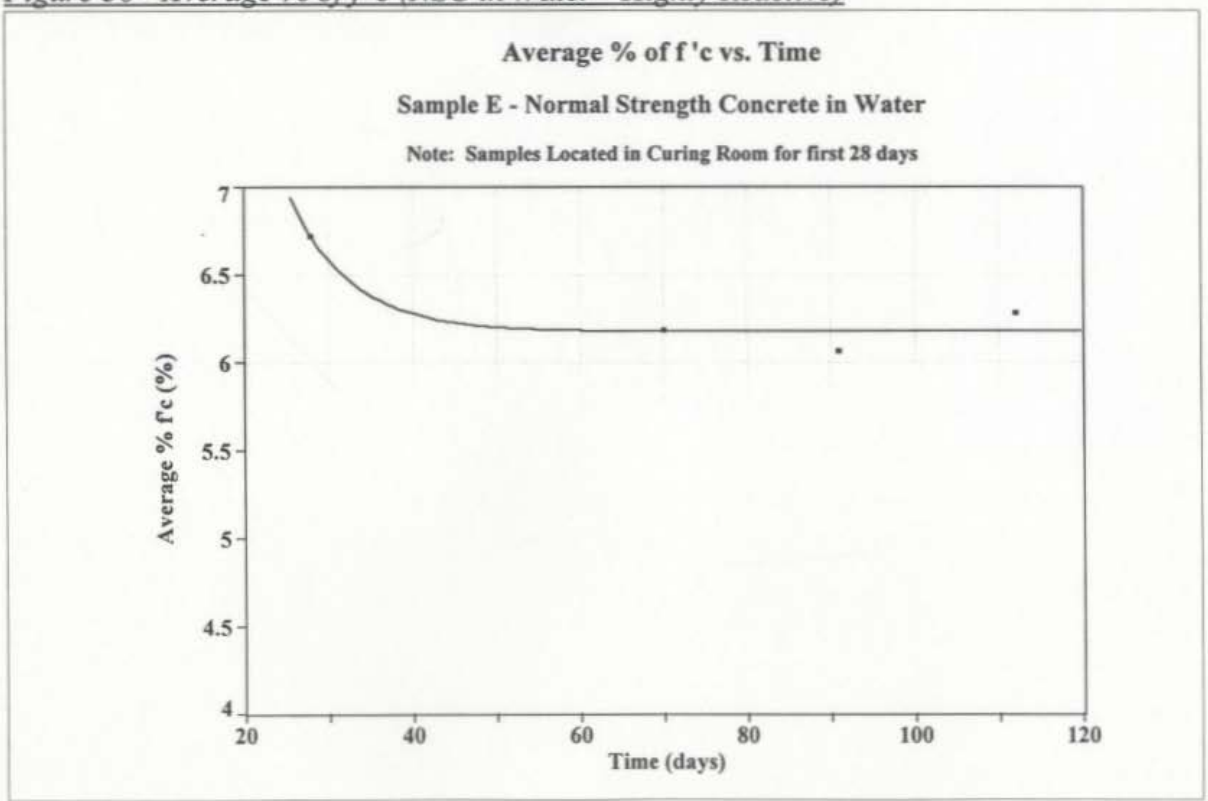

Table 26 - Tension Results (NSC in Solution - Highly Reactive)

Time (days)	Sample #	f_t MPa	Mean f_t Solution MPa	Avg. % of f 'c Solution	Std. Dev. Solution MPa	Coefficient of Variation
28 days	1 2 3	2.56 2.94 3.05	2.85	6.72 %	0.26	0.07
6 wk	1 2 3	2.00 2.08 1.84	1.97	4.65 %	0.12	0.01
9 wk	1 2 3	1.80 1.69 1.83	1.77	4.18 %	0.08	0.01
12 wk	1 2 3	1.92 1.81 1.67	1.8	4.25 %	0.12	0.01

Table 27 - Tension Results (NSC in Water - Highly Reactive)

Time (days)	Sample #	f_t MPa	Mean f_t Solution MPa	Avg. % of f 'c Solution	Std. Dev. Solution MPa	Coefficient of Variation
28 days	1 2 3	2.56 2.94 3.05	2.85	6.72 %	0.26	0.07
6 wk	1 2 3	2.77 2.38 2.71	2.62	6.18 %	0.21	0.04
9 wk	1 2 3	2.57 2.43 2.70	2.57	6.06 %	0.13	0.02
12 wk	1 2 3	2.95 2.84 2.19	2.66	6.28 %	0.41	0.17

4.3.3 Direct Tensile Strength (NSC - Moderately Reactive)

Testing results from normal strength concrete samples consisting of the potentially marginally reactive aggregate in direct tension also agrees quite well with results of previous experimentation by Zhen-hai and Xiu-qin (1987), Philips and Binsheng (1993). From the stress - strain diagram located in Figure 37, it can be seen that the ultimate tensile strength of the specimen was 2.78 MPa, with a corresponding strain 96 $\mu\epsilon$. The ultimate tensile strength amounted to 6.77 % of the ultimate compressive strength as measured after the initial 28 day curing period. These results also compare quite well with those determined from the normal strength concrete tested in direct tension utilizing the potentially highly reactive aggregate. Results using aggregate E recorded an ultimate tensile strength of 2.85 MPa (which amounted to 6.72 % of the ultimate compressive strength recorded at 28 days), and a corresponding strain at ultimate capacity of 115 $\mu\epsilon$. This is to be expected since both samples have not been subjected to the aggressive solution bath which would promote an alkali-aggregate reaction.

Samples located in the de-ionized water showed no apparent loss in ultimate tensile strength over the 12 week testing period. In fact, these specimens experienced a 6 % increase in ultimate tensile strength. However, an increase in the strain at ultimate tensile strength did increase to become approximately 230 $\mu\epsilon$.

Samples located in the NaOH solution showed a decrease in ultimate tensile strength of approximately 30% over the 12 week testing period. This decrease is slightly less than the

40% decrease experience from testing the samples that consisted of the more reactive aggregate, as was expected. In addition, the strain associated with the ultimate tensile strength was determined to be approximately 280 $\mu\epsilon$ at the time of failure, a 20 % increase from the ultimate strain of samples located in the de-ionized water.

Refer to Figures 38 and 39 for plots of average percent of ultimate compressive strength with time, as well as Tables 28 and 29 for tensile data analysis of samples from both environments.

Figure 37 - Direct Tensile Stress vs. Strain (NSC - Moderately Reactive)

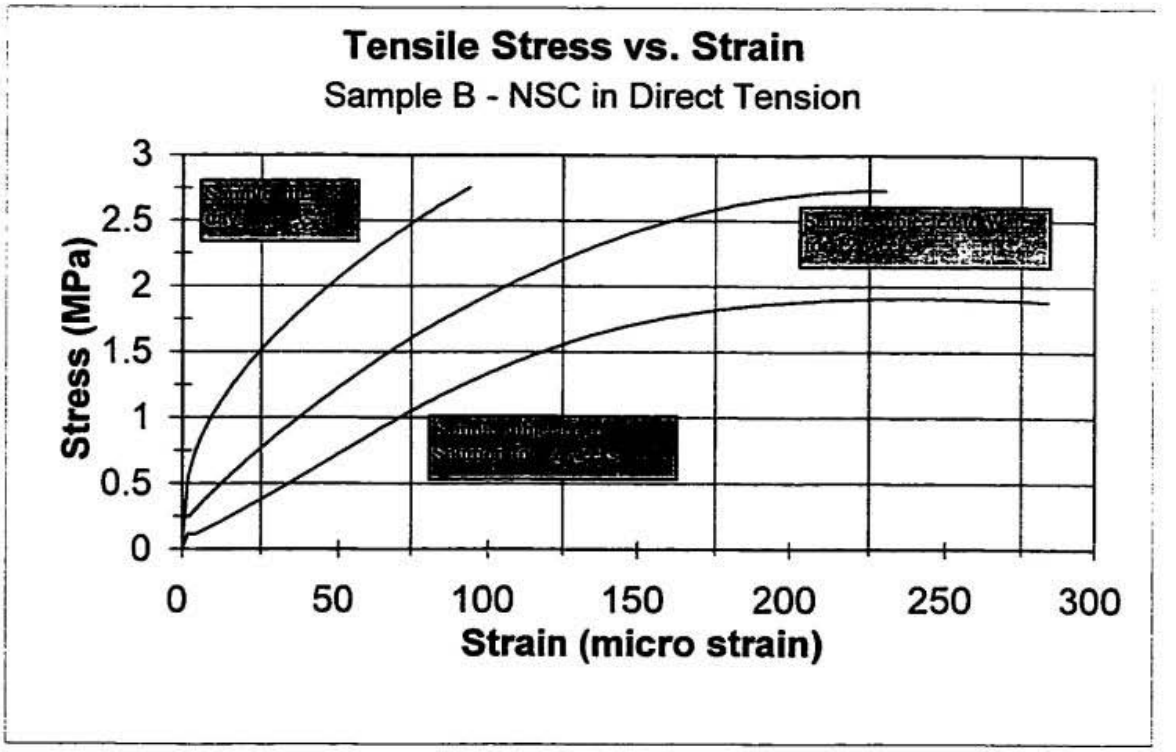

Figure 38 - Average % of f 'c (NSC in Solution - Moderately Reactive)

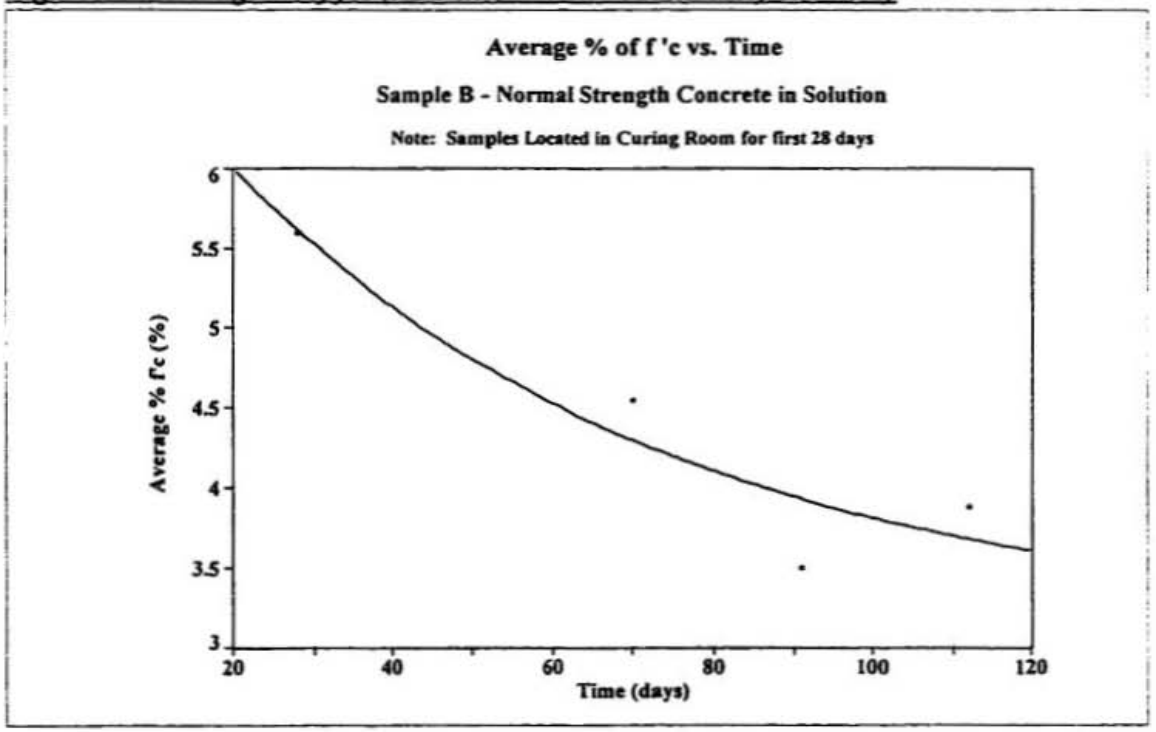

Figure 39 - Average % of f 'c (NSC in Water - Moderately Reactive)

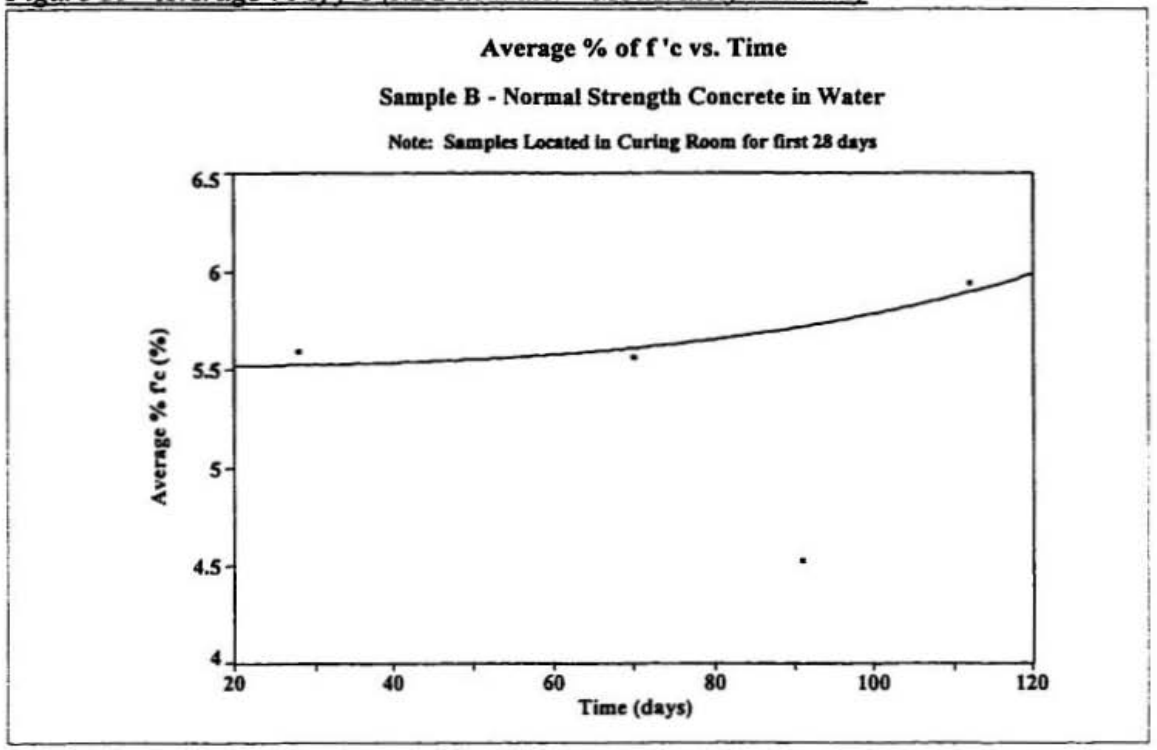

Table 28 - Tension Results (NSC in Solution - Moderately Reactive)

Time (days)	Sample #	f_t MPa	Mean f_t Solution MPa	Avg. % of f'c Solution	Std. Dev. Solution MPa	Coefficient of Variation
28 days	1 2 3	2.20 2.76 2.90	2.62	5.59 %	0.37	0.14
6 wk	1 2 3	2.07 2.35 1.96	2.13	4.54 %	0.2	0.04
9 wk	1 2 3	1.59 1.78 1.56	1.64	3.50 5	0.12	0.01
12 wk	1 2 3	1.93 1.62 1.90	1.82	3.88 %	0.17	0.03

Table 29 - Tension Test (NSC in Water - Moderately Reactive)

Time (days)	Sample #	f_t MPa	Mean f_t Solution MPa	Avg. % of f'c Solution	Std. Dev. Solution MPa	Coefficient of Variation
28 days	1 2 3	2.20 2.76 2.90	2.62	5.59 %	0.37	0.14
6 wk	1 2 3	2.78 2.61 2.42	2.61	5.56 %	0.18	0.03
9 wk	1 2 3	2.11 2.23 2.03	2.11	4.52 %	0.1	0.01
12 wk	1 2 3	2.63 3.04 2.69	2.79	5.94 %	0.22	0.05

4.3.4 Direct Tensile Strength (HSC - Highly Reactive)

As previously stated, Marzouk and Chen (1995) conducted research regarding high strength concrete specimens in direct tension. Using a similar testing procedures, with like samples, it was concluded that the 28 day average ultimate tensile strength of high strength concrete tested in direct tension was approximately 3.29 MPa, and that the corresponding average ultimate strain was measured as 122.0 $\mu\epsilon$. High strength concrete specimens tested throughout this investigation resulted in a 28 day ultimate tensile strength of 3.52 MPa, and a corresponding ultimate strain of 150 $\mu\epsilon$. These results are in good agreement considering slightly different mix designs, testing procedures, and sample sizes. In addition, Marzouk and Chen (1995) determined that the average ultimate tensile strength of the high strength concrete was approximately 4.8 % f 'c, whereas direct tension testing of high strength concrete using the highly reactive aggregate resulted in an average ultimate tensile strength of 4.9 %. Once again, these results are in good agreement. Refer to Figures 40 through 42, as well as Tables 30 and 31 for direct tension results and analysis of high strength concrete utilizing the potentially reactive aggregate.

Figure 41 indicates that the samples subjected to the NaOH solution experienced a continual decrease in ultimate tensile strength throughout the testing duration. At, the 12 week testing period, the ultimate tensile strength had decreased approximately 25 %, resulting in an average ultimate tensile strength of 2.71 MPa, or 3.71 % of f'c. However, figure 41 indicates that samples located in the de-ionized water increased in ultimate tensile strength by

approximately 35 %, resulting in an average ultimate tensile strength of 4.82 MPa, or 6.7 % of f'c.

These result seem to indicate that the high strength direct tension specimens located in the NaOH solution may have been more affected than the high strength compression specimens. This may be attributed to the fact that the tension specimens are only 37.5 mm thick, where as the compression specimens are 76.2 mm thick. As a result of this, more deleterious ions may have permeated the direct tension specimens, and promoted an alkali-aggregate reaction. In addition, the aggressive solution may have negated the effects of the secondary pozzolanic reaction of high strength concrete, which results in an improvement in strength, and micro structure. Furthermore, as previously stated, it is known that a decrease in material properties of samples subjected to an alkali-aggregate reaction are much more pronounced in tension testing than in compression testing due to the nature of crack formation.

Nonetheless, the high strength sample utilizing the potentially highly reactive aggregate in direct tension did not show an increase in strain associated with ultimate tensile strength.

Figure 40 - Direct Tensile Stress vs. Strain (HSC - Highly Reactive)

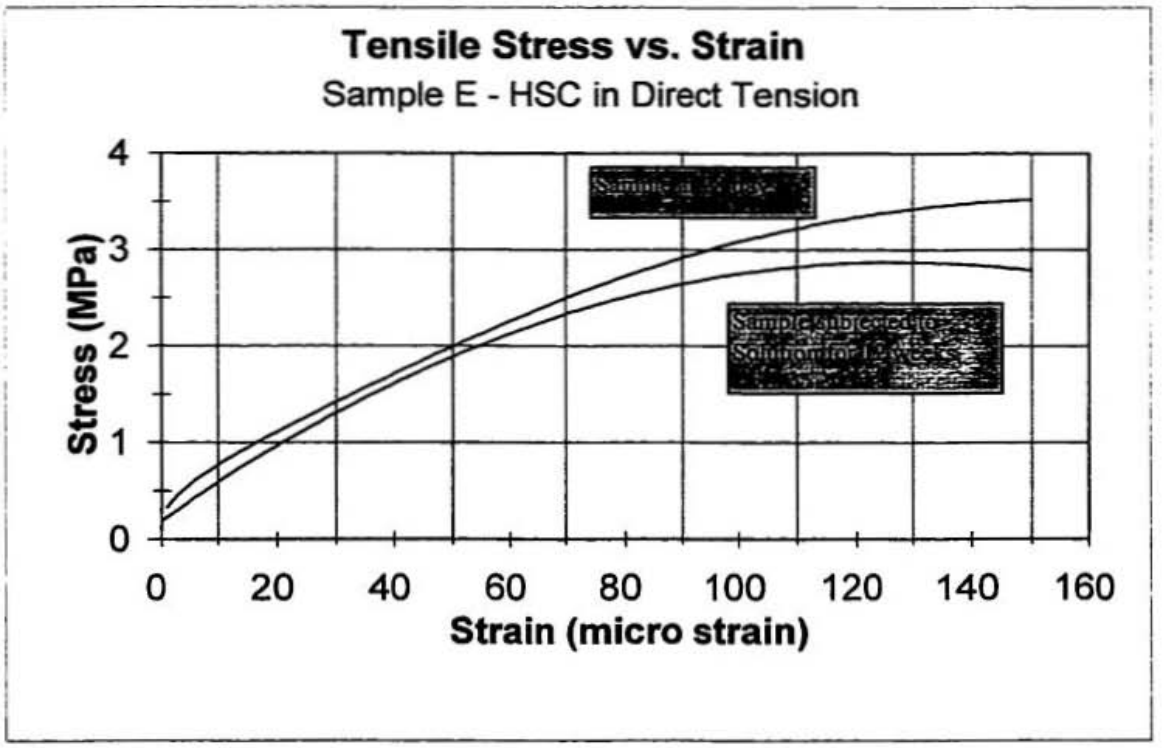

Figure 41 - Average % of f 'c (HSC in Solution - Highly Reactive)

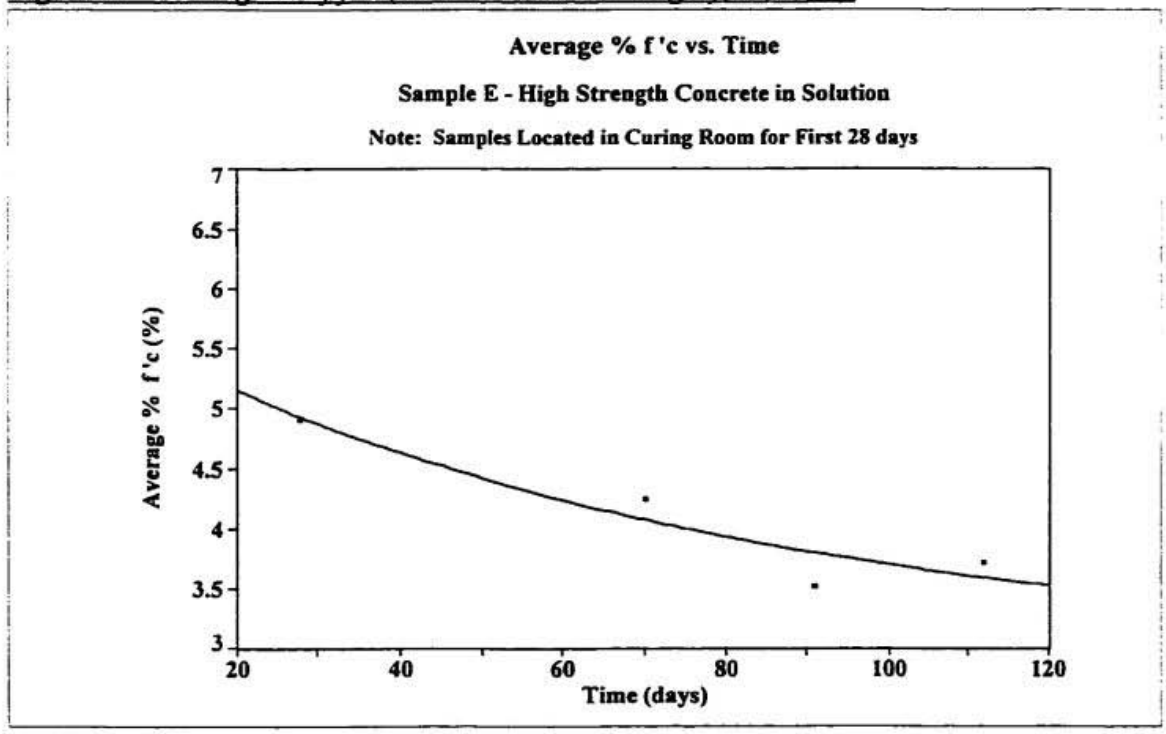

Figure 42 - Average % of f 'c (HSC in Water - Highly Reactive)

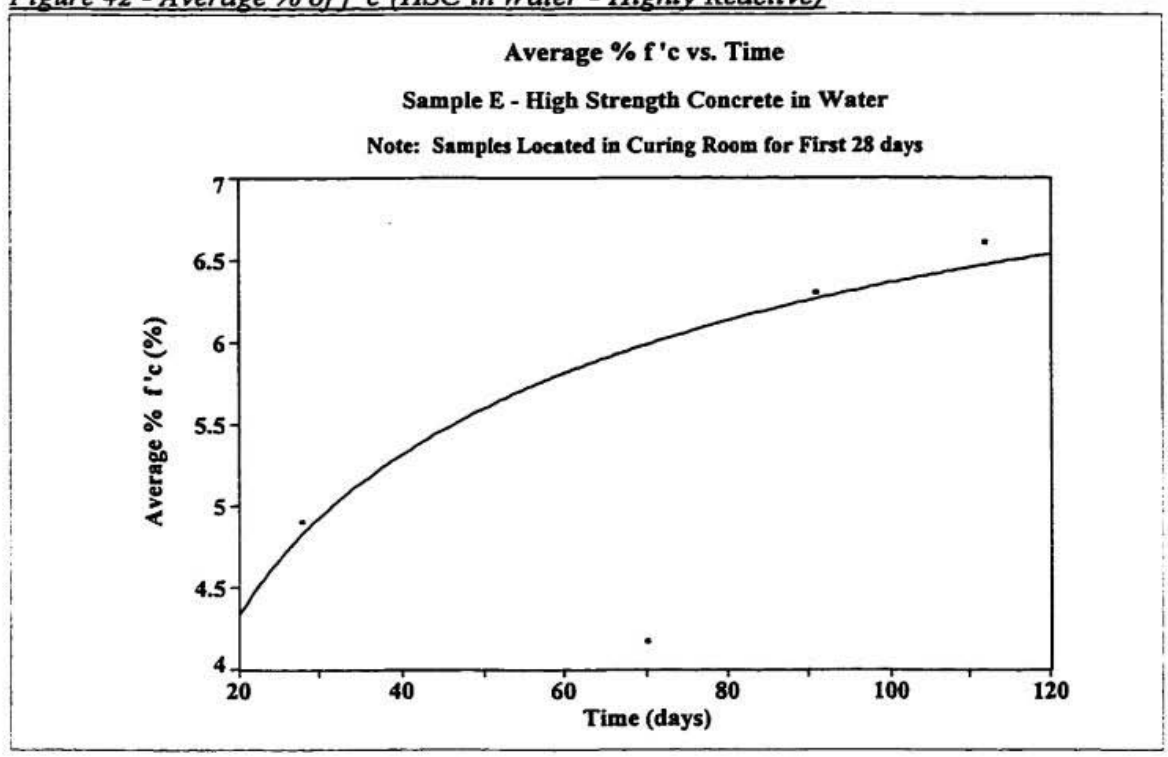

Table 30 - Tension Results (HSC in Solution - Highly Reactive)

Time (days)	Sample #	f_t MPa	Mean f_t Solution MPa	Avg. % of f'c Solution	Std. Dev. Solution MPa	Coefficient of Variation
28 days	1 2 3	3.71 3.45 3.57	3.58	4.90 %	0.13	0.02
6 wk	1 2 3	3.15 4.34 5.23	3.1	4.24 %	0.76	0.58
9 wk	1 2 3	3.40 3.45 3.68	2.56	3.51 %	0.11	0.01
12 wk	1 2 3	3.79 3.47 3.88	2.71	3.71 %	0.16	0.02

Table 31 - Tension Results (HSC in Water - Highly Reactive)

Time (days)	Sample #	f_t MPa	Mean f_t Solution MPa	Avg. % of f'c Solution	Std. Dev. Solution MPa	Coefficient of Variation
28 days	1 2 3	3.71 3.45 3.57	3.58	4.90 %	0.13	0.02
6 wk	1 2 3	4.63 4.27 3.63	3.05	4.17 %	0.37	0.14
9 wk	1 2 3	6.86 5.31 6.72	4.6	6.30 %	0.62	0.39
12 wk	1 2 3	6.25 6.73 6.84	4.82	6.70 %	0.23	0.05

4.3.5 Direct Tensile Strength (HSC - Marginally Reactive)

Stress - strain results from testing the high strength concrete in direct tension utilizing the potentially marginally reactive aggregate show that the 28 day ultimate tensile strength was 2.46 MPa, with a corresponding strain at ultimate strength of 250 $\mu\epsilon$. This ultimate tensile strength is approximately 3.42 % of the relating 28 day compressive strength, which is slightly lower than that provided through testing the high strength direct tension samples using the highly reactive aggregate. Refer to Figure 43 for stress - strain plot of the 28 day testing period samples.

Figures 44 and 45 represent the average ultimate strength of high strength specimens consisting of the marginally reactive aggregate (sample B) as a percentage of the corresponding 28 day ultimate compressive strength. From these figures, it is clear that both samples located in the water, and in the solution, experience a gain in ultimate tensile strength with time, similar to that of the high strength concrete consisting of the highly reactive aggregate. The trend curve fitted through both data sets show the 12 week ultimate tensile strength as approximately 3.5 % for samples located in the de-ionized water, and slightly over 3.5 % for samples located in solution.

The point associated with the 12 week break on Figure 44 was not considered when fitting the general trend. This was due to the fact the one of the direct tensile strengths recorded during testing was extremely low, and as a result was considered an anomaly. However, the

point was still considered in determining the average ultimate tensile strength for that testing period. Refer to Tables 32, and 33 for test results.

Figure 43 - Direct Tensile Stress vs. Strain (HSC - Moderately Reactive)

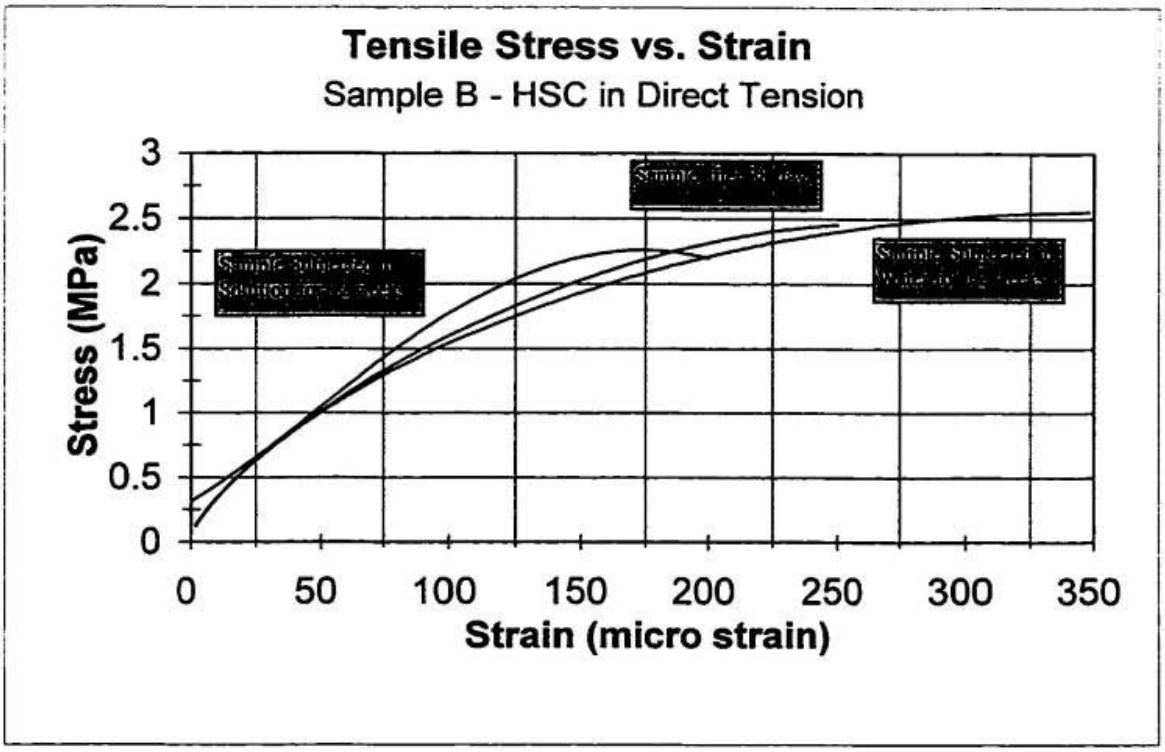

Figure 44 - Average % of f 'c (HSC in Solution - Moderately Reactive)

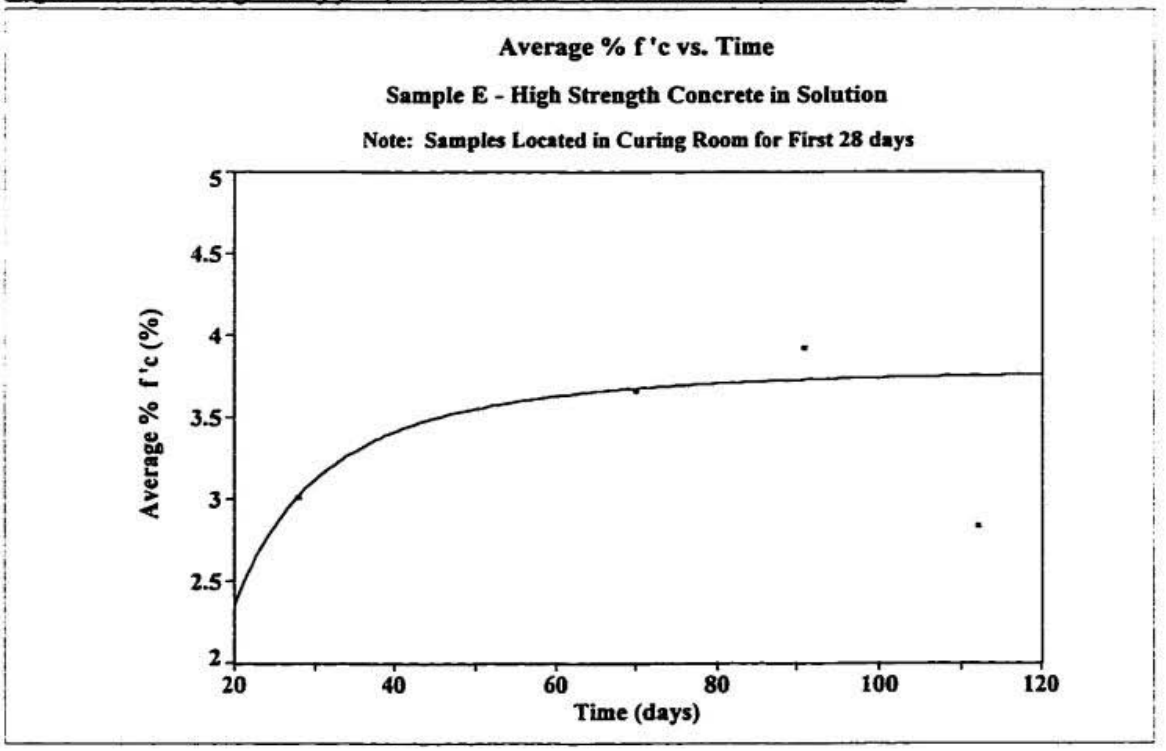

Figure 45 - Average % of f 'c (HSC in Water - Moderately Reactive)

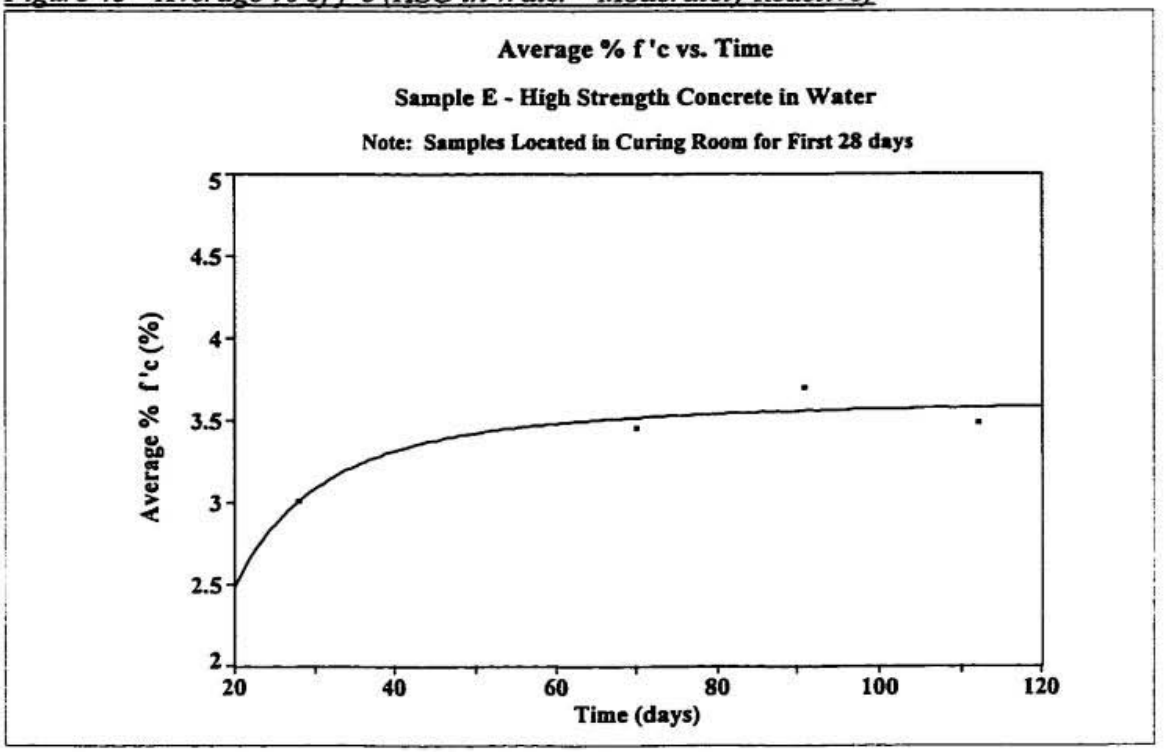

Table 32 - Tension Results (HSC in Solution - Moderately Reactive)

Time (days)	Sample #	f_t MPa	Mean f_t Solution MPa	Avg. % of f'c Solution	Std. Dev. Solution MPa	Coefficient of Variation
28 days	1 2 3	2.04 2.22 2.24	2.17	3.01 %	0.11	0.01
6 wk	1 2 3	2.70 2.62 2.58	2.63	3.66 %	0.06	0
9 wk	1 2 3	3.17 2.33 2.95	2.82	3.92 %	0.44	0.19
12 wk	1 2 3	2.16 2.16 1.79	2.04	2.83 %	0.22	0.05

Table 33 - Tension Results (HSC in Water - Moderately Reactive)

Time (days)	Sample #	f_t MPa	Mean f_t Solution MPa	Avg. % of f'c Solution	Std. Dev. Solution MPa	Coefficient of Variation
28 days	1 2 3	2.04 2.22 2.24	2.17	3.01 %	0.11	0.01
6 wk	1 2 3	2.87 2.29 2.28	2.48	3.45 %	0.34	0.11
9 wk	1 2 3	3.64 2.04 2.31	2.66	3.70 %	0.44	0.74
12 wk	1 2 3	2.41 2.55 2.55	2.5	3.48 %	0.08	0.01

4.4 Indirect Tension Results

4.4.1 General

In determining the tensile behaviour of concrete, researchers have relied on indirect tension testing methods (Clark (1990), Swamy and Al-Asali (1988)). The reasoning of such testing methods is that there is no CSA certified test that allows for the determination of the tensile parameters of concrete using the application of direct or uniaxial force. As a result, the indirect tension method has been the method of choice. ASTM C293-79 allows for the determination of the ultimate tensile strength of concrete prisms subjected to an indirect load, which is called the modulus of rupture, R . It is this parameter that is used in determination of the effects of an alkali-aggregate on the indirect tensile properties of concrete.

Research conducted by Swamy and Al-Asali (1988), and Swamy (1992) indicated that losses of 30% to 85% could occur depending on the aggregate type, and the exact testing regime utilized. However, the results from each particular investigation, are only relevant to that investigation. Direct comparison of results from all other research is not accurate since the results obtained are too affected by a multitude of parameters.

The following sections investigate the effects of an alkali-aggregate reaction on the modulus of rupture of concrete using two different aggregates.

4.4.2 Modulus of Rupture (NSC - Highly Reactive)

For the normal strength concrete samples consisting of the potentially reactive aggregate, the results show both the samples located in the water, and samples located in the solution, experience an increase in overall strength with time. The modulus of rupture of samples located in the NaOH solution, increase in strength from 4.16 MPa to 5.46 MPa over the 12 week testing period. This represents an increase of 30%. Samples located in the de-ionized water also experience in increase in the Modulus of Rupture from 4.16 MPa, to 5.65 MPa, over the same time frame. This represents an overall increase of approximately 36 %. Refer to Figures 46 and 47, as well as, Tables 34 and 35, for results and analysis for these specimens.

It was initially hypothesized that samples located in the NaOH solution would experience a decrease in overall indirect tensile strength for all of the testing periods. However, this is obviously not the case, and contradicts the findings of other researchers. Nonetheless, sample size may have attributed to achieving the increasing trend for the samples located in the solution. It would have taken much longer for the deleterious NaOH solution to permeate the larger prism samples (75 mm x 75 mm), than it would have to permeate the direct tension specimens (37.5 mm x 75 mm) to promote micro crack formation. However, since other researchers have shown the indirect tension test to be sensitive to the effects of alkali - aggregate reactivity (Swamy and Al-Asali (1988), and Clark (1990)), these results are deemed inconclusive. Moments may have been introduced if there was any eccentricity of the loading ram, or the load may not have been applied evenly, thus decreasing the net load bearing area.

Figure 46 - Avg. R vs. Time (NSC in Solution - Highly Reactive)

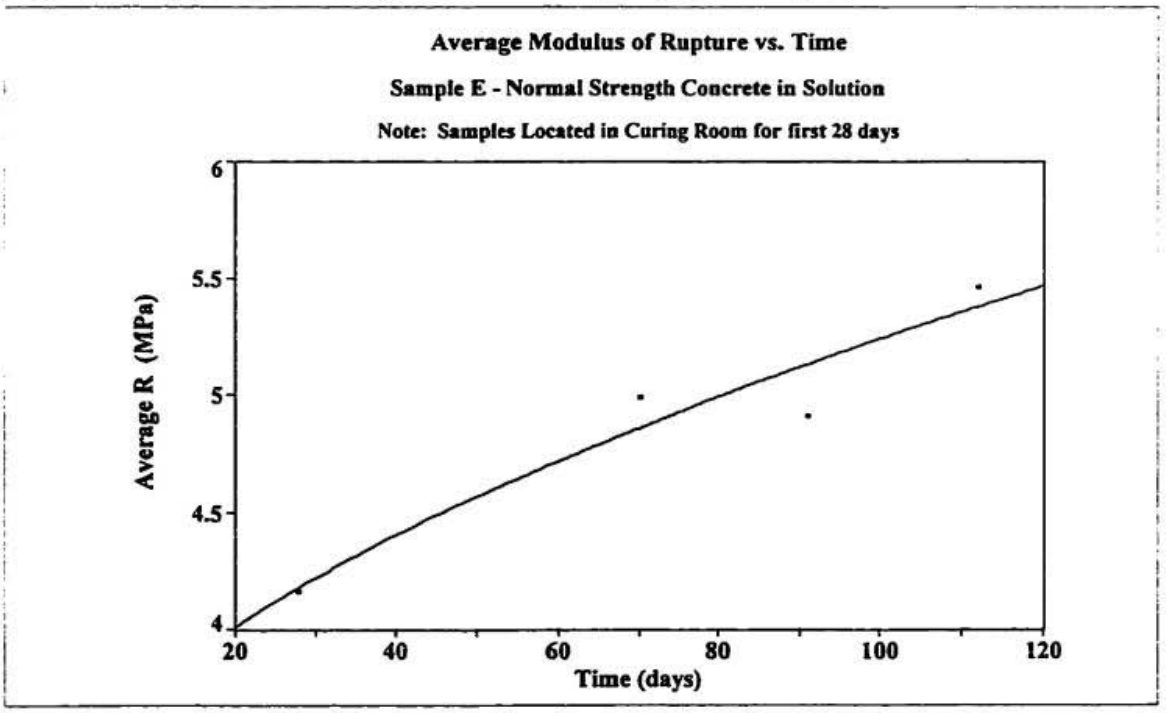

Figure 47 - Avg. R vs. Time (NSC in Water - Highly Reactive)

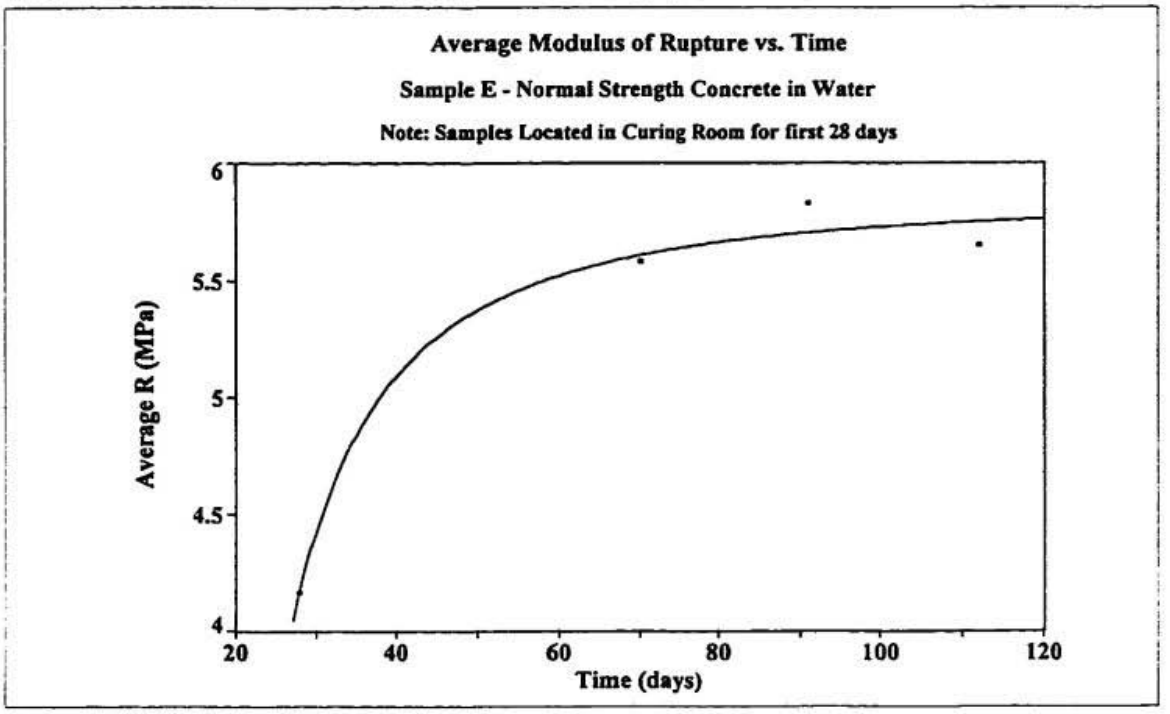

Table 34 - Indirect Tension Results (NSC in Solution - Highly Reactive)

Time (days)	Sample #	R MPa	Mean R Solution MPa	Avg. % of f'c Solution	Std. Dev. Solution MPa	Coefficient of Variation
28 days	1 2 3 4	5.04 4.00 3.92 3.76	4.16	9.81 %	0.51	0.26
6 wk	1 2 3	5.44 4.82 4.70	4.99	11.77 %	0.4	0.16
9 wk	1 2 3	5.53 4.71 4.48	4.91	11.57 %	0.55	0.3
12 wk	1 2 3	5.79 5.49 5.11	5.46	12.88 %	0.28	0.08

Table 35 - Indirect Tension Results (NSC in Water - Highly Reactive)

Time (days)	Sample #	R MPa	Mean R Solution MPa	Avg. % of f'c Solution	Std. Dev. Solution MPa	Coefficient of Variation
28 days	1 2 3 4	5.04 4.00 3.92 3.76	4.16	9.81 %	0.51	0.26
6 wk	1 2 3 4	5.80 4.87 6.43 5.22	5.58	13.16 %	0.69	0.47
9 wk	1 2 3	6.16 6.15 5.18	5.83	13.76 %	0.56	0.32
12 wk	1 2 3	5.40 5.59 5.97	5.65	13.34 %	0.24	0.06

4.4.3 Modulus of Rupture (NSC - Marginally Reactive)

Indirect, normal strength, tension samples consisting of aggregate B, the potentially marginally reactive aggregate, did, however, follow a similar trend to that determined by previous researchers (Swamy and Al-Asali (1988), Swamy (1992)). Samples subjected to the NaOH solution experienced a decrease in the modulus of rupture from 5.45 MPa (tested after the initial 28 day curing period) to 4.14 MPa, after being subjected to the solution for 12 weeks. This represents a decrease of approximately 25 %. Sample subjected to the de-ionized water remained, for the most part, at the same ultimate strength, 5.45 MPa, throughout the testing period. Refer to Figures 48 and 49, as well as, Tables 36 and 37 for corresponding results and analysis.

It is unclear why the normal strength concrete containing the moderately reactive aggregate did experience losses in modulus of rupture over the testing period, whereas the normal strength concrete containing the highly reactive aggregate experienced gains in modulus of rupture. Again, the only explanation would be a decrease in the net load bearing area due to skewness of the prisms, and / or any eccentricity of the loading ram which may have resulted in the application of moments.

Figure 48 - Avg. R vs. Time (NSC in Solution - Moderately Reactive)

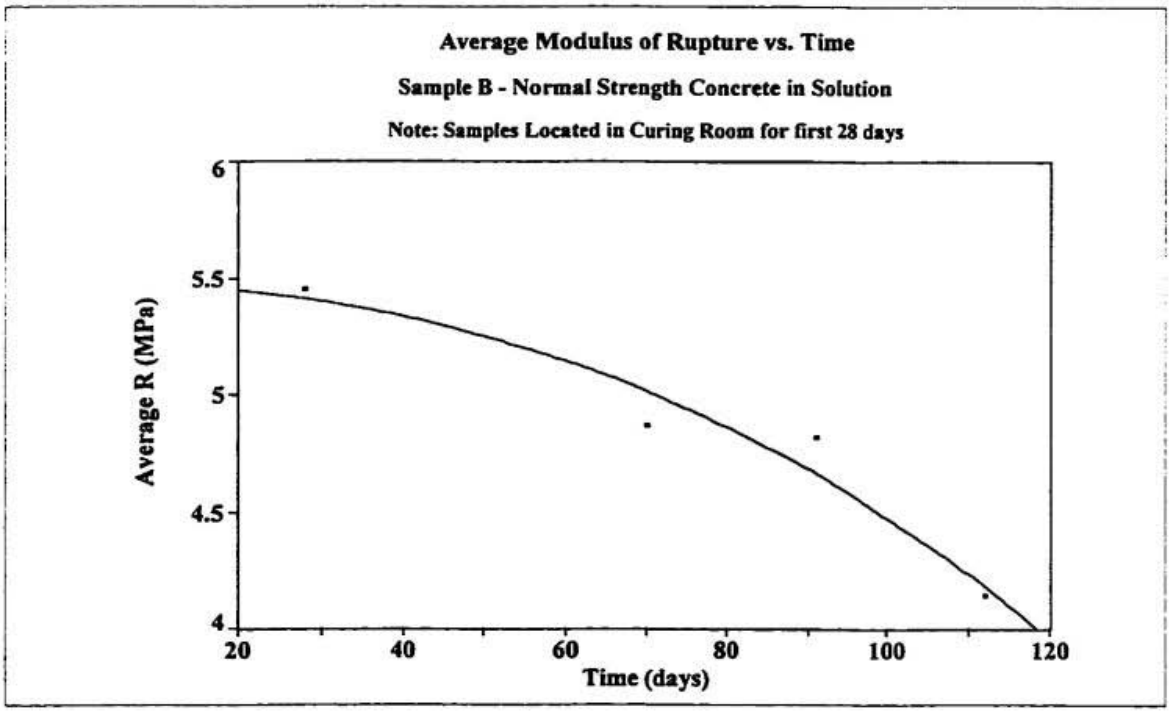

Figure 49 - Avg. R vs. Time (NSC in Water - Moderately Reactive)

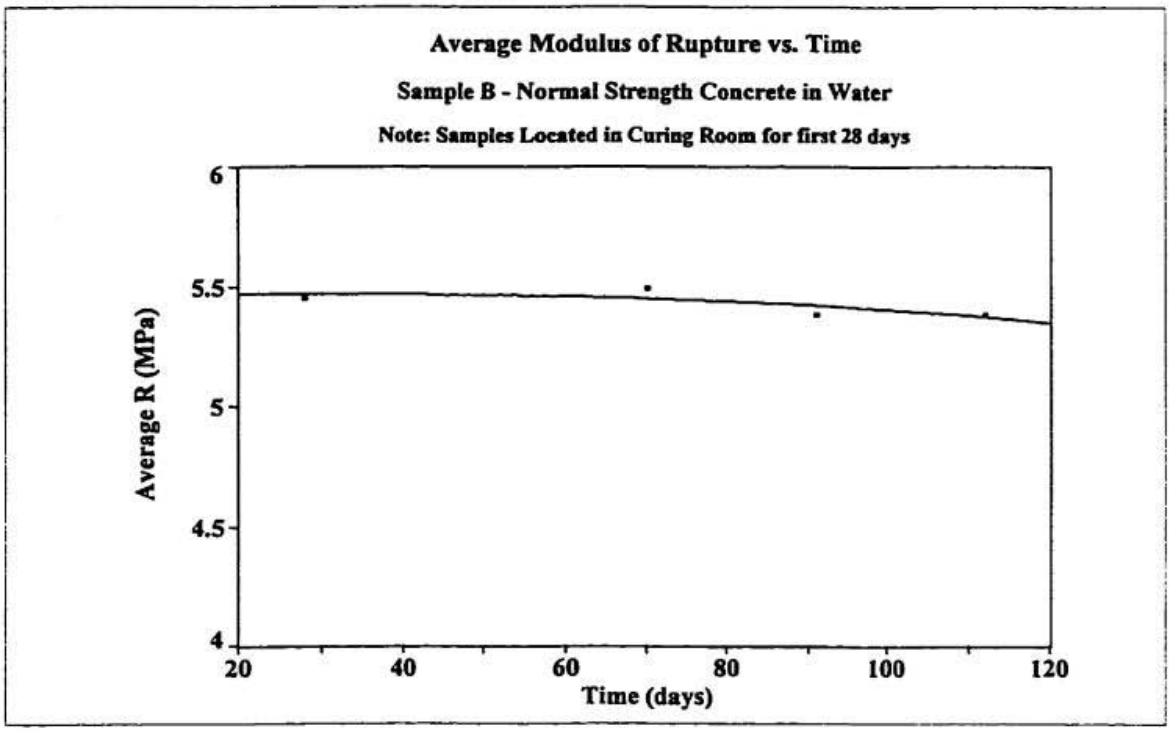

Table 36 - Indirect Tension Results (NSC in Solution - Moderately Reactive)

Time (days)	Sample #	R MPa	Mean R Solution MPa	Avg. % of f'c Solution	Std. Dev. Solution MPa	Coefficient of Variation
28 days	1 2 3 4	5.03 5.59 5.44 5.76	5.45	11.63 %	0.31	0.1
6 wk	1 2 3	4.77 4.64 5.21	4.87	10.40 %	0.3	0.09
9 wk	1 2 3	4.42 4.83 5.21	4.82	10.28 %	0.4	0.16
12 wk	1 2 3 4	4.37 3.51 4.37 4.33	4.14	8.84 %	0.42	0.18

Table 37 - Indirect Tension Results (NSC in Water - Moderately Reactive)

Time (days)	Sample #	R MPa	Mean R Solution MPa	Avg. % of f'c Solution	Std. Dev. Solution MPa	Coefficient of Variation
28 days	1 2 3 4	5.03 5.59 5.44 5.76	5.45	11.63 %	0.31	0.1
6 wk	1 2 3	6.12 5.08 5.27	5.49	11.71 %	0.56	0.31
9 wk	1 2 3	5.12 5.15 5.86	5.38	11.47 %	0.42	0.17
12 wk	1 2 3 4	5.73 5.46 4.96 5.94	5.38	11.48 %	0.48	0.23

4.4.4 Modulus of Rupture (HSC - Highly Reactive)

To the author's knowledge, no literature has been published regarding the effects of an alkali-aggregate reaction on the modulus of rupture of high strength concrete specimens. However, testing was conducted on similar high strength concrete specimens to determine the modulus of rupture alone, which provides a good basis for analysis of specimens tested herein. Marzouk and Chen (1995) determined the modulus of rupture of high strength concrete prisms, similar to that used throughout this investigation. It was determined that the modulus of rupture was approximately 9.4% f'c, with the modulus of rupture being approximately 200% of the direct tensile strength.

Testing of the 28 day high strength concrete specimens using the potentially highly reactive aggregate determined the modulus of rupture to be 8.39 MPa, or 11.49 % of f'c. This overall strength is approximately 230 % of the direct tensile strength (4.9 % of f'c), which is in good agreement with that determined by Marzouk and Chen (1995), who confirmed the relation to be approximately 200 % of the direct tensile strength.

Samples located in the de-ionized water experienced an increase in strength of approximately 50 %, from 8.39 MPa to 12.48 MPa. This increase in strength can, once again, be attributed to the secondary pozzolanic reaction, as previously discussed. Samples located in the solution experienced a small increase in overall strength from 8.39 MPa to 9.39 MPa, an increase of approximately 10 %. Since the only difference between both holding tanks is the

solution type, the NaOH solution is the direct result of the minimized increase in modulus of rupture. Refer to Figures 50 and 51, as well as, Tables 38 and 39, for results and analysis.

Figure 50 - Avg. R vs. Time (HSC in Solution - Highly Reactive)

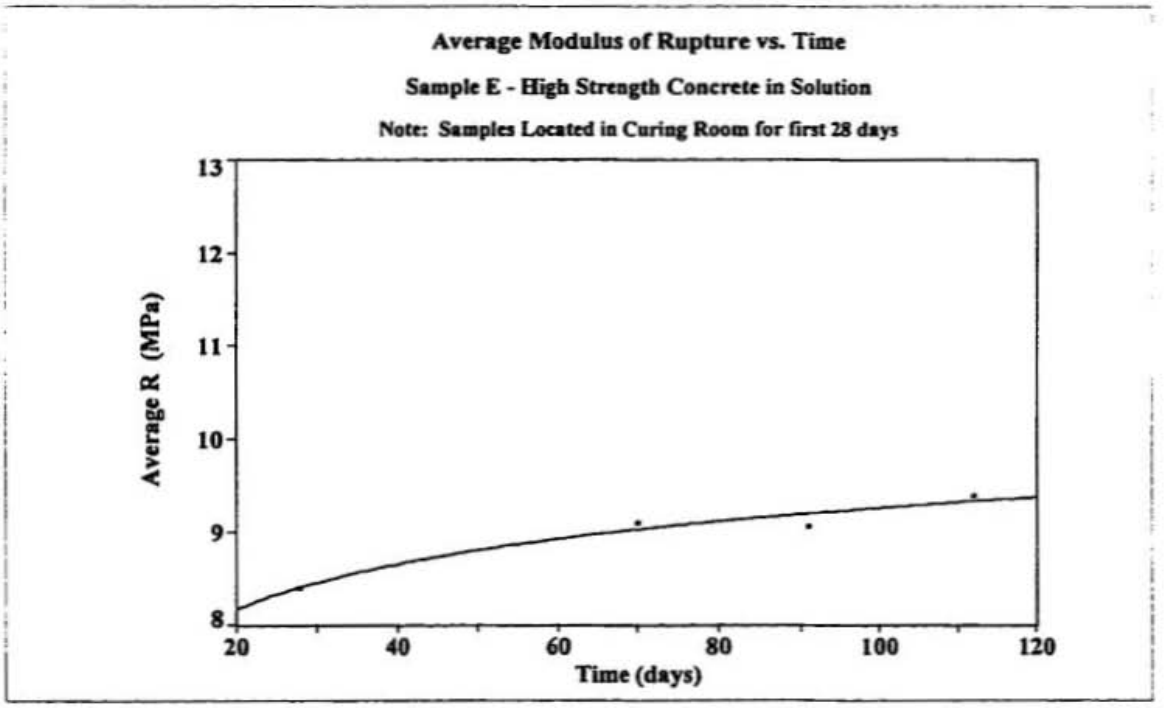

Figure 51 - Avg. R vs. Time (HSC in Water - Highly Reactive)

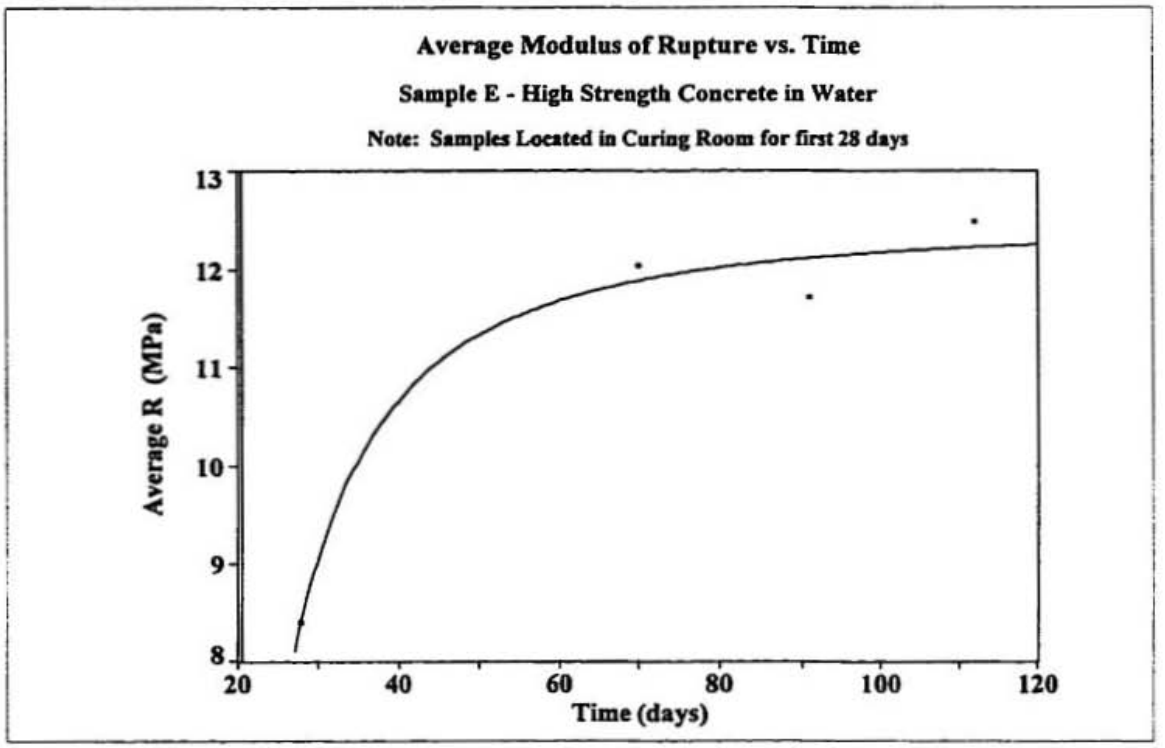

Table 38 - Indirect Tension Results (HSC in Solution - Highly Reactive)

Time (days)	Sample #	R MPa	Mean R Solution MPa	Avg. % of f'c Solution	Std. Dev. Solution MPa	Coefficient of Variation
28 days	1 2 3	7.69 8.10 9.38	8.39	11.49 %	0.88	0.78
6 wk	1 2 3	6.80 8.48 8.58	7.95	10.90 %	1	1
9 wk	1 2 3	9.99 8.16 9.00	9.05	12.40 %	0.92	0.84
12 wk	1 2 3	8.52 9.49 10.12	9.38	12.84 %	0.8	0.65

Table 39 - Indirect Tension Results (HSC in Water - Highly Reactive)

Time (days)	Sample #	R MPa	Mean R Solution MPa	Avg. % of f'c Solution	Std. Dev. Solution MPa	Coefficient of Variation
28 days	1 2 3	7.69 8.10 9.38	8.39	11.49 %	0.88	0.78
6 wk	1 2 3	13.66 10.33 12.15	12.04	16.50 %	1.67	2.79
9 wk	1 2 3	11.39 11.69 12.06	11.71	16.04 %	0.34	0.11
12 wk	1 2 3	11.13 13.08 13.24	12.48	17.10 %	1.17	1.37

4.4.5 Modulus of Rupture (HSC - Marginally Reactive)

Samples located in both the solution and the de-ionized water experienced an overall increase in modulus of rupture throughout the testing period. For samples located in the de-ionized water, the 28 day testing resulted in an average modulus of rupture of 5.91 MPa, representing 8.21 % of f 'c. This again compared well with results of experimentation conducted by Marzouk and Chen (1995) who determined the modulus of rupture of high strength concrete to be approximately 9.4% f 'c. Testing of samples determined that at the 12 week testing period, the modulus of rupture of specimens from both groups increased to approximately 10 % of f 'c, an increase of approximately 20 %. This trend is quite similar to that observed in the high strength specimens consisting of the highly reactive aggregate (Refer to Figures 52 and 53, as well as, Tables 40, and 41).

Figure 52 -Avg. R vs. Time (HSC in Solution - Moderately Reactive)

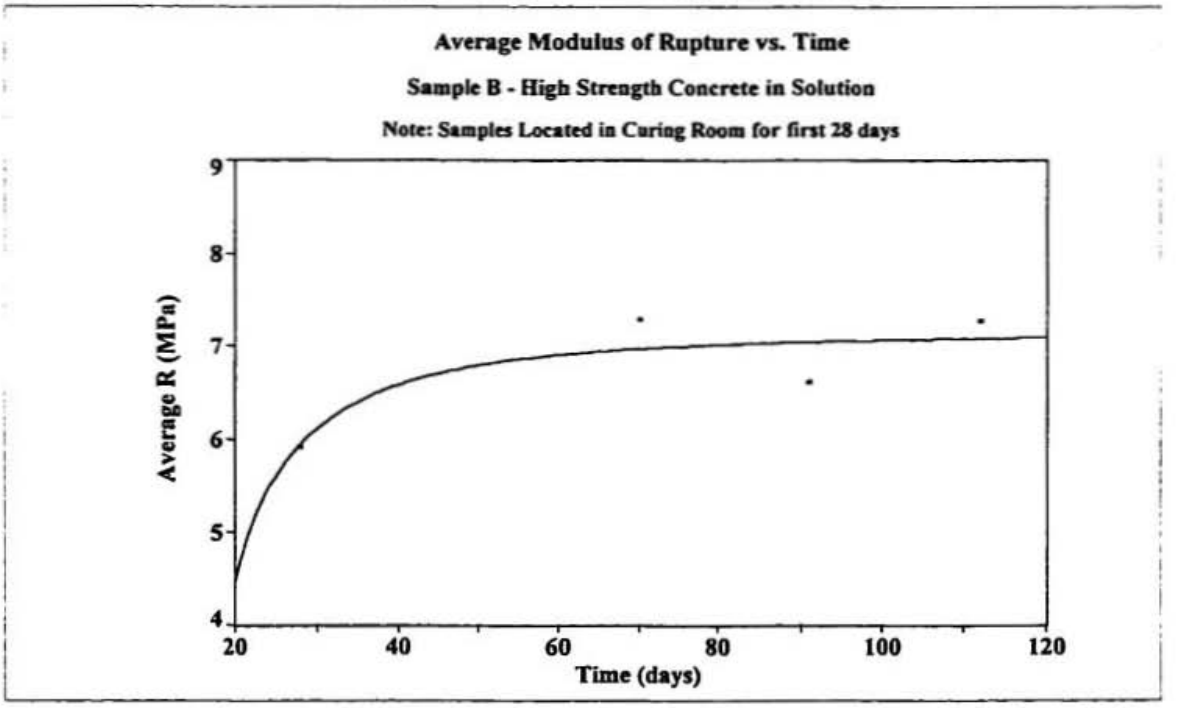

Figure 53 -Avg. R vs. Time (HSC in Water - Moderately Reactive)

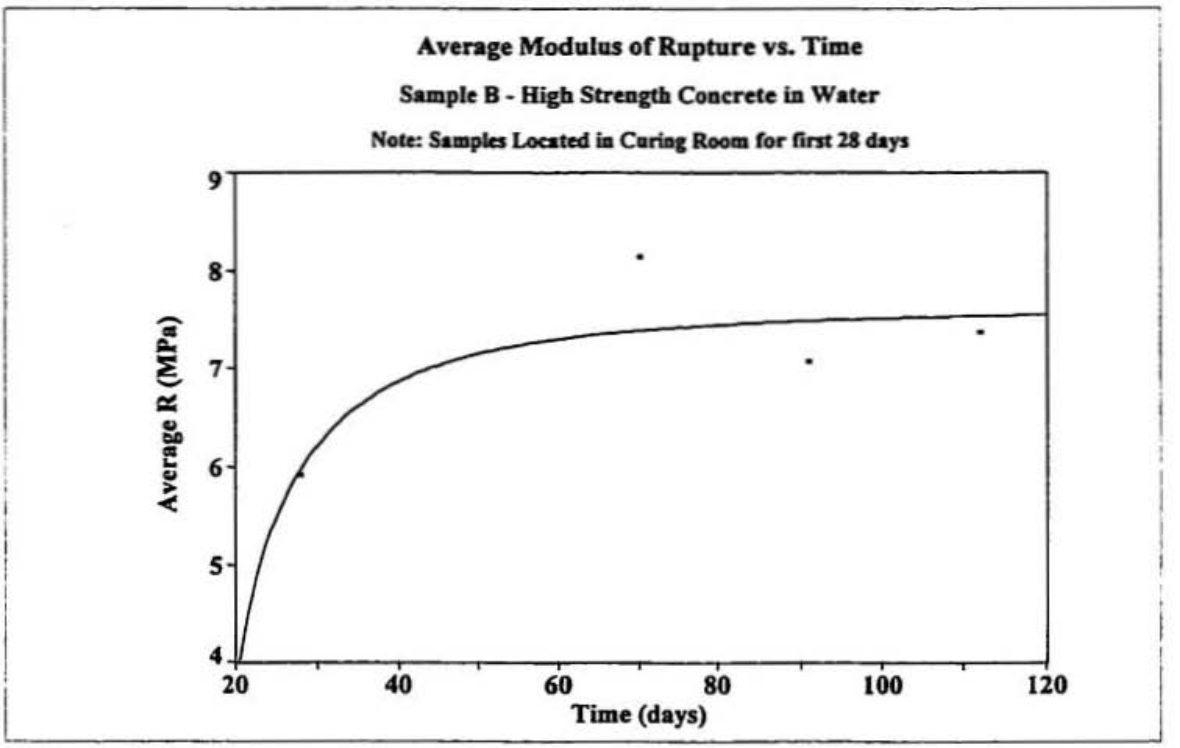

Table 40 - Indirect Tension Results (HSC in Solution - Moderately Reactive)

Time (days)	Sample #	R MPa	Mean R Solution MPa	Avg. % of f'c Solution	Std. Dev. Solution MPa	Coefficient of Variation
28 days	1 2 3	5.77 5.39 6.57	5.91	8.21 %	0.61	0.37
6 wk	1 2 3	7.31 6.14 8.38	7.28	10.12%	1.12	1.25
9 wk	1 2 3	7.43 6.42 5.94	6.6	9.17 %	0.76	0.57
12 wk	1 2 3	7.35 7.74 6.69	7.26	10.10 %	0.53	0.28

Table 41 -Indirect Tension Results (HSC in Water - Moderately Reactive)

Time (days)	Sample #	R MPa	Mean R Solution MPa	Avg. % of f'c Solution	Std. Dev. Solution MPa	Coefficient of Variation
28 days	1 2 3	5.77 5.39 6.57	5.91	8.21 %	0.61	0.37
6 wk	1 2 3	7.41 9.34 7.66	8.14	11.31 %	1.05	1.1
9 wk	1 2 3	7.11 7.02 7.08	7.07	9.83 %	0.06	0
12 wk	1 2 3	6.84 7.40 7.84	7.36	10.23 %	0.5	0.25

4.5 Freeze Thaw Results

4.5.1 General

Pulse velocity and dynamic measurement techniques have proven to be very useful in determining the initiation of concrete deterioration caused by alkali-aggregate reactivity for both highly reactive and slowly reactive aggregates. This is due to the fact that each technique is very sensitive to changes in the internal micro-structure, and can register measurable losses in mechanical properties before any visual observation cracking occurs. Experimentation conducted by Swamy (1992, 1995) has indicated losses in ultrasonic pulse velocity and dynamic modulus of elasticity can be quite severe, however, these experiments were not conducted in conjunction with freeze-thaw cycling of specimens.

All specimens, both normal and high strength, that are to be subjected to freeze-thaw cycling will first be submerged in either de-ionized water or the NaOH solution for a period of 6 weeks, after the initial 28 day curing period. It is believed that this time frame will allow the initiation of an alkali-aggregate reaction in specimens submerged in the aggressive NaOH solution.

It is predicted that the normal strength specimens containing the potentially highly reactive aggregate will experience greater losses in both the ultrasonic pulse velocity and the dynamic modulus of elasticity than for the normal strength concrete containing the potentially marginally reactive aggregate. Due to the increased resistance of the micro structure of high strength concrete to freeze-thaw cycling, it is believed that samples containing both aggregate

samples will behave quite similarly, experiencing no appreciable difference in ultrasonic pulse velocity or dynamic modulus of elasticity.

Marzouk and Jiang (1994) conducted extensive investigations regarding the effects of freeze-thaw cycling on the properties of high and normal strength concrete. After subjecting the samples to 300 freeze - thaw cycles, the relative dynamic modulus of elasticity was determined to be 88 % of the initial for high strength concrete, and 73 % for the normal strength concrete. These values indicate the increased durability of high strength concrete to freeze-thaw cycling. Testing conducted throughout this experimentation is expected to show similar reductions for samples initially subjected to the de-ionized water, in both the high strength and normal strength samples. However, greater losses in dynamic modulus and pulse velocity are expected for samples initially subjected to the aggressive NaOH, and more so for samples consisting of the potentially reactive aggregate.

4.5.2 Freeze - Thaw Results (NSC - Highly Reactive)

Determination of the dynamic modulus of elasticity for the normal strength concrete consisting of the potentially reactive aggregate revealed significant differences throughout the complete testing period. Samples located in the de-ionized water experienced only a 10% decrease in dynamic modulus after being subjected to 300 freeze-thaw cycles. However, samples located in the solution for 6 weeks after the initial curing period experienced a 24 % decrease in dynamic modulus after being subjected to 300 freeze- thaw cycles with respect to the 28 day value. These values indicate that concrete experiencing an alkali-aggregate

reaction is more prone to increased deterioration as a result of freeze-thaw cycling, as indicated by previous researchers (Davies and Oberholster (1989), Ludwig (1989), Swamy (1992), and Swamy (1994)) . Refer to Figures 54 and 55.

Ultrasonic pulse velocity measurements were also recorded on each specimen at the various intervals, in both the longitudinal and transverse direction (refer to Figures 56 and 57). Results of longitudinal pulse velocity measurements indicate that losses on the order of 13 % were observed in samples after 300 freeze - thaw cycles that were initially located in the NaOH solution. However, samples initially subjected to the de-ionized water for a period of 6 weeks, indicated a loss of less than 5 % in pulse velocity after being subjected to 300 freeze - thaw cycles. Losses in transverse pulse velocity measurements were quite similar, with samples initially subjected to the de-ionized water experiencing a 10% decrease, whereas specimens initially located in the NaOH solution experienced approximately 13 % decrease in pulse velocity. The effect of an alkali-aggregate reaction on the durability of concrete is substantiated.

Figure 54 - Effects of F-T Cycling on Ed - NSC (Highly Reactive)

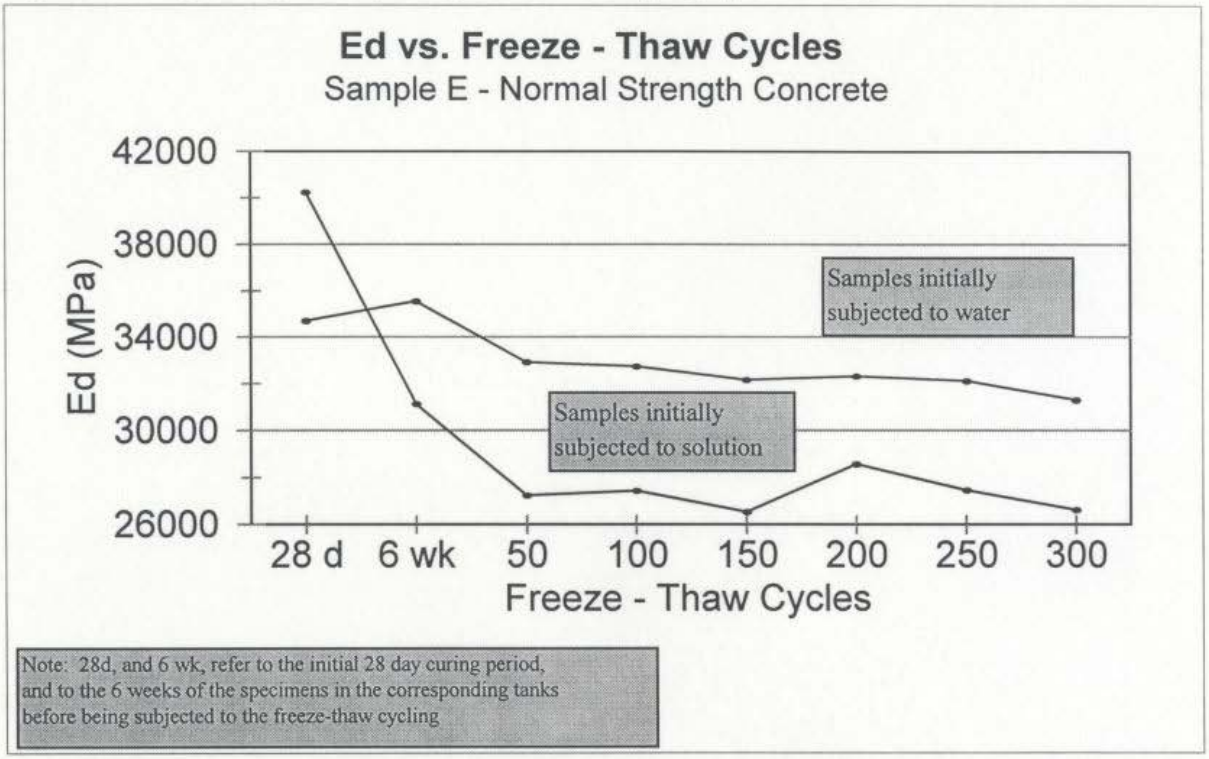

Figure 55 - Effects of F-T Cycling on Relative Ed - NSC (Highly Reactive)

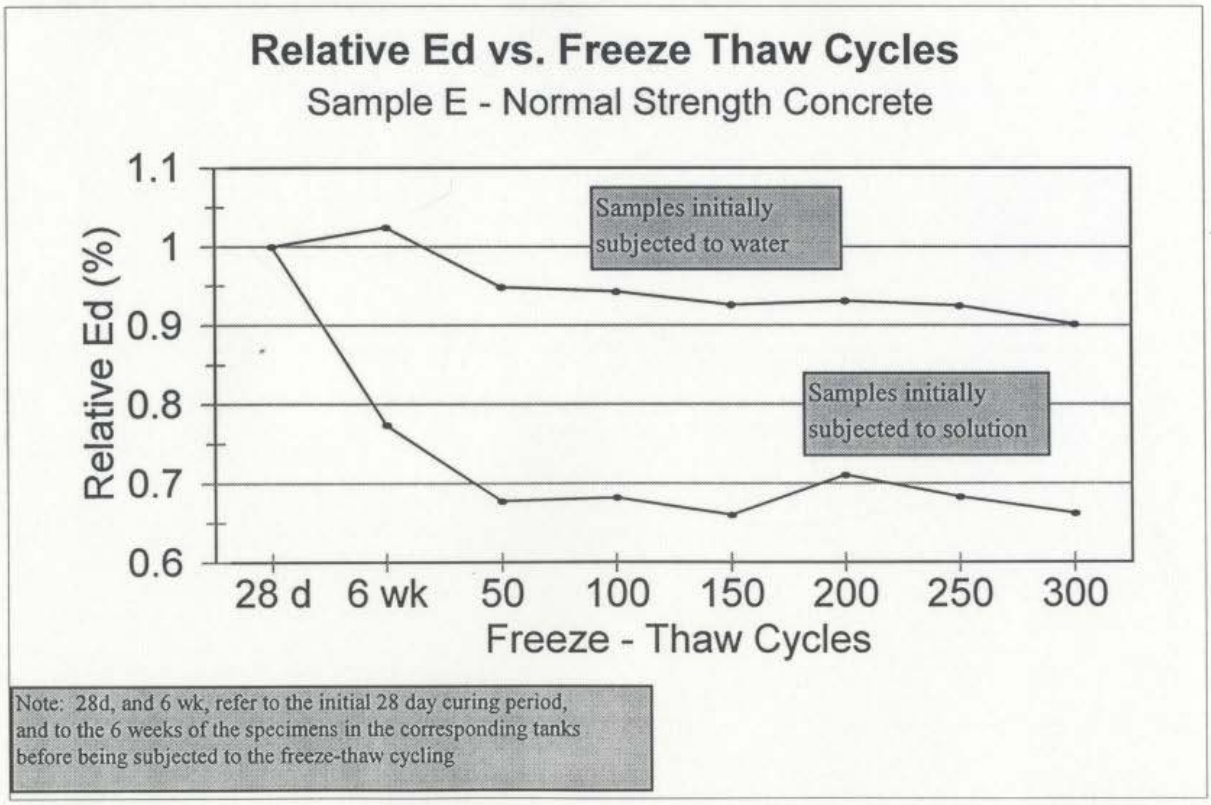

Figure 56 - Effects of F-T Cycling on Pulse Velocity - NSC (Highly Reactive)

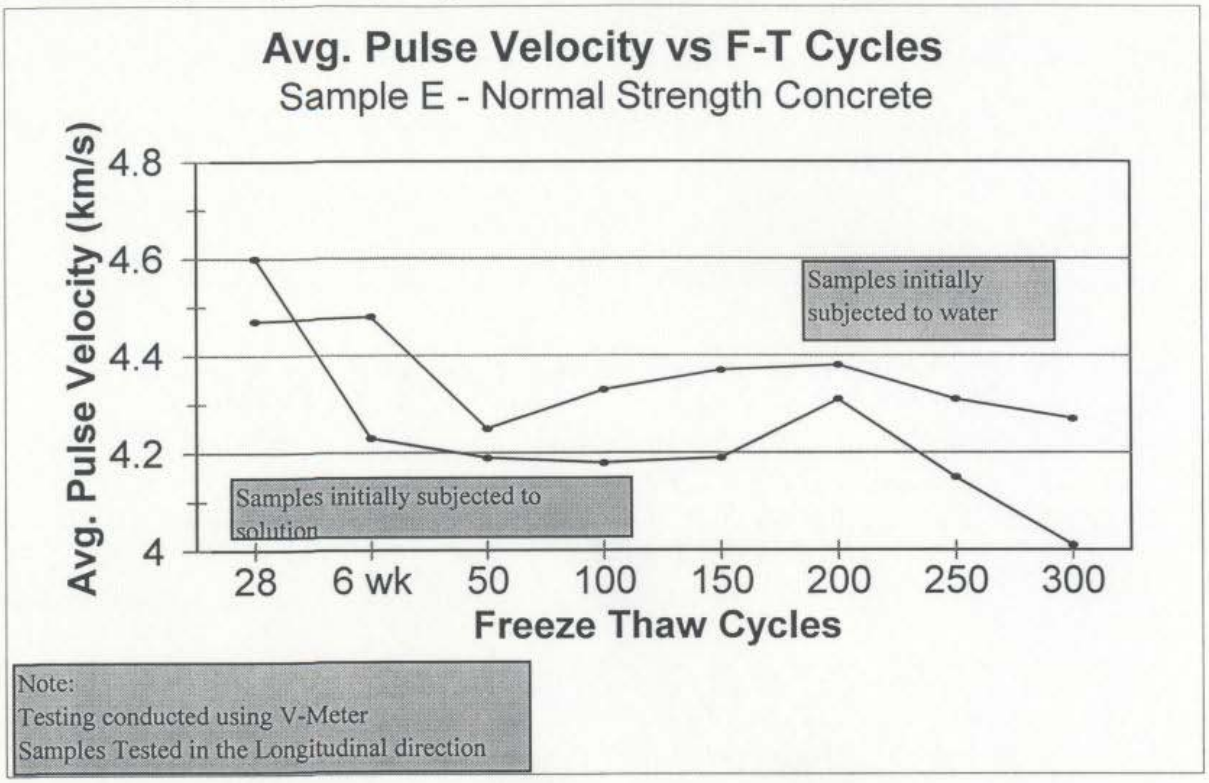

Figure 57 - Effects of F-T Cycling on Pulse Velocity - NSC (Highly Reactive)

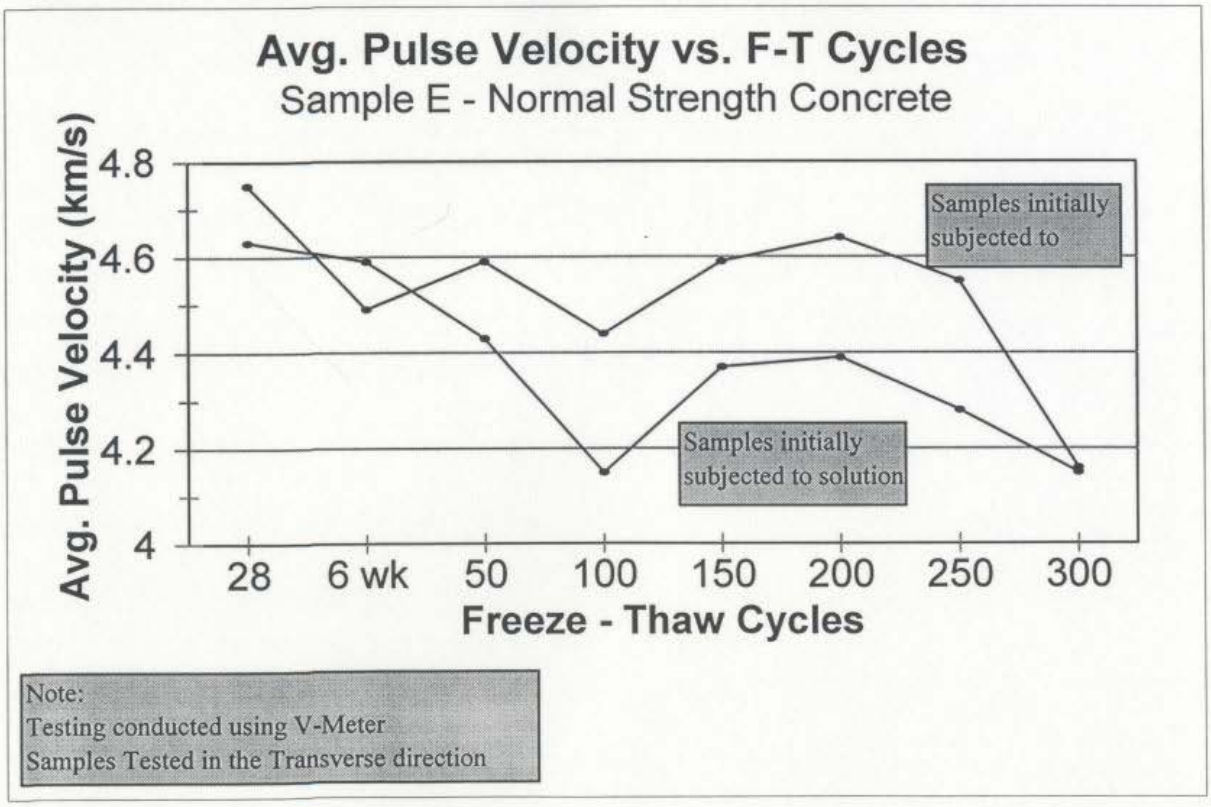

4.5.3 Freeze-Thaw Results (NSC - Moderately Reactive)

The dynamic modulus of elasticity determined on the normal strength consisting of the potentially marginally reactive aggregate (aggregate B) resulted in unexpected results. Samples initially submerged in the de-ionized water before undergoing the freeze-thaw cycling process revealed results quite similar to the corresponding testing of normal strength concrete consisting of the potentially highly reactive aggregate. Losses in the dynamic modulus of elasticity were approximately 6.5 % after undergoing 300 freeze - thaw cycles. However, samples that were initially submerged in the solution for 6 weeks prior to the freeze - thaw cycling process, experienced losses in dynamic modulus of elasticity on the order of 60 %. These losses are much greater than the 24 % loss in dynamic modulus determined from samples consisting of the potentially highly reactive aggregate, and are contrary to what is believed should have been apparent. However, progressive deterioration of the ends of the prisms with increased freeze - thaw cycling were noticed by the author throughout the testing period. Such deterioration may be explained by inadequate compaction of the samples at the time of placement into the forms. Refer to Figures 58 and 59.

Determination of both longitudinal, and transverse, pulse velocities for normal strength concrete samples consisting of the potentially marginally reactive aggregate also followed the same trend as that of the dynamic modulus of elasticity. For samples initially located in the de-ionized water, longitudinal pulse velocities were recorded as marginally increasing at 0.7%, whereas the same samples experienced a loss in transverse pulse velocity of less than 2 %. However, samples initially submerged in the NaOH solution experienced losses in

longitudinal pulse velocities of approximately 30 %, and losses in transverse pulse velocity of approximately 37 %. However, the pulse velocity measurements recorded in the transverse direction may produce less accurate results, since the longitudinal measurements have a much longer distance of travel, which results in less error due to the resolution of time measurement (Marzouk and Jiang, 1994). Refer to Figures 60 and 61.

Nonetheless, these results are not consistent with those initially expected, especially when considering the fact that a less reactive aggregate has resulted in markedly significant increases in losses to both the dynamic modulus of elasticity, as well as pulse velocity measurements.

Figure 58 - Effects of F-T Cycling on Ed - NSC (Moderately Reactive)

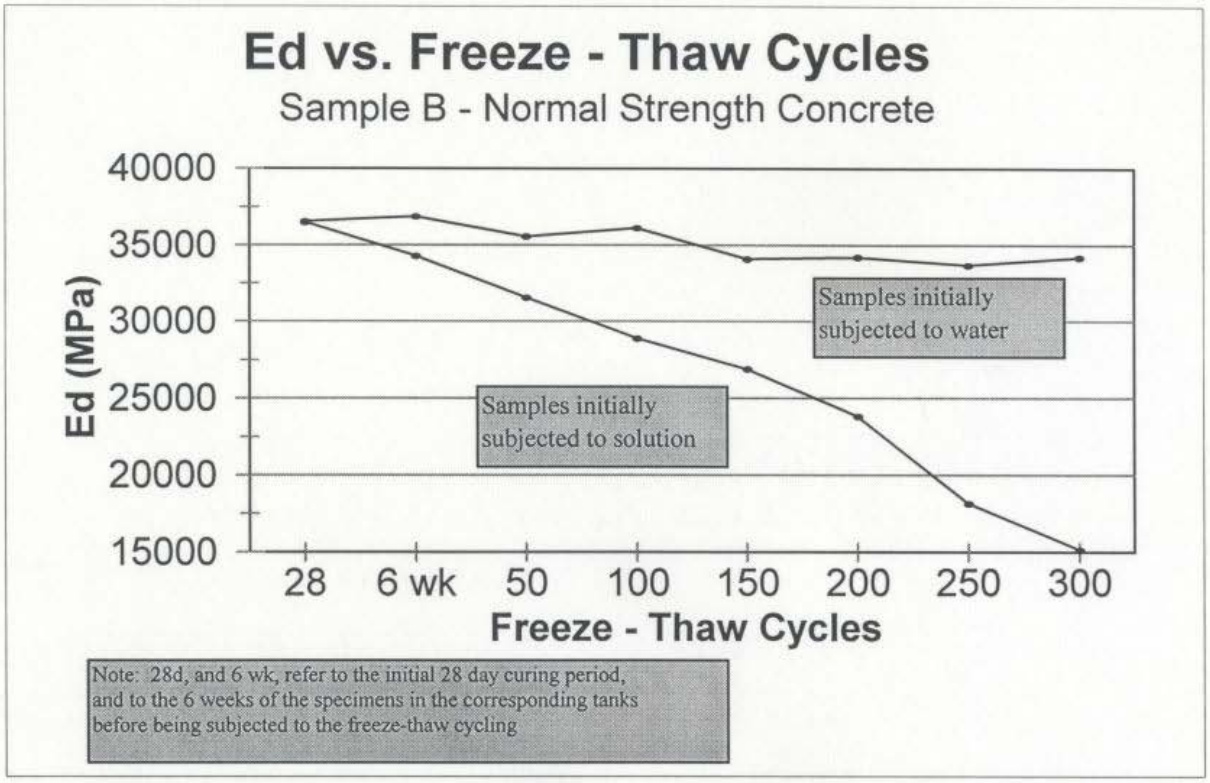

Figure 59 - Effects of F-T Cycling on Relative Ed - NSC (Moderately Reactive)

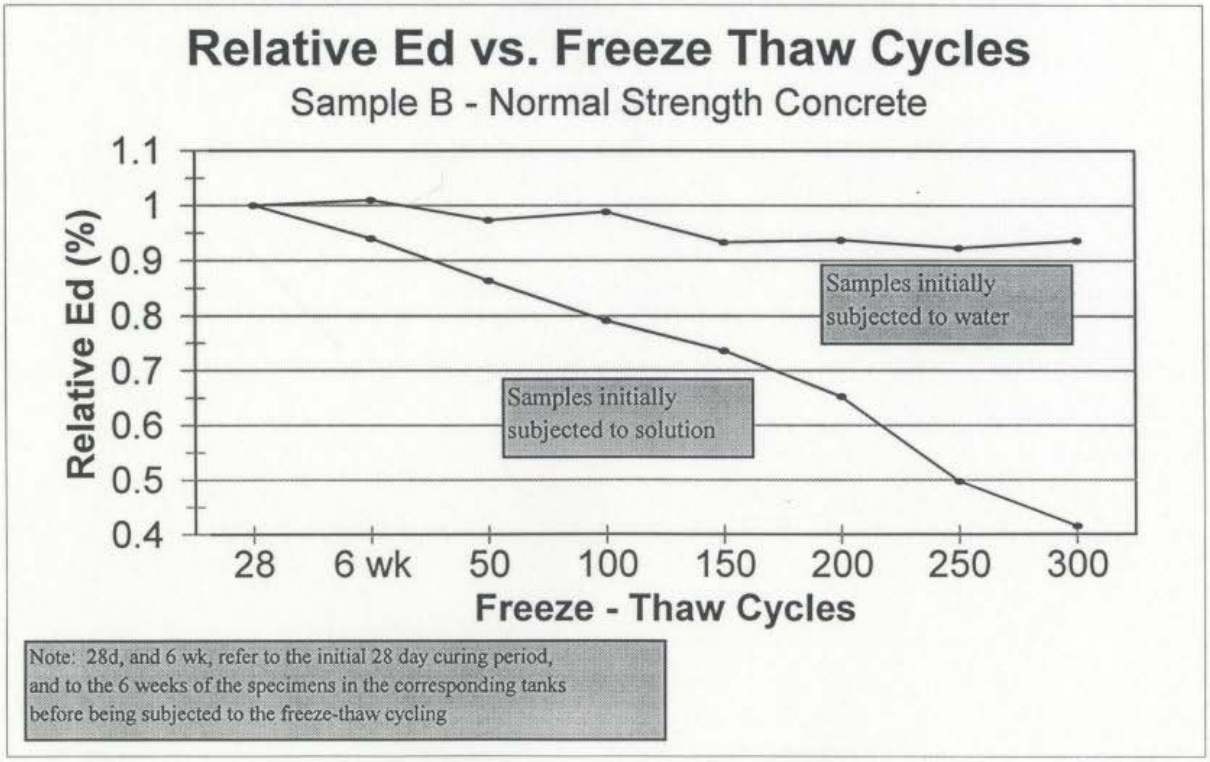

Figure 60 - Effects of F-T Cycling on Pulse Velocity - NSC (Highly Reactive)

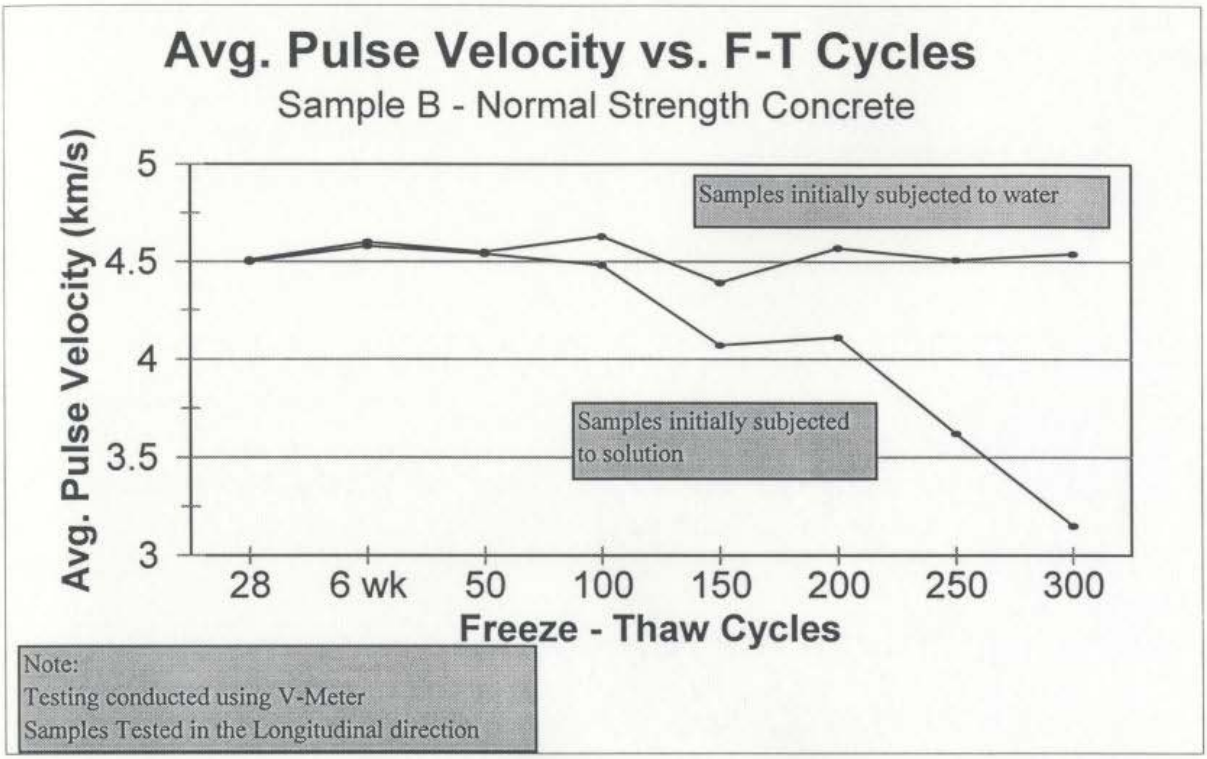

Figure 61 - Effects of F-T Cycling on Pulse Velocity - NSC (Highly Reactive)

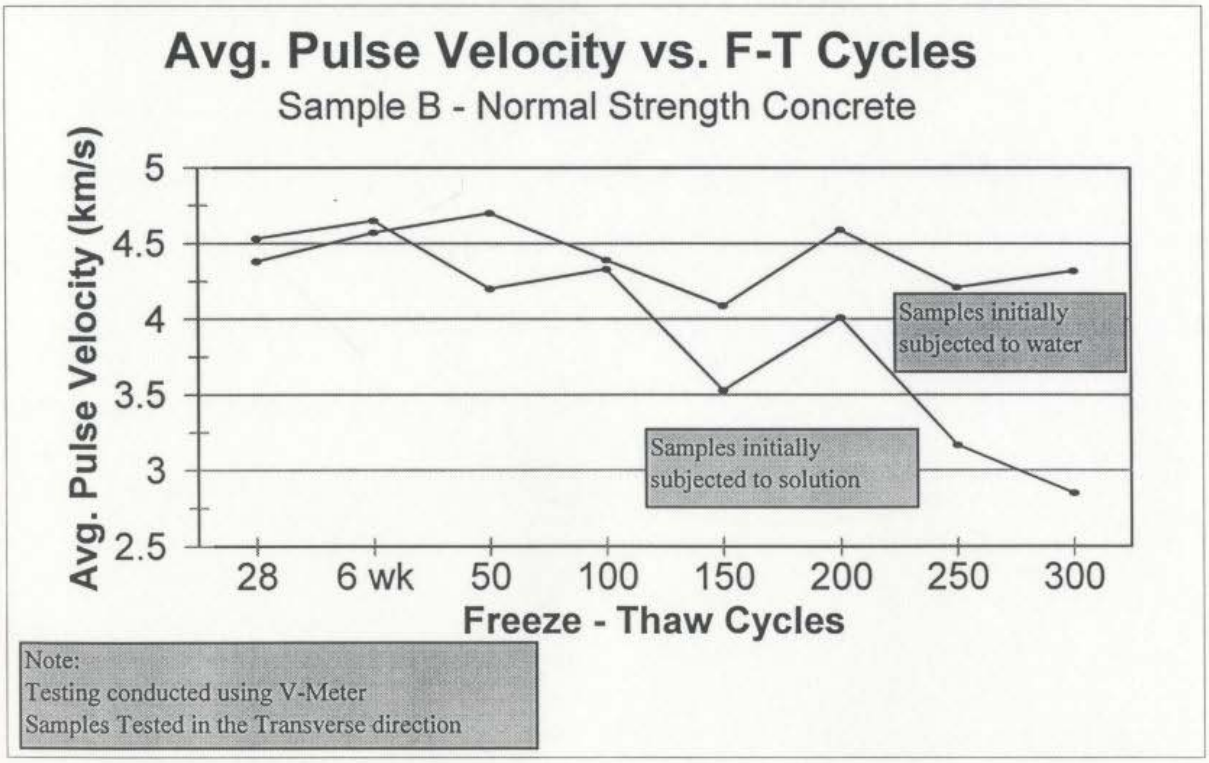

4.5.4 Freeze-Thaw Results (HSC - Highly Reactive)

High strength concrete samples initially subjected to de-ionized water and aggressive NaOH solution consisting of the potentially reactive aggregate did not show any losses in either the dynamic modulus of elasticity, longitudinal pulse velocity, or transverse pulse velocity. Refer to figures 62 through 65.

The dynamic modulus of elasticity for samples subjected to water and solution did show an initial increase after being in the respective tanks for a period of 6 weeks. However, after undergoing 300 freeze-thaw cycles, both samples returned to almost exactly the same value. In addition, pulse velocity measurements for both high strength concrete samples consisting of the potentially highly reactive aggregate followed a similar trend. After being subjected to 300 freeze - thaw cycles, the resulting ultrasonic pulse velocity recorded was almost equal to that recorded after the initial 28 day curing period.

These results confirm the improved durability of high strength concrete to freeze - thaw cycling. Testing conducted by Marzouk and Jiang (1994) revealed that two high strength specimens also had experienced losses in dynamic modulus of elasticity of less than 5 % for specimens that were 20 mm x 75 mm x 300 mm. The results obtained herein are deemed consistent with that of Marzouk and Jiang (1994).

Figure 62 - Effects of F-T Cycling on Ed - HSC (Highly Reactive)

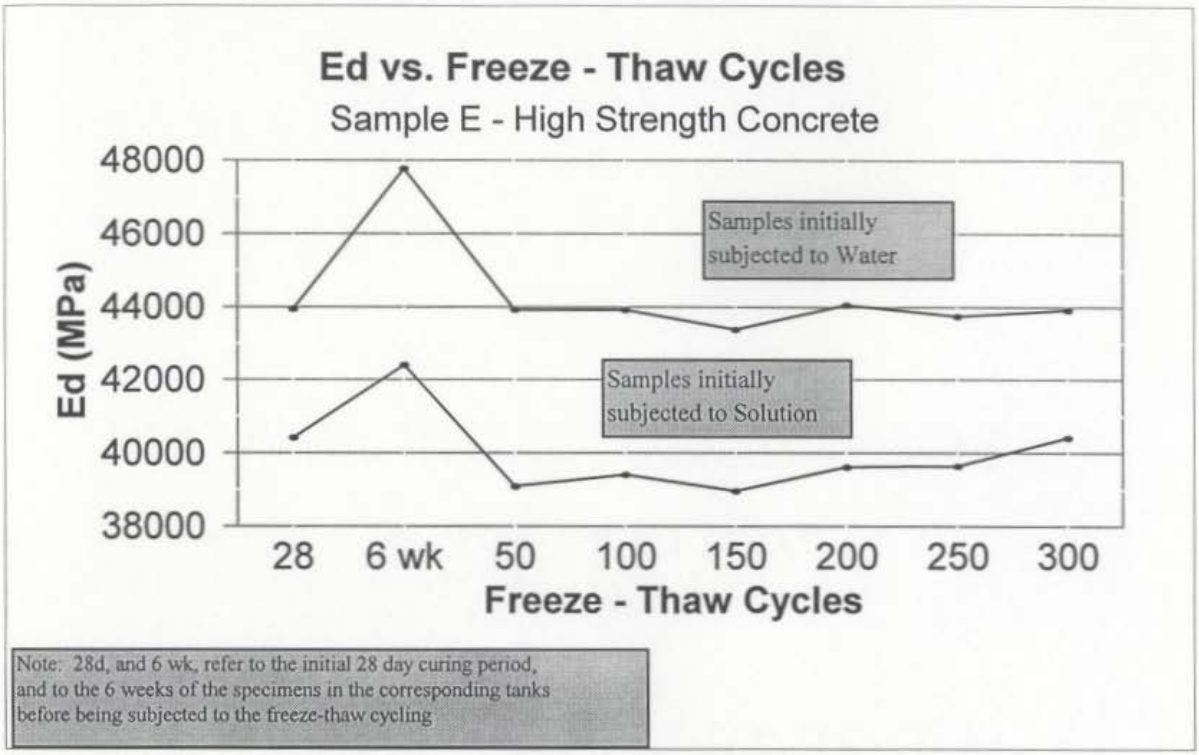

Figure 63 - Effects of F-T Cycling on Relative Ed - HSC (Highly Reactive)

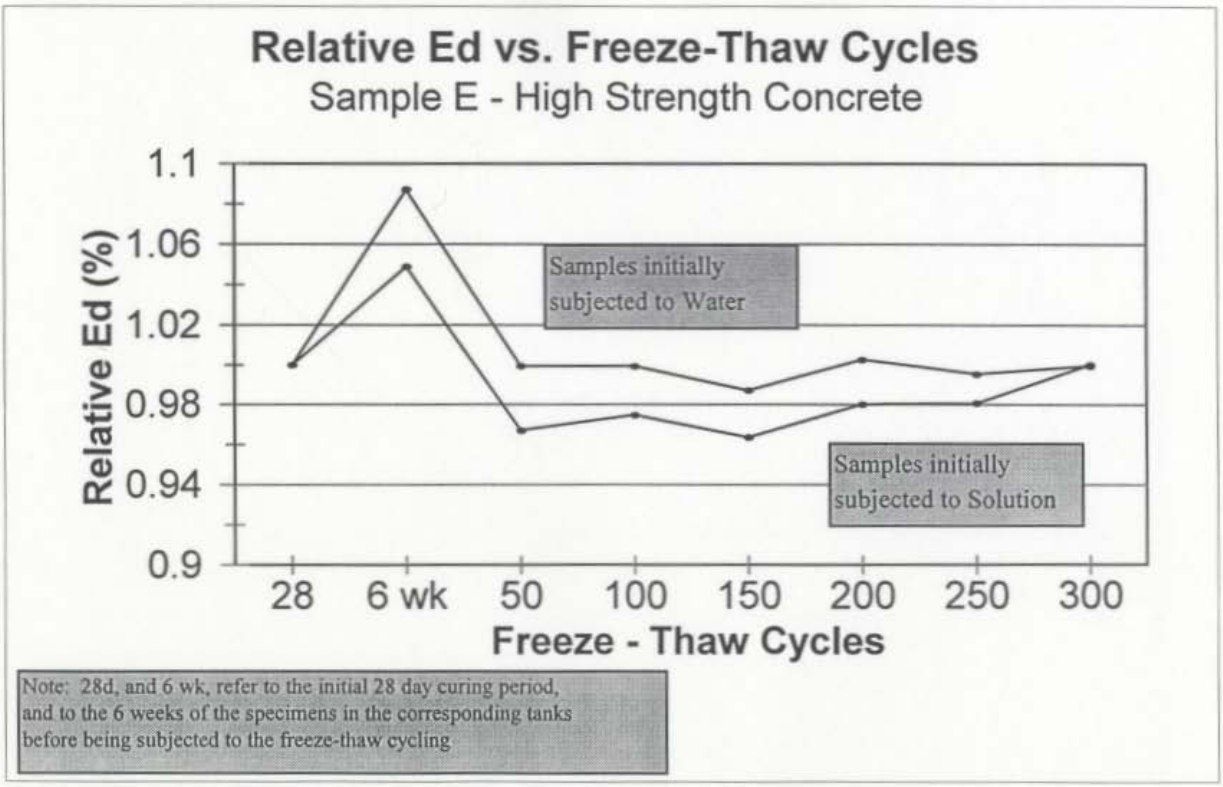

Figure 64 - Effects of F-T Cycling on Pulse Velocity - HSC (Highly Reactive)

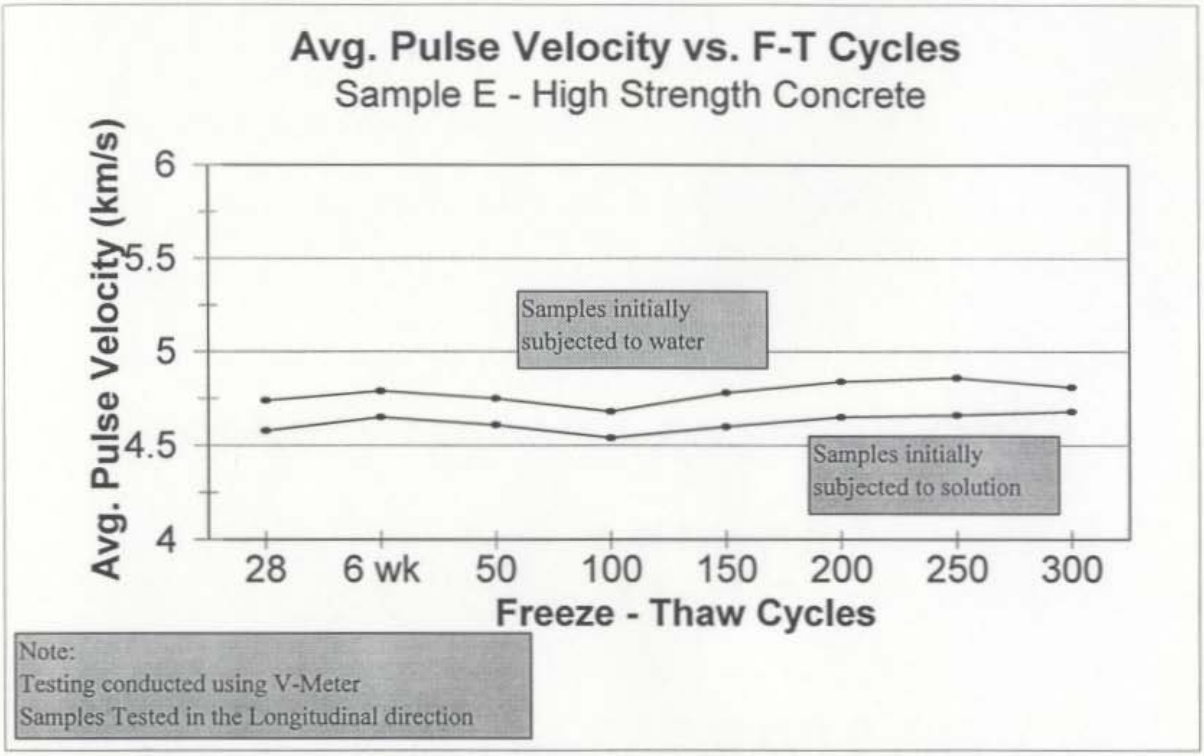

Figure 65 - Effects of F-T Cycling on Pulse Velocity - HSC (Highly Reactive)

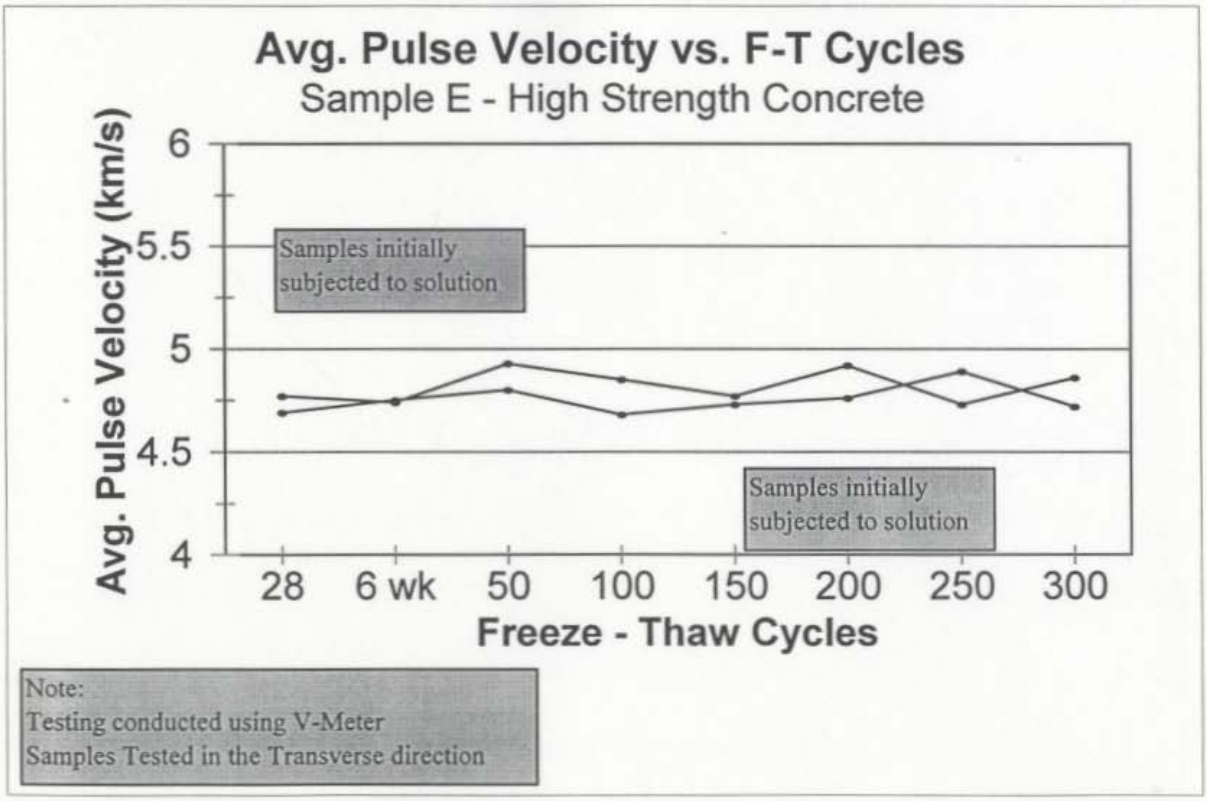

4.5.5 Freeze-Thaw Results (HSC - Moderately Reactive)

High strength concrete samples consisting of the potentially marginally reactive aggregate followed a very similar trend to that found of high strength concrete using the potentially reactive aggregate. The only exception was that of the transverse pulse velocity which experienced only minor decreases. However, due to the increased error associated with the shorter distance of pulse travel, the transverse ultrasonic pulse velocity has been considered not to decrease throughout the testing duration. Refer to figures 66 through 69.

Both samples located in the water, and in the aggressive NaOH solution did show a substantial increase (on the order of 7 %) in the dynamic modulus of elasticity after being submerged in the respective tanks for a period of 6 weeks. This trend was also evident in the high strength concrete consisting of the potentially highly reactive aggregate, and is the result of the secondary reaction due to the elevated storing temperatures. However, after both sample sets underwent 300 freeze - thaw cycles, the dynamic modulus, as well as the longitudinal ultrasonic pulse velocity, was determined to be approximately 3% higher for those contained in the solution, and 5% higher for those contained in the de-ionized water.

When comparing these results with those obtained from the high strength concrete utilizing the potentially highly reactive aggregate, it is seen that the potentially marginally reactive aggregate experiences slightly higher gains in material properties after the complete testing period, which is expected. These results, as with those obtained from testing the high strength concrete with the potentially highly reactive aggregate, again confirm the increased

durability of high strength concrete to repeated freeze - thaw cycling. Considering sample size, these results are also deemed consistent with that determined by Marzouk and Jiang (1994).

Figure 66 - Effects of F-T Cycling on Ed - HSC (Moderately Reactive)

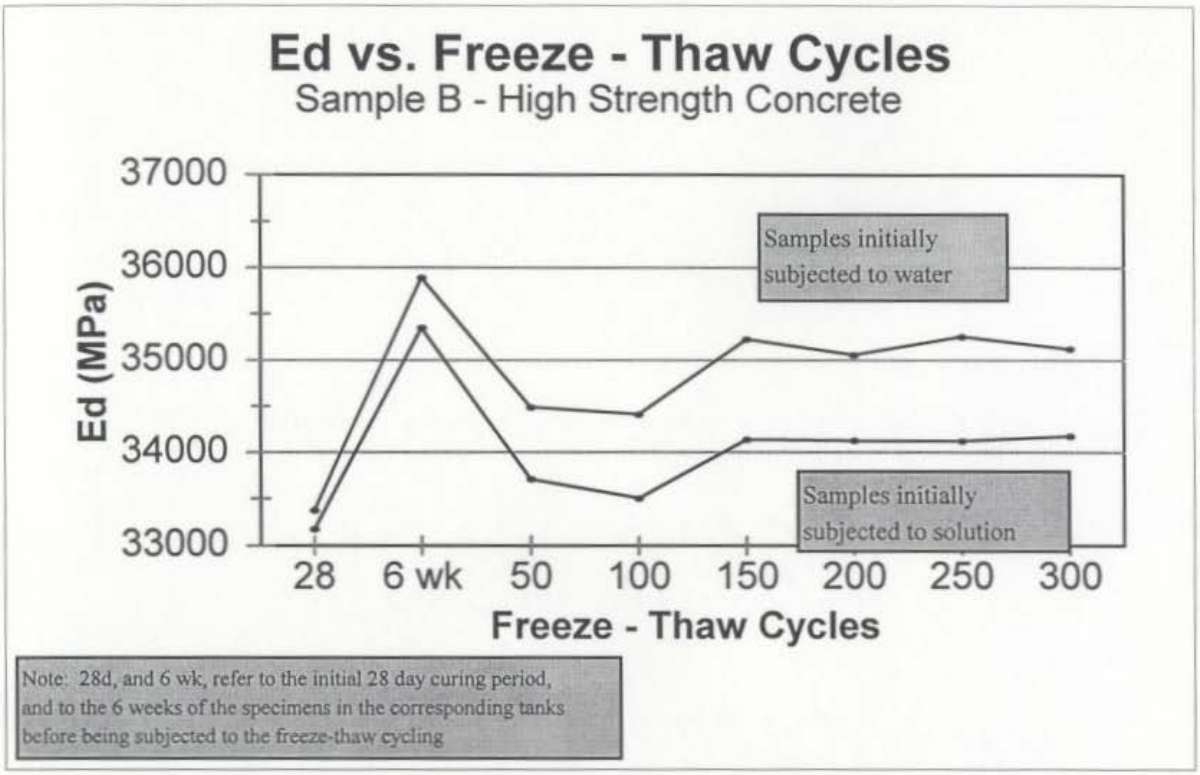

Figure 67 - Effects of F-T Cycling on Relative Ed - HSC (Moderately Reactive)

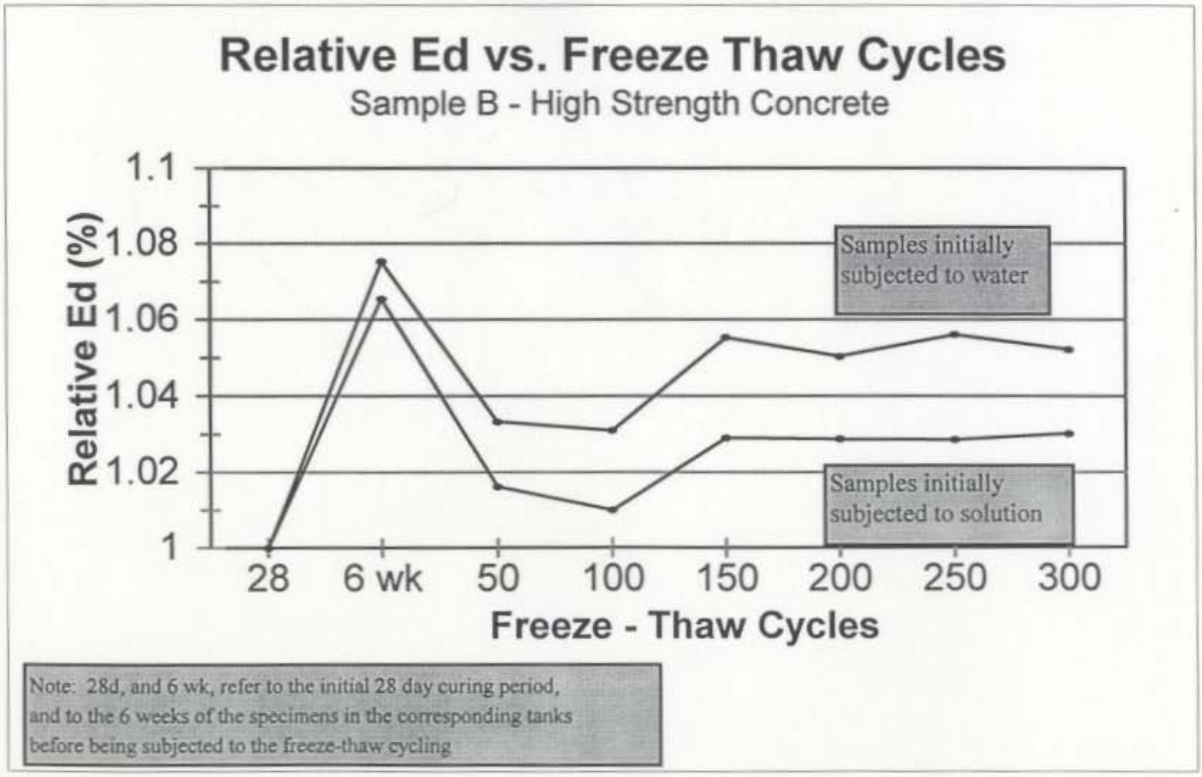

Figure 68 - Effects of F-T Cycling on Pulse Velocity - HSC (Moderately Reactive)

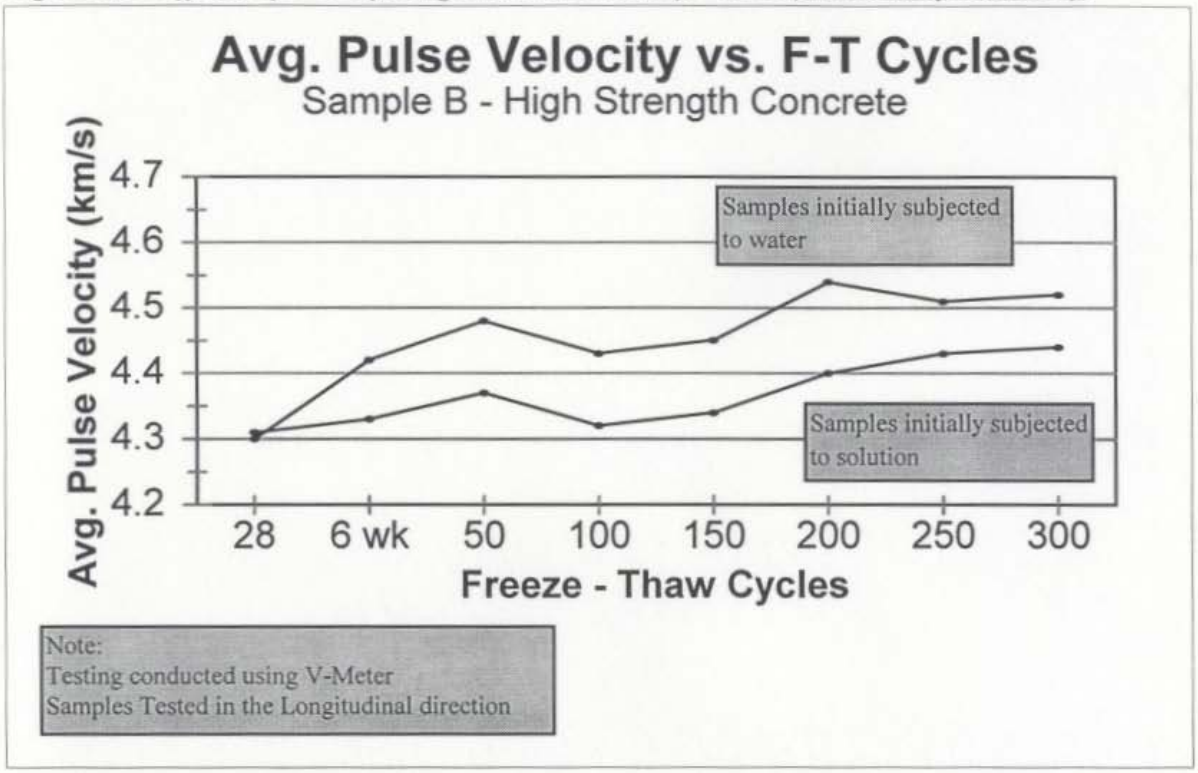

Figure 69 - Effects of F-T Cycling on Pulse Velocity - HSC (Moderately Reactive)

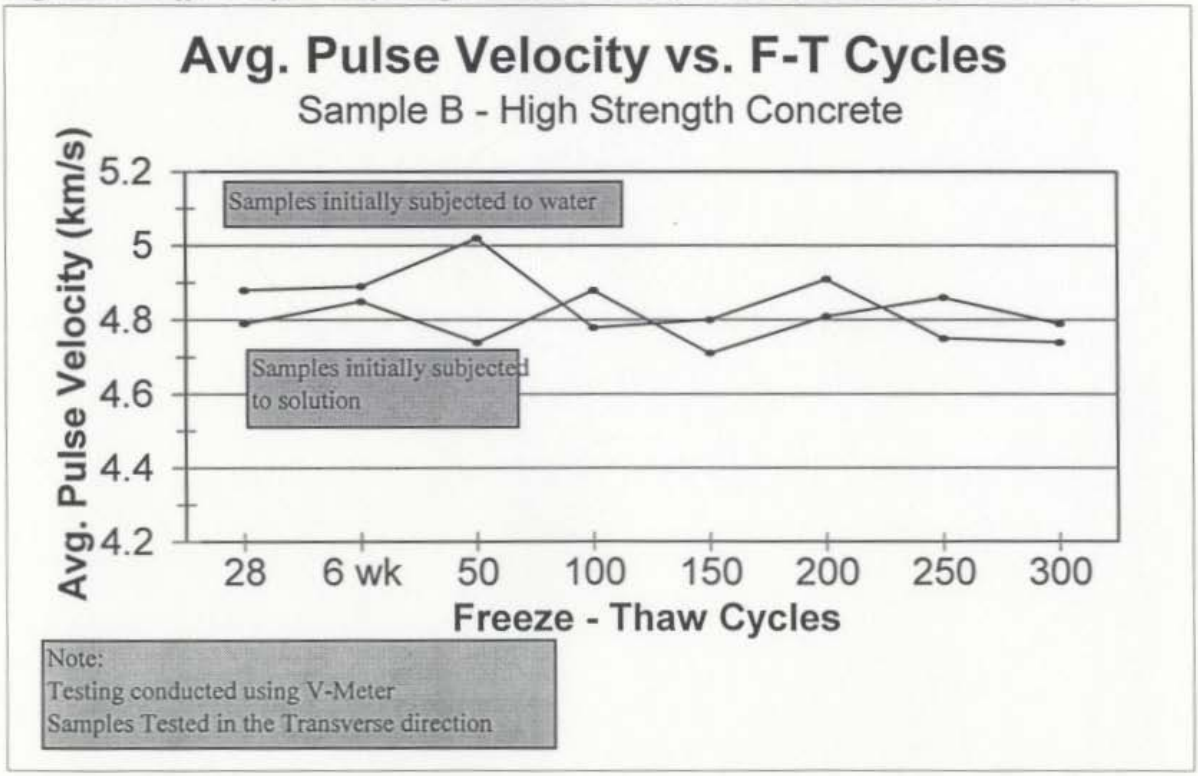

4.6 Creep Results

4.6.1 General

Creep is defined as the gradual increase in strain of concrete under a sustained stress, and is very important in the design of modern day structures. Often, the rate of application of the pre-determined load can affect the amount of instantaneous strain resulting on the specimen. However, for all samples tested, the load was generally applied in the same manner. It is important to re-iterate that all samples tested were not subjected to shrinkage due to the fact that they were stored in the curing room (100% RH @ 23°C), therefore, all charts represent pure creep.

When creep occurs in concrete, it is actually the volume of hydrated cement paste which undergoes creep. The aggregates act in restraint, and are usually not likely to creep, especially with normal weight aggregates. However, the aggregates modulus of elasticity, porosity, and mineralogical content all effect the overall value of creep obtained. In addition, the type of cement, fineness of cement, chemical admixtures, and supplementary cementing materials used in the mix design, storage temperature, specimen size, and relative humidity all affect the overall creep of the concrete. For this investigation, all of the previously mentioned items remain the same, except for the aggregate type. However, both aggregate types have approximately the same material properties, with the only difference being the reactivity of the aggregate. Therefore, any differences between creep experienced in concrete using both aggregates types, for both the normal and high strength mix design, will be the direct result of the aggregates reactivity only.

Creep has been found to continue for a very long period of time, if not indefinitely. However, after the application of the initial load, it can be seen that creep will continually decrease with time, and apparently tend toward some limiting value after an infinite period. It is important to note that the rate of creep increases with an increase in the strength - strain ratio for both normal and high strength concrete (Marzouk (1991), Neville (1995)).

Creep of both normal and high strength concrete at room temperature is influenced, for the most part, by the movement of evaporable water from the tobermorite gel. However, lower creep strains are usually experienced by high strength concrete compared with normal strength concrete. These results can be explained by the secondary hydration process between the calcium hydroxide and silica of high strength concrete. This reaction results in the degree of hydration being more developed in high strength concrete than that found in normal strength concrete, and thus a stronger, more durable, micro structure (Ali and Kesler (1964), Marzouk (1991), Neville (1995)).

Since the creep test is a prolonged compression test, it is assumed that the normal strength concrete specimens subjected to the NaOH solution will experience more creep, or compressibility, than those submerged in the de-ionized water. Rotter (1995) states that creep of specimens experiencing an alkali-aggregate reaction is 2 to 4 times larger than that of unaffected specimens. In addition, it is assumed that the normal strength concrete consisting of the potentially highly reactive aggregate will experience higher creep than that consisting of the potentially marginally reactive aggregate due to the formation of a higher

percentage of gel, which will be weaker than the hardened cement paste, and thus be more compressible (Refer to Section 4.1).

To the authors knowledge, no creep testing has been performed on high strength concrete specimens with regard to alkali-aggregate reactivity. However, research conducted by the Portland Cement Association has shown that high strength concrete usually experiences 40 to 70 % of the specific creep of normal strength concrete, and that creep strains are reduced as the hydration process of high strength concrete proceeds. This is due to the fact that the improving micro structure slows the moisture diffusion (Farny at al., 1994).

The improved qualities of high strength concrete would lead one to assume that the effects of the solution will not be as great as for normal strength concrete specimens (Refer to Section 4.1). Since the aggregate type is the only variable, any observed differences will be the result of the reaction alone.

4.6.2 Creep of Normal Strength Concrete

Normal strength concrete containing the potentially reactive aggregate in solution was observed to creep 1.94 times the amount observed in the same sample set subjected to the de-ionized water after a period of 90 days (Refer to Figure 70). This result is, once again, attributed to the formation of micro cracks occurring from the alkali-aggregate reaction (as explained in section 4.1), and is consistent with that reported by Rotter (1995). Creep samples consisting of the potentially reactive aggregate in solution were determined to creep

1.47 times that of like samples in the de-ionized water tank (Refer to Figure 71). The reduction in creep is the result of a decreased alkali-aggregate reaction occurring within the specimens, which is the direct result of the aggregate mineralogy.

Figure 70 - Creep of Concrete - NSC (Highly Reactive)

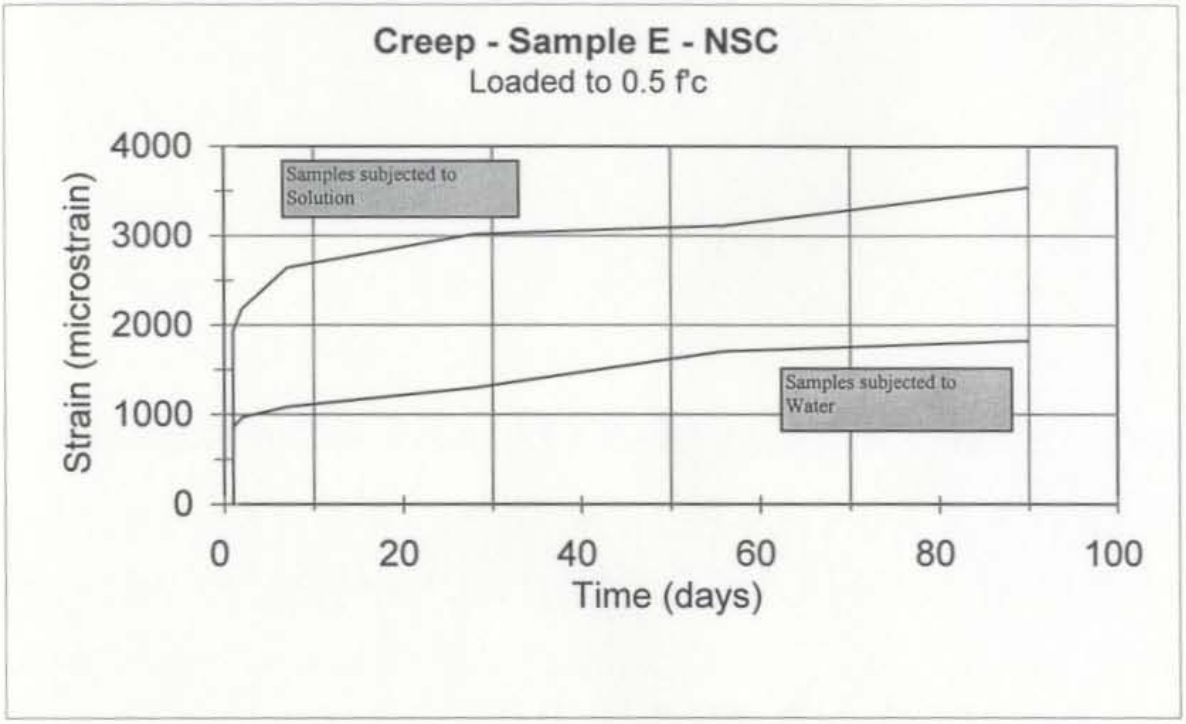

Figure 71 - Creep of Concrete - NSC (Moderately Reactive)

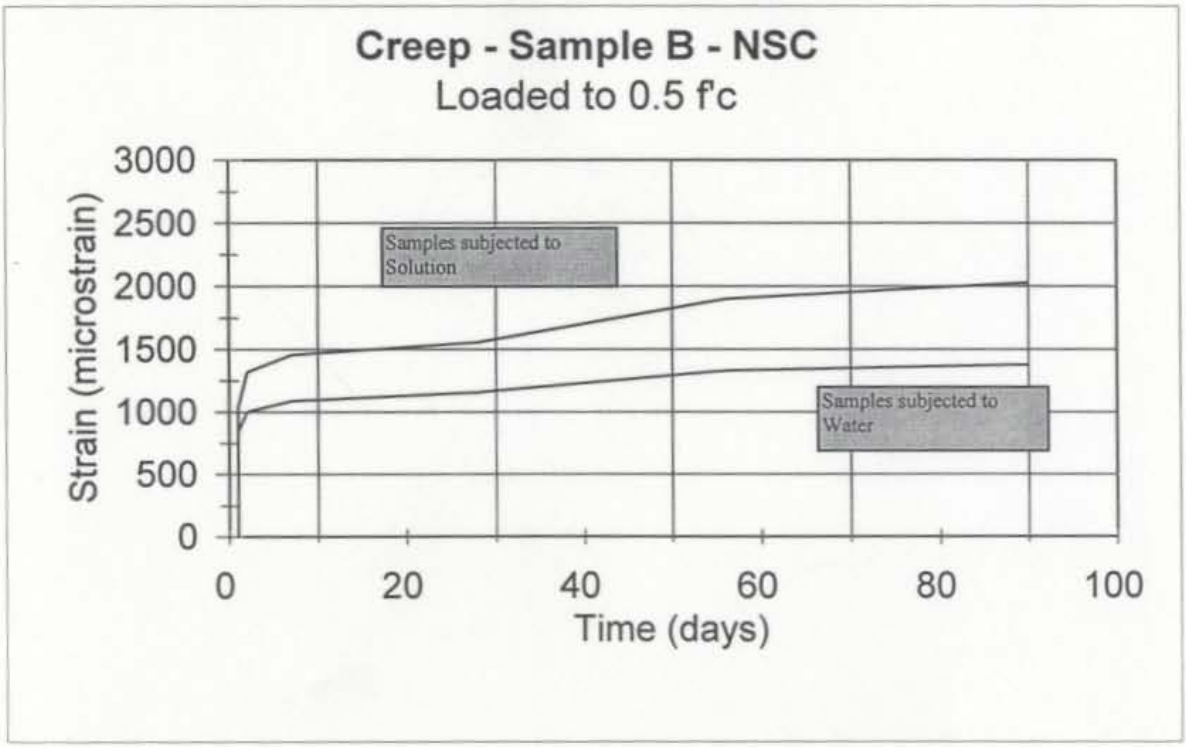

4.6.3 Creep of High Strength Concrete

High strength concrete containing the potentially highly reactive aggregate (aggregate E) was also observed to experience an increased amount of creep with respect to like samples containing the potentially marginally reactive aggregate (aggregate B). For the specimens containing aggregate E, those subjected to solution were observed to creep an average of 1.44 times that of its counterpart located in the de-ionized water (Refer to Figure 72). However, samples containing aggregate B, and subjected to NaOH solution, were observed to creep 1.29 times that of those contained in water (Refer to Figure 73). These results also substantiate the improved micro-structural qualities of high strength concrete with respect to normal strength concrete as reviewed in section 4.6.1.

Figure 72 - Creep of Concrete - HSC (Highly Reactive)

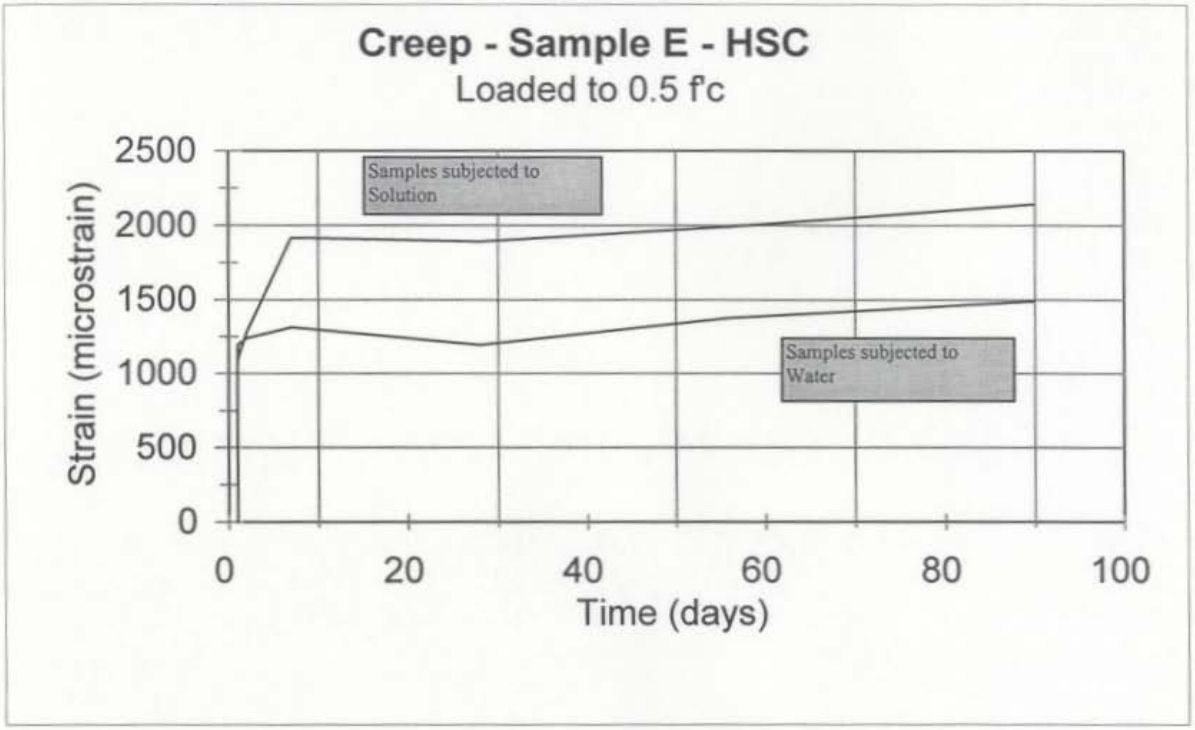

Figure 73 - Creep of Concrete - HSC (Moderately Reactive)

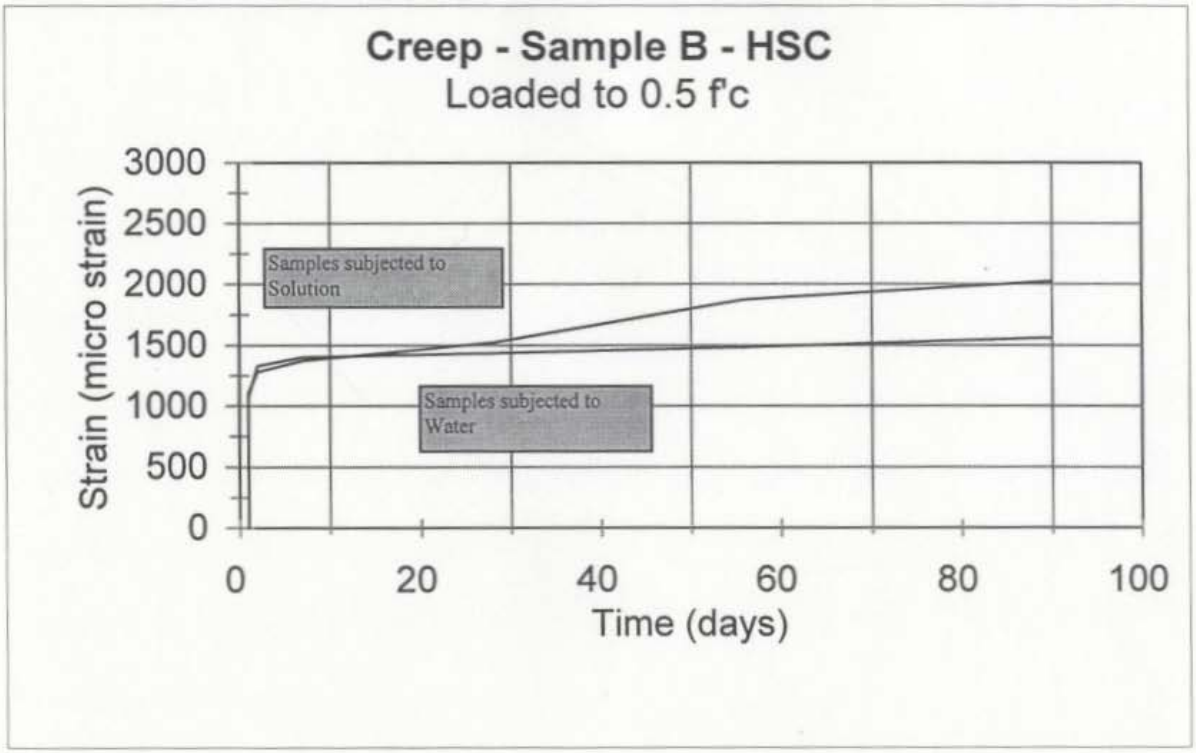

5.0 Effect of AAR on Beam Moment-Curvature

5.1 General

Research regarding alkali-aggregate reactivity has, for the most part, been concerned with the effects on the mechanical properties of concrete. Some researchers have generated either macro or micro models to aid in the overall understanding of the phenomenon. However, most have failed to bridge the gap between the experimental and practical on a level that is useful to the design engineer.

In the following section, the effects of theoretical expansive strains resulting from an alkali-aggregate reaction on the moment-curvature response of two common beam sections are investigated. These beams, an I-section, and a Tee-section, were chosen because they are present in many modern day structures, such as in buildings, and especially bridges. The analysis of these sections is based on strain compatibility and equilibrium equations, and will be introduced later.

The theoretical expansive strains, assumed to be the result of an alkali-aggregate reaction, will be considered with respect to the long term response of the section. The expansive strains chosen were 0 $\mu\epsilon$, 250 $\mu\epsilon$, 500 $\mu\epsilon$, and 1000 $\mu\epsilon$. A limiting value of 1000 $\mu\epsilon$ was chosen because Habita et al. (1992) showed that for a well-reinforced rectangular beam that was subjected to aggressive agents in order to facilitate an alkali-aggregate reaction, the largest expansive strain measured was of the order of 500 $\mu\epsilon$. It is believed that under actual in-service conditions, 1000 $\mu\epsilon$ is probably a limiting value.

5.2 Methodology

5.2.1 General

In order to better understand the procedures involved in the determination of the moment-curvature response, several parameters, and assumptions must be set forth.

For purposes of analysis, it is assumed that the section remains symmetrical about the vertical axis, that the concrete is only subjected to strains in the axial direction, and that the strains remain uniform over the width of any defined section. However, strains vary linearly over the depth of the section (i.e., plane sections remain plane). In addition, the members to be investigated will only be subjected to flexural loads (no axial loads).

In determining the moment-curvature response of a beam subjected to pure flexure, the most convenient method is to assume a concrete strain at the top of the section, and then, through trial and error, determine the strain at the bottom of the section which results in zero axial

load. Calculating the bottom strains for varying top concrete strains will allow the determination of the complete moment-curvature response of the section.

The methodology used in the determination of moment-curvature response is based on the following equilibrium equations.

$$\int_{Ac} f_c \, dA_c + \int_{As} f_s \, dA_s + \int_{Ap} f_p \, dA_p = N \qquad (5.1)$$

$$\int_{Ac} f_c \, y \, dA_c + \int_{As} f_s \, y \, dA_s + \int_{Ap} f_p \, y \, dA_p = -M \qquad (5.2)$$

Several additional compatibility equations, material stress-strain relationships, and assumptions are also required to determine the moment - curvature response of a section.

Initially, as previously stated, the strain in the concrete at the top of the section is assumed. The correct corresponding strain at the bottom of the section is determined by calculating the strain at the bottom of the section which, in conjunction with several compatibility equations, results in zero axial load from equation 5.1. Secondly, the transformed area (A_{trans}), transformed section modulus (I_{xx}), and section centroid (y_{trans}) must be determined in order to know the location about which moments are to be calculated.

Investigating any section can be accomplished by either simulating short or long term loading conditions. Since the compatibility and material property equations need be modified for long term investigations, these topics will be introduced separately.

5.2.2 Short Term Moment - Curvature Response

The mechanical properties important in the determination of either response are the ultimate concrete strength (f'c), strain at ultimate strength (ϵ'_c), and the modulus of elasticity (E) are required. For purposes of this investigation, the modulus of elasticity has been calculated using the ultimate strength from the following equation, where f'c was assumed to be 35 MPa.

$$E_{ct} = 5500\sqrt{f'_c} \text{ (MPa)} \qquad (5.3)$$

Using the initial tangent modulus (E_{ct}), the strain at ultimate strength can be determined from the following equation.

$$E_{ct} = 2\frac{f'_c}{\varepsilon'_c} \qquad (5.4)$$

The overall strain in any prestressed reinforcement can be determined from the following equation,

$$\varepsilon_{pf} = \varepsilon_c + \Delta\varepsilon_p \qquad (5.5)$$

In addition, the stress in the prestressing strands can be calculated using the Ramberg-Osgood equation as follows.

$$f_p = 200000\ \varepsilon_{pf} \left\{ 0.025 + \frac{0.975}{\left[1 + \left(118\ \varepsilon_{pf}\right)^{10}\right]^{0.1}} \right\} \leq 1860\ \text{MPa} \qquad (5.6)$$

The overall force in the prestressing strands can then be calculated using the following equation.

$$F_P = f_p\ A_P \qquad (5.7)$$

The final strain in non-prestressed reinforcement is assumed to be equal to the strain in the concrete at that location. Therefore,

$$\varepsilon_s = \varepsilon_c \qquad (5.8)$$

In addition, the stress in the non-prestressed reinforcement can be determined using the following equation.

$$f_s = E_s\ \varepsilon_s \leq f_r \qquad (5.9)$$

Using the following equation, the force in the non-prestressed reinforcement can be determined.

$$F_s = f_s\ A_s \qquad (5.10)$$

The force caused by the strains in the concrete is calculated based on the following equation.

$$F_c = \alpha \ f'_c \ \beta \ c \ B \tag{5.11}$$

where,

$$\alpha \ \beta = \frac{\epsilon_t}{\epsilon'_c} - [\epsilon_t / \epsilon'_c]^2 \tag{5.12}$$

and

$$\beta = \frac{4 - \epsilon_t / \epsilon'_c}{6 - 2 \ \epsilon_t / \epsilon'_c} \tag{5.13}$$

The correct strain at the bottom of the section corresponding to the strain at the top of the section has to ensure that the sum of the compressive and tensile forces generated from the aforementioned equations results in zero axial load. Finally, when the correct bottom and top strains have been chosen to ensure, with aid of the compatibility equations, that zero axial load exists, moments can be taken about the centroidal axis. The curvature for the particular moment can be determined from simple geometry.

5.2.3 Long Term Moment - Curvature Response

As with the short term response equations, the ultimate concrete strength (f 'c), strain at ultimate strength (ϵ 'c), and the modulus of elasticity (E) of concrete are required. However, the time dependant effects of creep, shrinkage, relaxation, and temperature must also be considered for each section. For the following long term investigations, no thermal effects were considered.

Creep can be accounted for by using a modified stress - strain relationship. If the ultimate strength of the cylinder (f'c) is known, the effective modulus of elasticity used in simulation of long term effects can be calculated using the following equation.

$$E_{c,eff} = \frac{E_{ct}}{1 + \phi} \tag{5.14}$$

The modified strain at ultimate strength of the cylinder used for long term loading can be calculated from the same equation as presented in Equation 5.4, however, the modulus of elasticity must be replaced with the effective modulus of elasticity.

It is assumed that the prestressing strands lose 3% of their initial stress due to relaxation. Therefore, the effective modulus of elasticity for the prestressing strands can be determined using the following equation.

$$E_{eff,p} = (1 - \text{Relaxation})\, E_p \tag{5.15}$$

The modulus of elasticity for non-prestressed reinforcement is assumed not to be affected by any long term loading.

As with the determination of the moment curvature response of a section under short term loading, the strains in the concrete at different locations throughout the section have to be determined. The compatibility equations used in determining the final strains under long term analysis need to include the effects of shrinkage and temperature.

The final strain in any prestressed reinforcement can be determined from the following equation,

$$\varepsilon_{pf} = \varepsilon_c + \Delta\varepsilon_p - \varepsilon_{pth} - \varepsilon_{AAR} \quad (5.16)$$

The final strain in non-prestressed reinforcement can be calculated using the following equation.

$$\varepsilon_{sf} = \varepsilon_c - \varepsilon_{sth} - \varepsilon_{AAR} \quad (5.17)$$

The final long term strain in the concrete can be calculated using the following equation.

$$\varepsilon_{cf} = \varepsilon_c - \varepsilon_{cth} - \varepsilon_{AAR} \quad (5.18)$$

As with the determination of the short term moment - curvature response, when the correct bottom and top strains have been chosen to ensure, with aid of the compatibility equations, that zero axial load exists, moments can be taken about the centroidal axis. However, for the prestressing strands, the Ramberg - Osgood Equation (Equation 5.6) must be modified to determine the strain at which the strands will rupture under long term loading. The ultimate stress of the strands remains unchanged. However, the effective modulus of elasticity must be used in the equation. Therefore,

$$f_p = 194000\ \varepsilon_{pf}\left\{0.025 + \frac{0.975}{\left[1 + \left(118\ \varepsilon_{pf}\right)^{10}\right]^{0.1}}\right\} \leq 1860\ \text{MPa} \qquad (5.19)$$

Using the modified modulus of elasticity, and ultimate strength of the prestressing strand, the prestressing strand is assumed to rupture at an ultimate strain (ϵ_{pu}) of 0.054 $\mu\epsilon$ (5.4 %).

The forces due to the non-prestressed reinforcement, and the concrete are calculated in the same manner as with the short term loading scenario. However, the strains used in the force equations must be those determined using the long term final strain equation as introduced above.

For the long term loading, several different theoretical AAR strains (250, 500, and 1000 $\mu\epsilon$) will be investigated, as well as long term effects without the incorporation of AAR strains. The effects of the different loading scenarios are shown in the following sections.

5.3 Tee - Section Moment - Curvature Response

Often with construction of bridges or floor systems, supporting beams and slabs are cast together in a continuous pour so that the entire system is monolithic. The slab, extending on either side of the beam is then considered as the flange, with the beam (web) and flange resulting in the formation of a Tee-section. The Tee-section chosen for analysis is shown in Figure 74.

For this particular section, it is assumed that the web has 7 layers of prestressing tendons located at 50mm intervals from the bottom of the section with 50mm of cover. It is also assumed that for each interval, a total area of 200 mm^2 of prestressing tendon exists. Particulars such as prestrain due to jacking, modulus of elasticity for the tendons, and ultimate strain before rupture can be found in Table 42.

It is assumed that there is no non-prestressed reinforcement located in the section, and that tension stiffening only occurs around the prestressing. Thermal strains are not included in this investigation, however, shrinkage strains of -0.48×10^{-3} are present. In addition, for the long term investigations, AAR strains of 0, 250, 500 and 1000 $\mu\epsilon$ will be investigated. Strains resulting from alkali-aggregate reactivity, since being expansive, are considered positive. However, it is assumed that the strains due to AAR will only affect non-prestressed reinforcement (in this case not present), and the surrounding concrete. This investigation is also conducted assuming several different layers of concrete, the dimensions and locations

of which are listed in the following table. The moment - curvature response of the section is located in Figure 75.

Figure 74 - TEE-Section Investigated

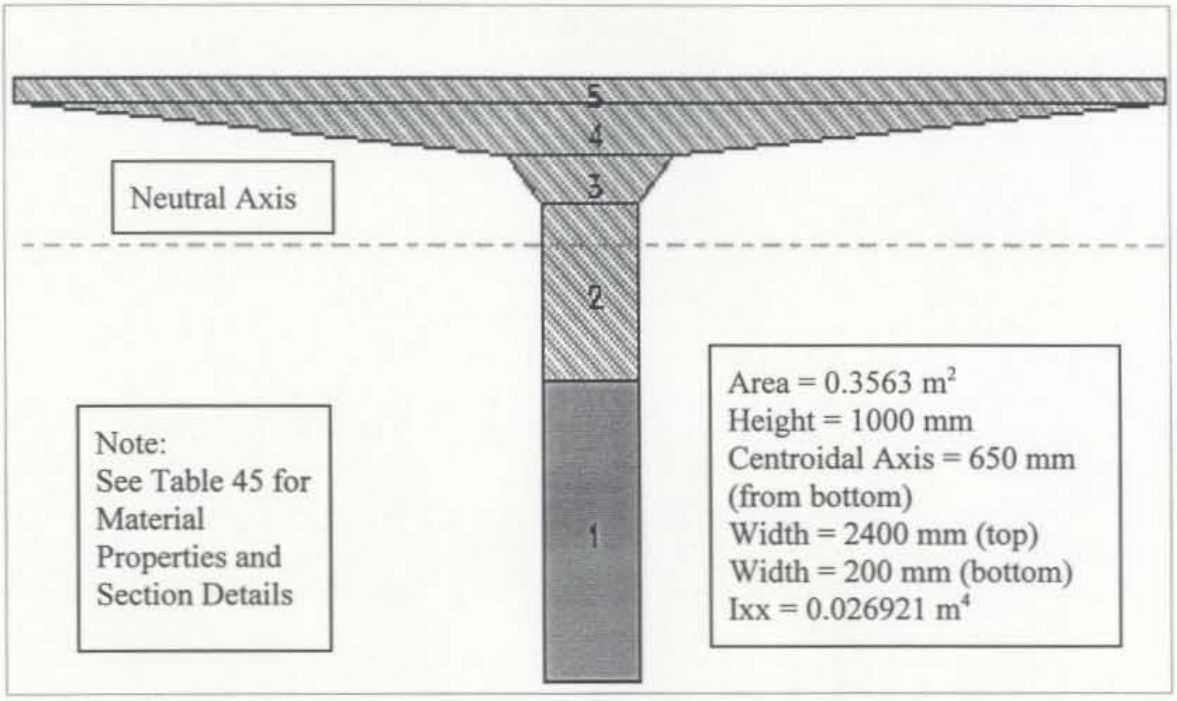

Figure 75 - Moment Curvature Response of Tee - Section

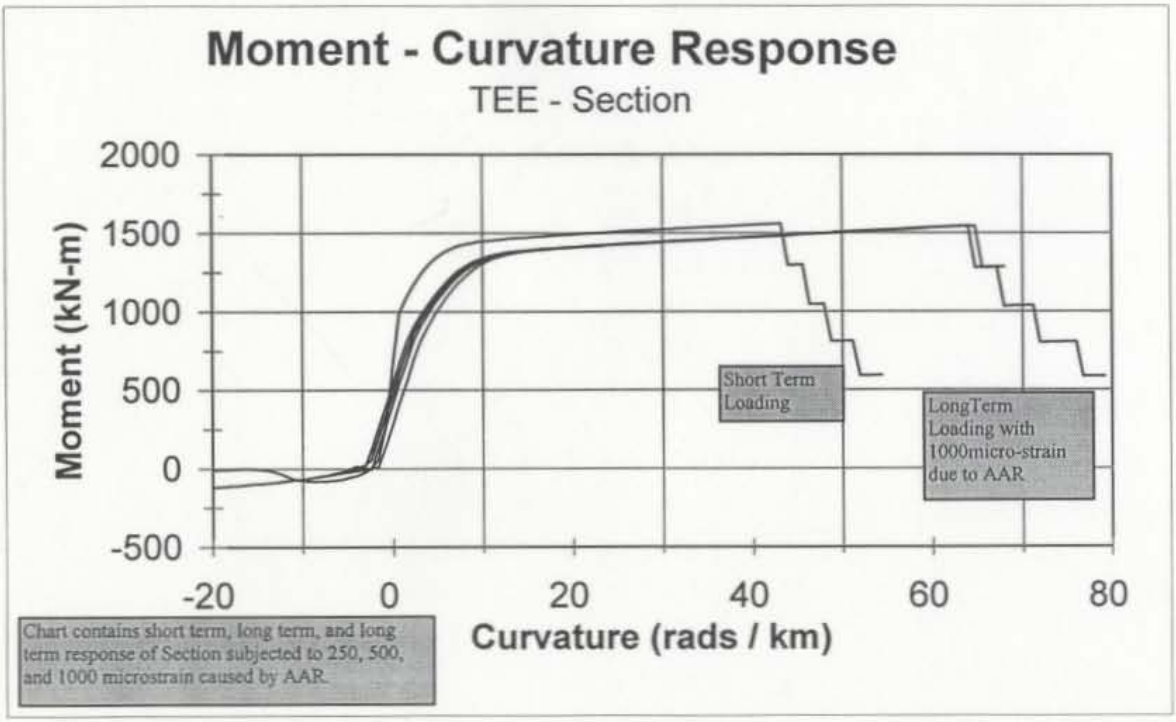

Table 42 - Tee - section Properties

Response Version 1 Data-File
Copyright 1990 A. Felber
Name of Section: **Tee-Beam**
Units M/U 'Metric/U.S.Customary': M
Number of Concrete Types (1-5): 2

Type Number	f'c [MPa]	ec' [Milli-Strain]	Tension Stiffening Factor
1	35.00	-7.959	0.70
2	35.00	-7.959	0.00

Number of Rebar Types (1-5): 0
Number of Tendon Types (1-5): 1

Type Number	[Ramberg-Osgood-Factors--] A	B	C	Elastic Modulus [MPa]	fpu [MPa]	ep rupture [Milli-Strain]
1	0.025	118.000	10.000	194000	1860	54.000

Height of Section: 1000 mm
Distance to Moment Axis: 650 mm

Shear Y/N 'Yes/No': N

Number of Concrete Layers (1-20): 5

Layer Number	y [mm]	bottomwidth [mm]	top width [mm]	height [mm]	Type Number
1	0	200	200	450	1
2	450	200	200	262	2
3	712	200	350	75	2
4	788	350	2400	75	2
5	862	2400	2400	38	2

Number of Tendon Layers (0-10) : 7

Layer Number	y [mm]	Area [mm^2]	Prestrain [Milli-Strain]	Type Number
1	50	200	6.000	1
2	100	200	6.000	1
3	150	200	6.000	1
4	200	200	6.000	1
5	250	200	6.000	1
6	300	200	6.000	1
7	350	200	6.000	1

5.4 I - Section Moment - Curvature Response

I - sections are often used as girders in prestressed bridge construction, and will be the next section considered in the moment - curvature response investigation. The section chosen for analysis is shown in Figure 76, whereas additional sectional properties are located in Table 43.

It is assumed that the I-section has 2 layers of prestressing tendons. The first is located at 50 mm from the bottom of the section with an area of 300 mm^2, whereas the second layer of prestressing is located at 100 mm from the bottom with an area of 200 mm^2. All other parameters regarding the ultimate stress of the tendons, and strain at which rupture occurs, in both the long and short term cases, remains identical to those considered during the Tee-section investigation.

The I-section is assumed to have an area of 600 mm^2 non-prestressed reinforcement located at 50 mm from the top of the section. This particular reinforcement is assumed to have a modulus of elasticity of 200E3 MPa, and an ultimate stress of 400 MPa. It is also assumed that the reinforcement will rupture at a strain of 40E-3 in both short and long term investigations.

Tension stiffening for the I - section is considered to occur around both kinds of reinforcement. Once again, thermal strains are not included in this investigation, however, shrinkage strains of -0.48E3 are present. As conducted for the Tee- section investigation,

theoretical expansive strains of 0, 250, 500 and 1000 $\mu\epsilon$ resulting from alkali-aggregate reactivity will be investigated, and that these strains will not affect the prestressed reinforcement. The different layers of concrete considered in this investigation, as well as other material and sectional properties are listed in Table 42. The moment - curvature response of the section is located in Figure 77.

Figure 76 - I-Section Investigated

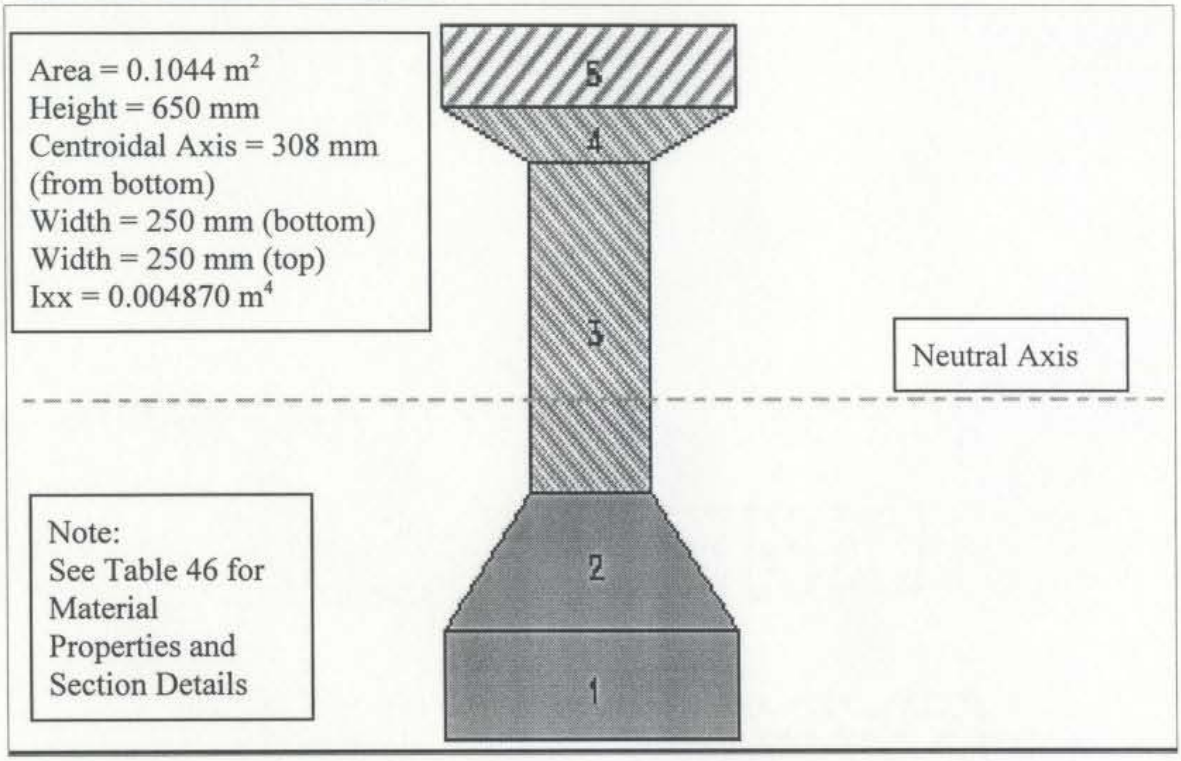

Figure 77 - Moment Curvature Response of I - Section

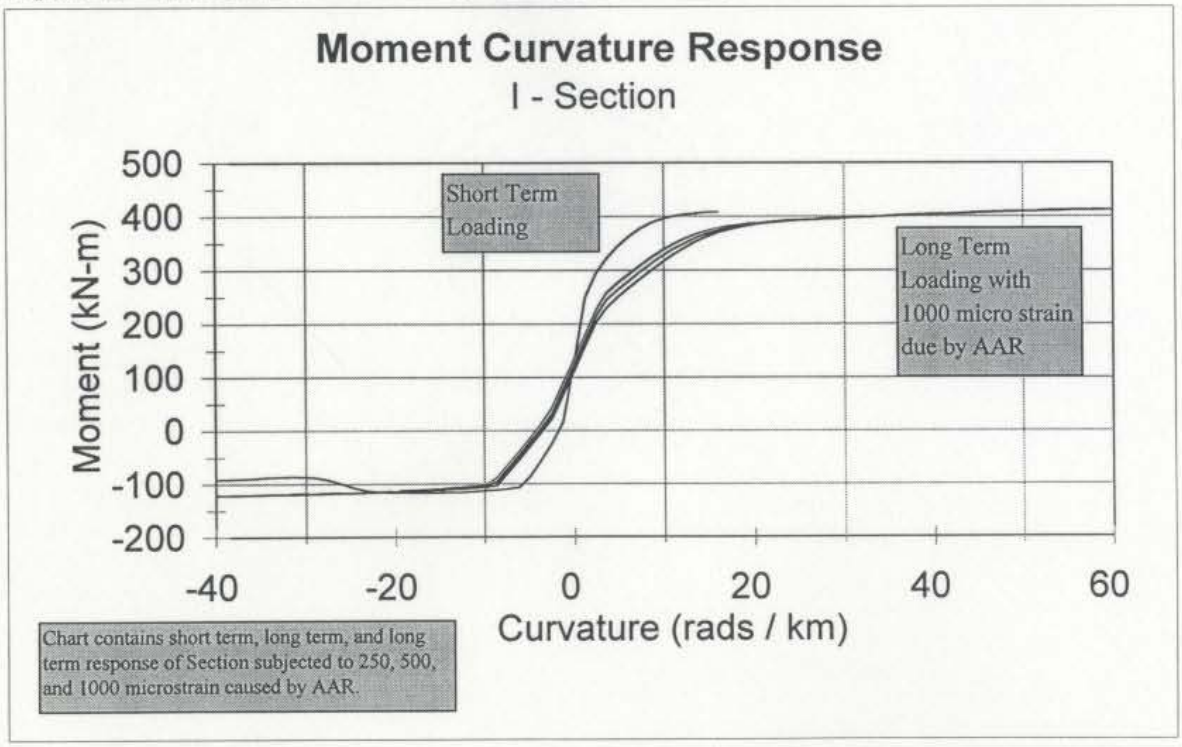

Table 43 - I - Section Properties

Response Version 1 Data-File
Copyright 1990 A. Felber
Name of Section: I-Section
Units M/U 'Metric/U.S.Customary': M
Number of Concrete Types (1-5): 2

Type Number	f'c [MPa]	ec' [Milli-Strain]	Tension Stiffening Factor
1	35.00	-7.959	0.70
2	35.00	-7.959	0.00
3	35.00	-7.959	0.70

Number of Rebar Types (1-5): 1

Type Number	Elastic Modulus [MPa]	fy [MPa]	esh [millistrain]	es rupture [millistrain]	fu [MPa]
1	200000	400	20.0	40.0	400

Number of Tendon Types (1-5): 1

Type Number	[Ramberg-Osgood-Factors--] A	B	C	Elastic Modulus [MPa]	fpu [MPa]	ep rupture [Milli-Strain]
1	0.025	118.000	10.000	194000	1860	54.000

Height of Section: 650 mm
Distance to Moment Axis: 308 mm
Shear Y/N 'Yes/No': N

Number of Concrete Layers (1-20): 5

Layer Number	y [mm]	bottomwidth [mm]	top width [mm]	height [mm]	Type Number
1	0	250	250	100	1
2	100	250	100	125	1
3	225	100	100	300	2
4	525	100	250	50	2
5	575	250	250	75	3

Number of Rebar Layers (0-10) : 1

Layer Number	y [mm]	Area [mm^2]	Type Number
1	600	600	1

Number of Tendon Layers (0-10) : 2

Layer Number	y [mm]	Area [mm^2]	Prestrain [Milli-Strain]	Type Number
1	50	300	6.000	1
2	100	200	6.000	1

5.5 Discussion of AAR effect on Beam Moment - Curvature Response

The I-section, and Tee-section previously investigated are representative of those often used in modern day construction. From the moment-curvature response of both, it can be seen that the curvature does increase somewhat when considering the short term response in conjunction with the long term response without the addition of strains resulting from alkali-aggregate reactivity. These findings are consistent with an analysis of any section with regard to moment-curvature response.

Examination of the results does show that even when a theoretical expansive alkali-aggregate strain of 1000 $\mu\epsilon$ is assumed to be present, the effects on the moment-curvature response are minimal. The reduction in moment capacity, and curvature of both sections is minimal (<5%). It is important to note that although the curvature of the sections increases slightly as the theoretical AAR strain is increased, the effect may be less in actual field performance conditions. The bond of the cement and the reinforcement should be considered. However, it is beyond the scope of this report.

These findings are consistent with those determined by Clayton et al. (1990), and Turdoff (1990), as reviewed in section 2.6.3. Turnoff concluded that for several prestressed concrete beams that had been affected by alkali-aggregate reactivity, the bending moment capacity of the section had not been affected. In fact, in some cases the capacity of the section had increased. Clayton et al. (1990) also concluded that for well-reinforced sections affected by alkali-aggregate reactivity, no adverse side effects were experienced.

6.0 Conclusions and Recommendations

Research over the past few decades has indicated than an alkali-aggregate reaction can be a catalyst in premature deterioration of concrete structures. In the past, alkali - aggregate research in Newfoundland was limited to petrographic examination of aggregates, accelerated mortar bar testing, and concrete prism testing. However, due to recent developments in Newfoundland regarding the Hibernia project, the Lower Churchill River, and the possibility of several other mega projects, research regarding the effect of an alkali-aggregate reaction on the mechanical properties of concrete was initiated. The following is a summary of the major findings, and includes recommendations for further research.

- A petrographic examination and accelerated mortar bar testing were conducted for 7 locations in the province to determine the aggregate's reactivity. Based on the results of the investigation, the aggregate's in Newfoundland can be classified into three types; potentially highly reactive, potentially moderately reactive, and non-reactive.

- Using the results of both the petrographic examination and the AMB testing, an extensive testing regime was initiated. This included over 800 samples of both normal and high strength concrete consisting of either a potentially highly reactive aggregate, or a potentially marginally reactive aggregate. Samples of both normal and high strength were equally divided, and placed in either a 80 °C solution bath containing water, the control environment, or 1M NaOH, to accelerate the reaction. Samples of both strengths, from both solution baths, were tested after the initial 28 day curing period, and at various intervals for an extended period of time. The mechanical properties tested included compression, direct tension, indirect tension, freeze thaw, and creep testing. The results of each test specimen, from both the water and solution baths, were then compared.
- The effects of an alkali-aggregate reaction on the mechanical properties of high strength concrete were minimal. This is attributed to the improved micro structure of high strength concrete, as well as the improved grain refinement, and decreased permeability which reduces the mobility of aggressive agents. In addition, the additional calcium silicate hydrates provided to the mix by the silica fume chemically "tie-up" alkalies in the concrete that may otherwise be available to initiate an alkali-aggregate reaction.
- In general, normal strength concrete samples containing the highly reactive aggregate experienced the greater losses in mechanical properties than the normal strength concrete containing the marginally reactive aggregate.

- The compressive strength of normal strength concrete containing the highly reactive aggregate experienced a decrease in ultimate compressive strength of 28%, and a decrease in modulus of elasticity of 80%. For the normal strength concrete containing the moderately reactive aggregate, the ultimate compressive strength remained almost constant, while a decrease in modulus of elasticity of 20% was recorded. These results are found to be consistent with that determined from other researchers.
- The ultimate tensile strength of both the normal strength concrete containing the highly and marginally reactive aggregate were found to be very sensitive to the effects of an alkali-aggregate reaction. The ultimate tensile strength of the normal strength concrete containing the highly and moderately reactive aggregate decreased by 37 %, and 31 % respectively. These results are attributed to the increased sensitivity of direct tension testing to the effects of the reaction.
- The effects of an alkali-aggregate reaction on the modulus of rupture of normal strength concrete specimens was deemed inconclusive. The modulus of rupture of specimens containing the highly reactive aggregate did not decrease during the testing period, whereas, specimens containing the moderately reactive aggregate experienced a decrease in the modulus of rupture. Such unexpected behaviour can be explained due to any eccentricity of the loading ram, or uneven loading application.
- The effects of freezing and thawing on the mechanical properties of normal strength concrete revealed that the specimens containing the highly reactive aggregate experienced a decrease of 13 % in ultrasonic pulse velocity over the testing period, whereas the specimens containing the moderately reactive aggregate experienced a

30 % decrease. It was expected to see a larger decrease for normal strength specimens containing the highly reactive aggregate. However, upon regular testing, it was noticed that the specimens containing the moderately reactive aggregate experienced a substantial amount of scaling, which may explain the results.

- Creep of normal strength concrete containing the highly reactive aggregate experienced a 94% increase in creep strain with respect to the control after a period of 90 days at a load equal to 50% of the ultimate compressive strength. Normal strength specimens containing the moderately reactive aggregate experienced a 48 % increase in creep strain with respect to the control after a period of 90 days at a load equal to 50% of the ultimate compressive strength. These results were expected, and are attributed to the weaker cement gel formed by the more aggressive alkali-aggregate reaction.
- The theoretical investigation of the effects on an alkali-aggregate reaction of the moment curvature of two common structural bridge beams was investigated. The concept of strain compatibility and equilibrium was used to determine the effects of the reaction on the long term moment - curvature response of each section. It has been found that the effect for both sections were minimal (<5%). These results are consistent with that determined from research conducted during the past decade involving pre-stressed, and well reinforced sections.

Recommendations for Future Research

- It is recommended that geochemical analysis involving either X-ray diffraction analysis, scanning electron microscope techniques, or petrographic examination be used to compare the products of an alkali-aggregate reaction of laboratory specimens and samples taken from in-service structures. In this manner, the mechanical properties of laboratory samples could aid in the prediction of field structure response over its in-service life. In addition, duration of submergence in solution could possibly be linked to actual field service years.
- It is recommended that future laboratory samples contain reinforcement. Research regarding reinforced concrete specimens may provide a better indication of the effects of an alkali-aggregate reaction on actual field performance of structures.

References

Ali, I. and Kesler, C.E. (1964). *Mechanism of Creep in Concrete*, Symposium on creep of Concrete, ACI special publication SP, 9,, 57-67

Arumugasaamy, P., and Swamy, R.N. (1978). *Moisture movements in reinforced concrete columns, Il Clemento*, 3: 121-128.

Alasali, M.M., Malhotra, V.M., Soles, J.A. (1990). *Performance of various test methods for assessing the potential reactivity of some Canadian aggregates*, International Workshop on Alkali-Aggregate Reactions in Concrete: Occurrence Testing and Control, J.A. Soles (Ed.), CANMET, Ottawa: (5).

Bach et al. (1992). *Load Carrying Capacity of Structural Members Subjected to Alkali-Silica Reactions*, The 9th International Conference on Alkali-Aggregate Reaction in Concrete: 9-21.

Bérubé, M.A., Duchesne, J. (1992). *Does Silica Fume Merely Postpone Expansion Due to Alkali-Aggregate Reaction*, The 9th International Conference on Alkali-Aggregate Reaction in Concrete: 71-80.

Blackwell, B.Q., et al. (1992). *The Use of Fly Ash to Suppress Deleterious Expansion Due to AAR in Concrete Containing Greywacke*, The 9th International Conference on Alkali-Aggregate Reactivity in Concrete:102-109.

Bragg, D., and Foster, K. (1992). *Relationship between petrography and results of alkali-reactivity testing, samples from Newfoundland, Canada*, The 9th International Conference on Alkali-Aggregate Reaction in Concrete:127-135.

Bragg, D.J. (1995). *Petrographic Examination of Construction Aggregates of Newfoundland*, Dept. of Natural Resources (Geological Survey), Government of Newfoundland and Labrador, Current Research, 95(1).

Bragg, D.(1996). *Alkali-Aggregate Reactivity in Newfoundland*, Department of Natural Resources, Government of Newfoundland and Labrador: 11-20.

Chana P S and Thompson D.M., (1992). *Laboratory Testing and Assessment of Structural Members Affected by Alkali-silica Reaction*, The 9th International Conference on Alkali-Aggregate Reaction in Concrete: 156-165.

Chatterji, S.A. (1989). *Simple Chemical Test Method for the Detection of Alkali Aggregate reaction Using Concrete Specimens*, Proceedings of the 8th International Conference on Alkali-Aggregate Reactivity: 295-299.

Chen, et al. (1990). *CANMET investigations of supplementary cementing materials for reducing alkali-aggregate reactions*, International Workshop on Alkali-Aggregate Reactions in Concrete: Occurrence, Testing and Control, J.A. Soles (Ed.), CANMET, Ottawa: (8).

Chen, Z. (1993). *Non-linear Analysis of High-Strength Concrete Slabs*. Master's Thesis, Memorial University of Newfoundland.

Clark, L.A. (1990). *Structural aspects of alkali-silica reaction*. Structural Engineering Review, 2:121-125.

Clayton et al. (1990). *The effects of alkali-silica reaction on the strength of prestressed concrete beams*. The Structural Engineer, 68 (15): 287-292.

Collins, M..and Mitchell. D. (1991). Prestressed Concrete Structures. New Jersey: Prentice Hall Publishing Co.

Connell, M.D., and Higgins, D.D. (1992). *Effectiveness of GGBS in Preventing ASR*, The 9th International Conference on Alkali-Aggregate Reaction in Concrete: 175-183.

Davies G., and Oberholster, R.E. (1989). *The Effect of Different Outdoor Exposure Conditions on the Expansion due to Alkali-Silica Reaction*, Proceedings of the 8th International Conference on Alkali-Aggregate Reactivity: 623-628.

Danay, A. (1994). *Structural Mechanics Methodology in Diagnosing and Assessing the Long-Term Effects of Alkali-Aggregate Reactivity in Reinforced Concrete Structures*, ACI Materials Journal: 54-62.

Diab, Y., and Prin, D. (1992). *Alkali-Aggregate Reaction Structural Effects: A Finite Element Model*, The 9th International Conference on Alkali-Aggregate Reaction in Concrete:261-268.

Doran, D.K., and Moore, J.F.A. (1989). *Appraisal of the Structural Effects of Alkali-Silica Reaction*, Proceedings of the 8th International Conference on Alkali-Aggregate Reactivity: 657-672.

Duchesne, J., and Bérubé, M. (1994). *Available Alkalies from Supplementary Cementing Materials*, ACI Materials Journal, 91 (3): 289-298.

Farbiarz, J., et al. (1989). *Alkali-Aggregate Reaction in Fly Ash Concrete*, Proceedings of the 8th International Conference on Alkali-Aggregate Reactivity: 240-246.

Farny, A., et al. (1994). *High Strength Concrete*. Portland Cement Association, Skokie, Ill.

Goltermann, P. (1994). *Mechanical Predictions on Concrete Deterioration. Part 2: Classification of Crack Patterns*. ACI Materials Journal, 92(1): 58-63.

Grattan - Bellew, P.E. (1990). *Alkali-aggregate reactivity highlights of current research including presentations at the 8th International Conference on Alkali-Aggregate*, International Workshop on Alkali-aggregate reactions in concrete: Occurrence, Testing, and Control, J.A. Soles (Ed.), CANMET, Ottawa: (1).

Guo, Z.H., and Zhang, X.Q., (1987). "Investigation of complete stress deformation curves for concrete in tension." ACI Materials Journal., 84(4), 278-285.

Habita et al. (1992). *Alkali-aggregate reaction structural effects: An experimental study*, The 9th International Conference on Alkali-Aggregate Reaction in Concrete: 403-409.

Hammersely, G.P. (1992). *Procedures for Assessing the Potential Alkali-Reactivity of Aggregate Sources*, The 9th International Conference on Alkali-Aggregate Reaction in Concrete: 411-419.

Hayes, J.P. (1990). Unpublished geology map of Newfoundland, Department of Mines and Energy, Mineral Development Division, Government of Newfoundland and Labrador, Version 2.0.

Heinz, D. and Ludwig, U. (1987). *Mechanism of secondary Ettringite Formation in Mortars and Concrete subjected to Heat Treatment, Concrete Durability*, Katherine and Bryant Mather International Conference, John M. Scanlon (Ed.), American Concrete Institute SP-100, 2: 2059-2072.

Hobbs, D.W. (1989). *Effect of Mineral and Chemical Admixtures on Alkali-Aggregate Reaction*, Proceedings of the 8th International Conference on Alkali-Aggregate Reactivity: 173-186.

Hobbs D.W. (1990). *Cracking and Expansion due to alkali-silica reaction: its effect on concrete*, Structural Engineering Review, 2: 65-70.

Hooton, R.D., and Rodgers, C.A. (1989). *Evaluation of Rapid Test Methods for Detecting Alkali-Reactive Aggregates*, Proceedings of the 8th International Conference on Alkali-Aggregate Reactivity: 439-444.

Hooton, R.D. (1992). *New Aggregate Alkali-Reactivity Test Methods*, Ministry of Transportation, Ontario (Research and Development Branch report).

Hudec, P.P., and Labri, J.A. (1989). *Chemical Treatments and Additives to Minimize Alkali Reactivity*, Proceedings of the 8th International Conference on Alkali-Aggregate Reactivity: 193-198.

Institution of Structural Engineers (1998): Structural Effects of alkali-silica reaction, p.31

Jawed I . (1992). *Alkali-Silica Reactivity - A Highway Perspective*, The 9th International Conference on Alkali-Aggregate Reactivity in Concrete: pp. 471- 476.

Jones, T.N., et al. (1990). *Mechanism of Expansion in Duggan Test for Alkali-Aggregate Reaction, Canadian Developments in Testing Concrete Aggregates for Alkali-aggregate reactivity*, Ministry of Transportation of Ontario, Report EM-92: 70-82.

Kawamura, M., et al. (1989). *Release of Alkalis from Reactive Andesitic Aggregates and Fly Ashes into Pore Solution in Mortars*, Proceedings of the 8th International Conference on Alkali-Aggregate Reactivity: 271-278.

Koyangi et al. (1992). *Mechanical Properties of Concrete Deteriorated by Alkali-aggregate Reaction under Various reinforcement Ratios*, The 9th International Conference on Alkali- Aggregate Reactivity: 556-563.

Leger, P., et al. (1990). *Numerical Simulation of concrete expansion in concrete dams affected by alkali-aggregate reaction: state of the art*, Canadian Journal of Civil Engineering, 22, 692-713.

Ludwig, U. (1989). *Effects of Environmental conditions on Alkali-Aggregate Reactions and Preventative Measures*, Proceedings of the 8th International Conference on Alkali-Aggregate Reactivity: 583-596.

Marzouk, H. (1991). *Creep of high-strength concrete and normal-strength concrete.* Magazine of Concrete Research, 43 (155):121-126.

Marzouk, H. and Chen, Z.W. (1995). *Fracture Energy and Tensile Properties of High Strength Concrete.* Journal of Materials in Civil Engineering, 7(2): 108-116.

Marzouk, H., Jiang, D. (1994). *Effects of Freezing and Thawing on the Tension Properties of High Strength Concrete.* ACI Materials Journal, 91(6).

May, I.M., and Wen, H.X. (1992). *The Modelling of the Effects of AAR Expansion on Reinforced Concrete Members*, The 9th International Conference on Alkali-Aggregate Reaction in Concrete: 638 - 647.

Mehta, P.K. (1988). *Durability of Concrete exposed to the Marine Environment*, International Conference on Performance of Concrete in Marine Environment, V.M. Malhotra (Ed.): 1-29.

Nielsen, K., et al, (1993). *Development of stresses in Concrete Structures with alkali-silica reactions*, Materials and Structures, 26:152-158.

Neville, A.M. (1995). Properties of Concrete: Fourth Edition, Longman Group Limited, England.

Oberholster, R.E. (1989). *Alkali-Aggregate Reactions in South Africa: Some Recent Developments in Research*, Proceedings of the 8th International Conference on Alkali-Aggregate Reactivity: 77-82.

Okada, K., et al. (1989). *Alkali-aggregate reaction: An Investigation on its Causes and strength Evaluation of Materials subjected to its Effects*, Proceedings of the 8th International Conference on Alkali-Aggregate Reactivity: 609-615.

Ono, K. (1990). *Strength and stiffness of alkali-silica reaction concrete and concrete members*, Structural Engineering Review, 2:121-125.

Palmer, D. (1978). *Alkali-Aggregate Reaction - Recent Occurrences in the British Isles*, Proceedings of the 4th International Conference on the Effects of Alkalies in Cement and Concrete: 285-298.

Philips D.V., and Bisheng Z. (1993). *Direct Tension on notched and un-notched plain concrete specimens*. Magazine of Concrete Research 45(162): 25-35.

Pleau, R. et al. (1989). *Mechanical Behaviour of Concrete affected by AAR*, Proceedings of the 8th International Conference on Alkali-Aggregate Reactivity: 721-726.

Rodgers, C.A. (1986). *Evaluation of the Potential for expansion and cracking of concrete caused by the alkali-carbonate reaction*, Cement, Concrete, and Aggregate (CCAGDP), 8 (1):13-23.

Rodgers, C.A. (1990). *Alkali-Aggregate Reactivity in Canada*, International Workshop on Alkali-aggregate reactions in concrete: Occurrence, Testing, and Control, J.A. Soles (Ed.), CANMET, Ottawa: (4).

Rotter, H. (1995). *Alkali-Aggregate Reaction: From basic Principles to structural behaviour - A literature review*, Hydro-Québec.

Sakaguchi, Y., et al. (1989). *The Inhibiting Effect of Lithium Compounds on Alkali-Silica Reaction*, Proceedings of the 8th International Conference on Alkali-Aggregate Reactivity: 229-234.

Schmitt J.W., and Stark, D.C., (1989). *Recent Progress in Development of the Osmotic Cell to Determine the Alkali-Silica Reactivity of Aggregates*, Proceedings of the 8th International Conference on Alkali-Aggregate Reactivity:

Shayan, A., and Quick, G. (1989). *Microstructure and Composition of AAR products in Conventional Standard and New Accelerated Testing*", Proceeding of the 8th International Conference on Alkali-Aggregate Reactivity: 475-482.

Sims, I., Higgins, D. (1992). *The Use of GGBS to Prevent ASR Expansion Caused by UK Flint Aggregates*, The 9th International Conference on Alkali-Aggregate Reaction in Concrete: 988-1000.

Stanton, T.E. (1940). *Expansion of concrete structures through reaction between cement and aggregate*. American Society of Civil Engineers, 66: 1781-1815.

Stark, D. (1990). *The moisture condition of field concrete exhibiting alkali-silica reactivity*, International Workshop on Alkali-Aggregate Reactions in Concrete: Occurrence, Testing, and Control, J.A. Soles (Ed.), CANMET, Ottawa: (2).

Swamy, R.N. (1994). *Alkali-Aggregate Reaction - The Bogeyman of Concrete*, Concrete Technology: Past, Present, and Future, Proceedings of V.Mohan Malhotra Symposium, American Concrete Institute:105-129.

Swamy, R.N. (1995). *Assessment and Rehabilitation of AAR-Affected Structures*, Proceedings of the 10th International Conference on Alkali-Aggregate Reactivity.

Swamy, R.N. (1995a). *Alkali-aggregate reaction: that was the monster that was*, International Workshop on Alkali-Aggregate Reactions in Concrete, B. Fournier (Ed.), CANMET, Ottawa,: 47-63.

Swamy, R.N. (1995b). *Effects of Alkali-Aggregate Reactivity on Mineral Stability and Structural Integrity*, International Workshop on Alkali-Aggregate Reactions in Concrete, B. Fournier (Ed.), CANMET, Ottawa:.293-309.

Swamy, R.N., and Al-Alasali, M.M. (1990). *Control of Alkali- Silica Reaction in Reinforced Concrete Beams*. ACI Materials Journal, 87 (1): 38-46.

Swamy, R.N., and Al-Alasali, M.M.(1988). *Engineering Properties of Concrete Affected by Alkali-Silica Reactivity*. ACI Structural Journal.

Swamy, R.N., and Al-Alasali, M.M.(1989). *Effect of Alkali-silica Reaction on the Structural Behaviour of Reinforced Concrete Beams*. ACI Structural Journal.

Swamy, R.N. (1992). *Alkali-Aggregate Reactions in Concrete: Material and Structural Implications*. Advances in Concrete Technology, V.M. Malhotra (ed.),Energy, Mines, and Resources, Ottawa: 533-581.

Thomas, M.D.A., et al. (1992). *Suppression of Damage from Alkali Silica Reactivity by Fly Ash in Concrete Dams*, The 9th International Conference on Alkali-Aggregate Reactivity in Concrete:1059-1066.

Turdoff, M.A. (1990). *Assessment of Pre-stressed Concrete Bridges Suffering from Alkali-Silica Reaction*. Cement and Concrete Composites, 12: 203-210.

Vivian, H.E. (1992). *The Mechanism of Alkali-Aggregate Reaction*, The 9th International Conference on Alkali-Aggregate Reaction in Concrete: 1085-1106.

Wang, H., and Gillott, J.E. (1992). *Combined Effect of Air-entraining agent and silica fume on alkali-silica reaction*", The 9th International Conference on Alkali-Aggregate Reactivity in Concrete:1100-1112.

Wee, T., et al. (1996). *Stress-Strain Relationship of High Strength Concrete in Compression*. Journal of Materials in Civil Engineering, ASCE, 8(2): 70-76.

Wood et al. (1989). *Physical behaviour of AAR damaged Concrete in Structures and in Test Conditions*, Proceeding of the 8th International Conference on Alkali-Aggregate Reactivity: 765-770.

Wood, J.G., et al. (1992). *Revision of the Structural Engineers Report - Structural Effects of Alkali Silica Reaction*, The 9th International Conference on Alkali-Aggregate Reaction in Concrete:1107 - 1112.

Zhen-hai, G., Xiu-qin, Z.(1987). *Investigation of Complete Stress-Deformation Curves for Concrete in Tension* , ACI Materials Journal: 278-285.